HÉCTOR LUIS HERNÁNDEZ HERNÁNDEZ

FORMATION AND CHARACTERIZATION OF NANOSTRUCTURED CONJUGATES FROM TARA GUM AND α-LACTALBUMIN OR β-LACTOGLOBULIN

Dissertation submitted to the Universidade Federal de Viçosa, as part of requirements of the Food Science and Technology Graduate Program, to obtain the title of *Magister Scientiae*.

VIÇOSA
MINAS GERAIS-BRASIL
2018

Ficha catalográfica preparada pela Biblioteca Central da Universidade Federal de Viçosa - Câmpus Viçosa

T

H557f
2018

Hernández Hernández, Héctor Luis, 1991-
Formation and characterization of nanostructured conjugates from tara gum and α-lactalbumin or β-lactoglobulin / Héctor Luis Hernández Hernández. --Viçosa, MG, 2018.
xix, 120 f. : il. (algumas color.) ; 29 cm.

Texto em inglês.
Orientador: Jane Sélia dos Reis Coimbra.
Dissertação (mestrado) - Universidade Federal de Viçosa.
Inclui bibliografia.

1. Soro de leite. 2. Proteínas. 3. Maillard, Reação de. 4. Glicosilação. I. Universidade Federal de Viçosa. Departamento de Tecnologia de Alimentos. Programa de Pós-Graduação em Ciência e Tecnologia de Alimentos. II. Título.

CDD 22. ed. 641.373

HÉCTOR LUIS HERNÁNDEZ HERNÁNDEZ

FORMATION AND CHARACTERIZATION OF NANOSTRUCTURED CONJUGATES FROM TARA GUM AND α-LACTALBUMIN OR β-LACTOGLOBULIN

Dissertation submitted to the Universidade Federal de Viçosa, as part of requirements of the Food Science and Technology Graduate Program, to obtain the title of *Magister Scientiae*.

APPROVED: August, 2nd 2018

Eduardo Basílio de Oliveira
(Co-advisor)

Igor José Boggione Santos
(Co-advisor)

Angélica Ribeiro da Costa

Jane Sélia dos Reis Coimbra
(Advisor)

DEDICATION

To all my family members: Nelcy Judith Hernández Espitia, Héctor Eduardo Hernández Luna, Carmen Enith Luna Perneth and Melany Hernández Hernández.

GRACIAS POR TODO EL APOYO Y CARIÑO INCONDICIONAL

BIOGRAPHY

HÉCTOR LUIS HERNÁNDEZ HERNÁNDEZ, son of Héctor Eduardo Hernández Luna and Nelcy Judith Hernández Espitia, was born in Cereté, Colombia, on September 16th, 1991. He attended his junior and secondary education at Colegio Militar Almirante Colón of Montería. As soon as he finalized his studies successfully, he joined the Universidad de Córdoba and graduated with B.Sc. degree in Food Engineering in 2015. After his graduation, he traveled to Brazil and he joined the Graduate Program in Food Science and Technology at the Universidade Federal de Viçosa in August 2016 and submitted his dissertation to defend in August 2018.

ACKNOWLEDGEMENTS

The *M.Sc* was possible due to valued contribution of many people and funding agencies who offered their technical skills, support and time**.**

First of all, I want to thank God for giving me knowledge, health, patience and strength to complete this stage of my life. I had hard moments, but with the presence of God in my life, I managed to overcome all hostilities and this was motivation to improve every day and to achieve the objectives.

To my mother Nelcy Hernández, father Héctor Eduardo Hernández and grandmother Carmen Luna for the strength, the constant collaboration, help, love, confidence and incentive for the development of this work.

Special thanks to the Conselho Nacional de Desenvolvimento Tecnológico (CNPq) and the program *Estudante-Convênio Pós-graduação (PEC-PG)* for the concession of the scholarship and for covering project expenses.

To the Universidade Federal de Viçosa (UFV) and the Departamento de Tecnologia de Alimentos (DTA) for the opportunity to develop this work.

I would like to thank especially my advisor Dr. Jane Sélia dos Reis Coimbra for the opportunity, for her support in my *M.Sc* studies, for the confidence, for her motivation and for sharing her vast knowledge.

To my co-advisor Dr. Igor José Boggione Santos for the friendship, for his valuable support and suggestions for my work.

To my co-advisor Dr. Eduardo Oliveira for his patience, support and for teaching me things about polysaccharides.

To Professor Reinaldo Teófilo for his support and help in the statistical analyses.

To the Centro Nacional de Pesquisa em Energia e Materiais (*CNPEM*) and the people from Laboratório de Espectroscopia e Calorimetria (LEC), in particular to Fernanda for all the technical support and lessons learned in the conduction of DSC, FI and CD analyses.

To Professors Nilda de Fátima Soares and Eber Medeiros, for the opportunity to work in the Laboratório de Embalagens (LABEM) in the conduction of DLS and Zeta potential analyses.

To Professor Sukarno Ferrereira for helping me in the AFM analysis in the Laboratório de Nanoscopia.

To the members of the Núcleo de Microscopia e Microanálise, in particular to Cristiane Cesário for the opportunity to develop the TEM analysis.

To María Claudia Negrete for the friendship, for helping me at all times, for her great cooperation and valuable advice and support for developing this project.

I owe a lot of gratitude to my friends in Brazil and Colombia, Kely de Paula, José Antônio Queiroz, Maurício Palmeira, Camila Saraiva, Camila Pinheiro, Pedro Calhau, Monique Ellen Torres, Thomás Valente, Luis Arteaga Blanco, Mariano Di Yorio, Gustavo Leite, Douglas Balbino, Victor Gonçalves, María Paulina Mendoza, Karina Vásquez, Yaremis Cabrera, Erika Giraldo, Harold Corrales, Olga Tovar, Charly de Aguas, Lizeth Álvarez and Andrea Vélez for the friendship and support.

I must thank my friends and colleagues from the Laboratório de Operações e Processos (LOP) for their help, assistance and valuable contributions over the time I developed my experiments.

SUMMARY

LIST OF FIGURES

CHAPTER 1

ARTICLE 1

ARTICLE 2

LIST OF TABLES

CHAPTER 1

ARTICLE 1

ARTICLE 2

LIST OF SYMBOLS AND ABBREVIATIONS

aa – Amount of amino acids

a_w – Water activity

AFM – Atomic force microscopy

BI – Browning index

c – Protein concentration

CCD – Central composite design

CD – Circular dichroism

DSC – Differential scanning calorimetry

D_h – Hydrodinamic diameter

DLS – Dynamic light scattering

F_{air} – Air flow rate

FI – Fluorescence intensity

F_r – Feeding rate

HR – Hydrodynamic radius

TG – Tara gum

TEM – Transmission electronic microscopy

MM – Molar mass

OPA – Ortho-phthalaldehyde

PDI – Polydispersity index

RH – Relative humidity

T_{inlet} – Inlet air temperature

T_{outlet} – Outlet air temperature

α-la – α-lactalbumin

β-lg – β-lactoglobulin

ζ – Zeta potential;

ΔH_d – Enthalpy change of denaturation

l– path length

ESI– Emulsion stability index

T_d – Denaturation temperature

CPI– Canola protein isolate

GA– Gum Arabic

WPI– Whey protein isolate

U_E– Electrophoretic mobility

ε– Dielectric constant

η–Viscosity

VD – Volume distribution

WPH – Whey protein hydrolyzed

SBP – Sugar beet pectin

CFG – Corn fiber gum

ABSTRACT

HERNÁNDEZ, Héctor Luis, *M.Sc*., Universidade Federal de Viçosa, August, 2018. **Formation and characterization of nanostructured conjugates from tara gum and α-lactalbumin or β-lactoglobulin.** Advisor: Jane Sélia dos Reis Coimbra. Co-advisors: Eduardo Basílio de Oliveira and Igor José Boggione Santos.

The conjugation of proteins with polysaccharides has been used to improve and/or enhance the technical-functional properties of proteins, to increase the thermal stability of proteins and to form nanostructures able to act as carrier of bioactive compounds. Due to the differentiated functionality of conjugates, Chapter I presents a review on the techniques used to produce and to characterize proteins/polysaccharides conjugates formed via Maillard reaction. Articles 2 and 3 describe the formation and characterization of, respectively, α-lactalbumin (α-la) and β-lactoglobulin (β-lg) conjugates with Tara gum (TG), as well as the obtaining and characterization of nanostructures formed from these conjugates. The conjugates were obtained through Maillard reaction using the dry-heating method. Dispersions containing protein and polysaccharide (mass ratio 1:1) were initially lyophilized and/or spray-dried in order to evaluate the effect of the drying technique, and subsequently heated to 60 ° C and relative humidity of 79 % for up to 9 days. The formation of the conjugates was evaluated by measures of the browning index and by using the ortho-phthalaldehyde test. Variance analysis and Tukey test were used as criteria to determine the most appropriate incubation time for obtaining the conjugates. Nanostructures from conjugates were synthesized under different physicochemical conditions (temperature, pH and heating time) and characterized by dynamic light scattering, zeta (ζ-) potential, fluorimetry and circular dichroism. The thermal stability parameters (denaturation temperature, T_d; change of enthalpy, ΔH) were determined by differential scanning calorimetry, as well as the technical-functional properties (foam ability and emulsion stability index) of pure proteins, mixtures of protein+TG and nanostructures. The morphology of the nanostructures was evaluated by transmission electron microscopy and atomic force microscopy. The progress of the Maillard reaction increased with the increment of the heating time, with a larger extension in the systems formed with lyophilized mixtures. The most appropriate time of glycosylation for the two studied systems was 2 days. Nanostructures from β-lg-TG conjugates presented electrostatic instability with ζ-potential values varying from -30 to 30 mV. Systems containing β-lg-TG, formed at process condition of 50 °C, pH 9.2, 45' and dried by spray (SD) showed excellent emulsifying stability. Nanostructures from α-la-TG conjugates

showed a conical shape with a mean hydrodynamic diameter ranging from 34.3 to 290.1 nm, depending on the system and the conditions used. Systems of α-la-TG (SD) formed at conditions of 50 °C, pH 9.2, 45’ showed T_d = 67.50 °C indicating better thermal stability when compared to the control (pure α-la; T_d = 63.56 °C). Changes were observed in the secondary structure of nanostructures formed from α-la-GT system, mainly a decrease in α-helix content.

RESUMO

HERNÁNDEZ, Héctor Luis, *M.Sc*., Universidade Federal de Viçosa, agosto de 2018. **Formação e caraterização de conjugados nanoestruturados de goma tara e α-lactoalbumina ou β-lactoglobulina**. Orientadora: Jane Sélia dos Reis Coimbra. Coorientadores: Eduardo Basílio de Oliveira e Igor José Boggione Santos.

A conjugação de proteínas com polissacarídeos é utilizada para o melhoramento e/ou intensificação das propriedades técnico-funcionais das proteínas, aumento da estabilidade térmica das mesmas e formação de nanoestruturas destinadas à incorporação de compostos bioativos. Face à busca por sistemas proteicos com propriedades diferenciadas, o Capítulo I apresenta uma revisão sobre as técnicas de obtenção e caracterização de conjugados de proteínas e polissacarídeos formados por reação de Maillard. Os artigos 2 e 3 descrevem a formação e caracterização de conjugados de α-lactoalbumina (α-la) e β-lactoglobulina (β-lg), respectivamente, com goma tara (TG), bem como a obtenção e caracterização de nanoestruturas a partir destes conjugados. Os conjugados foram obtidos por meio da reação de Maillard utilizando o método de aquecimento a seco. Dispersões contendo proteína e polissacarídeo (razão mássica 1:1) foram incialmente secas por liofilização e/ou atomização com o objetivo de avaliar o efeito da técnica de secagem sobre as propriedades dos pós. Posteriormente, foram aquecidas a 60 °C e mantidas em ambiente de umidade relativa de 79 % por até 9 dias. A formação dos conjugados nos diferentes sistemas foi determinada por medidas do índice de escurecimento e pelo teste orto-ftalaldeído. Foram utilizados a análise de variância e o teste Tuckey como critérios para determinação do tempo de incubação apropriado para a obtenção dos conjugados. As nanoestruturas dos conjugados obtidas em diferentes condições físico-químicas (temperatura, pH e tempo de aquecimento) foram caracterizadas via espalhamento dinâmico de luz, potencial zeta (ζ), fluorimetria e dicroísmo circular. Foram determinados os parâmetros de estabilidade térmica (temperatura de desnaturação, T_d; variação da entalpia, ΔH) por meio da técnica de calorimetria diferencial de varredura, bem como as propriedades técnico-funcionais (habilidade de formação de espuma e índice de estabilidade de emulsão) das proteínas puras, misturas de proteína+TG e das nanoestruturas. A morfologia das nanoestruturas foi avaliada usando a microscopia eletrônica de transmissão e microscopia de força atômica. Em geral a extensão da reação de Maillard aumentou com o tempo de aquecimento, tendo uma maior extensão em conjugados obtidos de misturas liofilizadas. O tempo de glicosilação mais apropriado foi de 2 dias. Sistemas contendo β-lg-TG, secos em *spray*

dryer (SD) apresentaram instabilidade eletrostática com valores de potencial ζ na faixa de -30 a 30 mV. As condições de processamento de 50 °C, pH 9,2, 45’ para o sistema β-lg-TG (SD) apresentou excelente estabilidade emulsificante. Nanoestruturas de conjugados de α-la-TG mostraram um formato cônico com diâmetro médio hidrodinâmico variando entre 34,3 e 290,1 nm. As condições de processamento de 50 °C, pH 9,2, 45’ para o sistema α-la-TG (SD) apresentaram T_d = 67.50 °C, um indicativo de uma melhor estabilidade térmica quando comparado ao controle (α-la; T_d = 63.56 °C). Foram observadas mudanças na estrutura secundária das nanoestruturas de conjugados de α-la-GT, como a diminuição do conteúdo de α-hélice.

GENERAL INTRODUCTION

Proteins play a very important role in several industries, mainly in the food industry. These biomolecules are present in many foods, they have high nutritional value and exhibit capacity to improve techno-functional properties such as solubility, foam formation and stability, emulsification, film formation and gelification (Alahdad, Ramezani, Aminlari, & Majzoobi, 2009; Adjonu, Doran, Torley, & Agboola, 2014).

Among several proteins present in nature, there are the whey proteins. Whey is the liquid coproduct obtained from the production of cheese and other dairy products (Onwulata, C., Huth, 2008; Fagani, 2016).

These proteins are characterized for being a family of macromolecules with different structural characteristics. Among this protein group, one finds a greater proportion of β-lactoglobulin (β-lg) and α-lactalbumin (α-la) which when purified or concentrated, can be used in the food industry as stabilizing, emulsifying, gelling, antioxidant and antimicrobial agents enhancing diverse techno-functional properties (Jiménez-Castaño, Villamiel, & López-Fandiño, 2007; Abraham et al., 2016). Moreover, these compounds can be used for the synthesis of carrier matrices of bioactive compounds, polypeptides, drugs and vaccines (Liu, Jiao, Wang, Zhou, & Zhang, 2008).

However, a greater industrial application of these proteins is limited due to their conformational and functional instability under normal food processing conditions, in which high rates of deformation, flow, extreme temperatures and presence of proteolytic agents are involved (Oliver, Melton, & Stanley, 2006; Y. Liu, Zhao, Zhao, Ren, & Yang, 2012).

A low-cost method for improving the protein stability is a development of nanostructures obtained by conjugation of these proteins with polysaccharides through the Maillard reaction. In these conjugates, the protein and the polysaccharide are linked by a covalent bond between the ε-amino group of the lysine residues, and the carbonyl group of the polysaccharides, due to the Maillard reaction, which occurs naturally under controlled conditions of time, temperature, and relative humidity (Kato, 2002; J. Liu, Ru, & Ding, 2012). In addition, polysaccharides are thermally stable, safe, hydrophilic, biodegradable, abundant in nature, have a low-cost processing and have

diverse and numerous reactive groups, with a wide range of molar masses and different chemical compositions, which contribute to their diversity in structure and in property (Liu et al., 2008).

Nanostructures obtained by conjugation of proteins with polysaccharides are an effective form to improve or/and intensify techno-functional properties (Sanmartín, Arboleya, Villamiel, & Moreno, 2009; Corzo-Martínez, Sánchez, Moreno, Patino & Villamiel, 2012; Álvarez, García, Rendueles, & Díaz, 2012; Spotti et al., 2013; Kasran, Cui, & Goff, 2013) and also have potential use in controlled release system and nanoencapsulation. Several studies show that egg protein, soy protein and casein conjugated with polysaccharides (e.g. dextran, chitosan or galactomannan) improve their solubility, gelling properties, emulsifiers and thermal stability (Usui et al., 2004; Al-Hakkak & Al-Hakkak, 2010; Li et al., 2013; Kasran et al., 2013). Li, Shaoyong Yu, Ping Yao & Jiang, (2008) studied the formation of nanogels from lysozyme-dextran conjugate obtained via the Maillard reaction. Nanogels have the potential to be used in controlled release systems. Among diverse polysaccharides present on the market, one can find the tara gum (TG), which is recognized as food additive in several countries and it is mainly used as a thickener and stabilizer whose rheological properties are crucial for the consistency and viscosity of food products (Sittikijyothin, Torres, & Gonçalves, 2005). In addition, some studies described the possibility of using this biomolecule in the formation of gels, films and coatings with other polysaccharides and/or proteins (Cerqueira et al., 2009). There are many studies that report the behavior of the tara gum, however, research involving conjugation of whey proteins with tara gum are scarce (Jiménez-Castaño et al., 2007).

In this work, the formation of conjugates of α-lactalbumin or β-lactoglobulin with tare gum was studied with the aim of enlarge the use of whey proteins. The nanostructures formed from these conjugates were taken to the structural and morphological characterization, as well as to the evaluation of the technical-functional properties (foaming properties and emulsifying properties). Thus, the expectation is that this work may contribute to a greater dissemination of the potentialities of the use of protein and polysaccharide conjugates in the food industry.

CHAPTER 1

Review on the techniques used for produce and characterize protein-polysaccharide conjugates obtained by Maillard reaction

Review on the techniques used for produce and characterize protein-polysaccharide conjugates obtained by Maillard reaction

1. Whey Proteins

Whey is commonly defined as the liquid co-product originated from the production of cheeses and casein (De Wit, 2001; Onwulata, C., Huth, 2008). However, this definition can be extended to a broader concept that encompasses its various methods of production, thus whey would be the liquid co-product resulting from the extraction of casein from milk. Whey represents about 80 to 90% of the total milk volume and it has a yellowish-green coloration due to the presence of riboflavin (vitamin B_{12}) in its composition. It contains nutrients such as proteins, lactose and mineral salts, mainly (De Wit, 2001; Alves et al., 2014; Maganha, 2006).

Whey contains about 0.8 % of proteins; this percentage may vary depending on the breed of the cattle, the feed supplied and the country of origin (Jara & Pilosof, 2011). Table 1 shows the approximate fractionation of proteins present in whey obtained by enzymatic coagulation, their approximate concentration, isoelectric point and molecular weight.

Milk whey proteins are characterized by globular structures containing some disulfide bonds, which confer structural stability to the macromolecules. Fractions, or whey peptides, consist of α-lactalbumin (α-la), β-lactoglobulin (β-lg), bovine serum albumin (BSA), lactoferrin (Lf), immunoglobulins (Igs), lactoperoxidase (LP) and glycomacropeptides (GMP). These fractions may vary in size, molecular weight and function, providing special features (Boaglio, Bassani, Picó, & Nerli, 2006; Oliveira et al., 2007).

These proteins are characterized by having good gelling ability, emulsification, foaming, elaboration of protective films and capsules, excellent nutritional value and various physiological properties, therefore they have potentially several technological applications (Wong, Camirand, Pavlath, Parris, & Friedman, 1996; Sgarbieri, 2005).

Table 1. Approximate fractionation of proteins present in whey obtained by enzymatic coagulation.

Protein	Content (% whey dry base)	Concentration ($g \cdot L^{-1}$)	Isoelectric point	Molecular weight (kDa)
β-Lactoglobulin (β-Lg)	48 - 58	2.0 - 4.0	5.4	18
α-Lactalbumin (α-La)	13 - 19	0.6 - 1.7	4.4	14
Glycomacropeptide (GMP)	12 - 20	1.2 - 1.5	<3.8	8.6
Bovine serum albumin (BSA)	6	0.1 - 0.4	5.1	66
Immunoglobulins (Igs)	8 - 12	0.6 - 1.0	5-8	150
Lactoferrin (LF)	2	0.02 - 0.4	7.9	77
Lactoperoxidase (LP)	0.5	0.02	9.6	78

Source:(Onwulata, C., Huth, 2008; Fidelis, 2011) (adapted).

1.1. β-lactoglobulin (β-lg)

β-lg is characterized by having a globular three-dimensional structure, presenting in its primary structure 162 amino acid residues, molecular weight of approximately 18.3 kDa, isoelectric point equal to 5.4 (Bromley, Krebs, & Donald, 2005; Alves, Brenneisen, Ninni, Meirelles, & Maurer, 2008; Wijaya, Van der Meeren, & Patel, 2017). It is the most abundant whey protein and presents high solubility (~ 97%) over a wide pH range, but mainly at low pH values (pH 3), being stable at thermal treatments under these conditions (Chatterton, Smithers, Roupas, & Brodkorb, 2006).

The specific structure of β-1g, of the lipocalin type (Figure 1), forms a kind of cup of hydrophobic character that confers functional properties of great application in the food industry, such as emulsification, foam formation, gelation and interaction with molecules responsible for the aroma and flavor of the product (Morr, C. V.; Foegeding, 1990; Poppi; F.A., Costa; M.R., de Rensis; C.M.V.B., Sivieri, 2010).

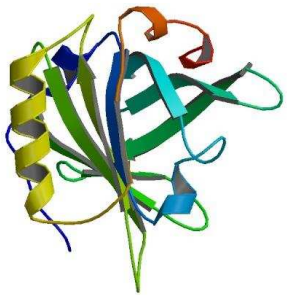

Fig. 1. Tertiary structure of β-lg. Source: Loch, Polit, Goreki, Bonarek, & Kurpiewska (2011), PDB.

When the hydrophobic cup of β-lg is exposed, for example, in heat denaturation, aggregates are formed by hydrophobic interactions. These aggregation properties can be manipulated by changing the temperature, pH and ionic strength. Under prolonged heating at low pH and low ionic strength, a transparent "fine wire" gel is formed, in which the protein molecules join together in long rigid fibers and can also produce nanoparticles (Ko & Gunasekaran, 2006).

1.2. α-lactalbumin (α-la)

α-1a is a globular and monomeric protein composed by 123 amino acids, molar weight of about 14 kDa and isoelectric point equal to 4.4. This protein has 13 potentially reactive amino groups, including the amino terminal group. The stability of α-1a depends on many factors such as pH, presence of salts, source, purity and protein concentration (Gu et al., 2001). α-la consists primarily of an α-helical domain and a small β-sheet domain (Figure 2), which are held together by a disulfide bond where the Ca^{2+} binding site is located (Permyakov & Berliner, 2000).

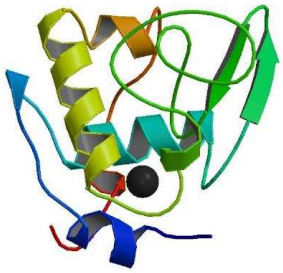

Fig. 2. Tertiary structure of α-la. Source: Chrysina, Brew, & Acharya, (2000) PDB.

α-la has nutritional properties and also assists the immune system. By forming complexes with differentiated cells, it avoids its degradation and increases the immune response of these cells activated by bacteria or components of the bacterial cell wall (Spencer et al., 2010). Its amino acid composition is indispensable for newborns and has high digestibility (Graveland-Bikker & de Kruif, 2006). The shape of the α-lactalbumin linked to lactose may prevent intestinal infections inhibiting the adhesion of pathogenic microorganisms on the surface of the lumen due to the lack of lactosamine required for adhesion (Kamau, Cheison, Chen, Liu, & Lu, 2010).

1.3. Techno-functional properties of proteins

In addition to their nutritional properties, proteins have specific techno-functional properties that facilitate food processing. These properties are also used in the formulation of new products. Among the techno-functional properties are water retention capacity, solubility, viscosity, gelation, aroma retention capacity (hydrodynamic properties or hydration properties) and emulsification, foaming, oil and film-forming properties (properties related to the protein surface) (Kilara & Vaghela, 2000).

1.3.1. Foam ability

Foams consist of an aqueous continuous phase and a gaseous dispersed phase (air). Many processed foods are foam-like products such as creams, ice creams, meringues, breads, mousses, etc. In most of these products, proteins are the main surface active agents that aid in the formation and stability of the dispersed gaseous phase (Fennema, Damodaran & Parkin, 2010).

Among the basic requirements for a protein to be a good foaming agent are the ability to adsorb rapidly at the air-water interface during agitation, to undergo rapid conformation and rearrangement at the interface, and to form a cohesive viscoelastic film through intermolecular interaction (Hettiarachchy & Ziegler, 1994).

The two most commonly used ways to measure these properties are: foaming activity and foam stability. Foaming activity indicates when a protein has the capacity to foam and to what extent does the volume increase over the volume of the solution (Haque & Kito, 1983). Foam stability refers to the ability of a formed foam to retain the maximum volume after a set period of rest (Kinsella & Melachouris, 1976).

1.3.2. Emulsifying properties

Emulsion is a heterogeneous system consisting of an immiscible liquid, completely diffuse in aqueous phase, in the form of droplets with a diameter greater than 0.1 micron. The formation of an emulsion requires energy to keep the droplets dispersed in the continuous phase, being intrinsically unstable; over time, the droplets of the dispersed phase will be attracted, resulting in the separation of the phases. The forces involved in the stability of the emulsion depend on the balance of the forces associated with the oil-water interface. It is deduced that this is thermodynamically unfavorable and, for this reason, such a process shows minimal stability, which can be

increased by the addition of surface active agents (Araújo, 2011). Proteins are amphiphilic molecules, migrating spontaneously to an oil-water interface. In this way, the proteins form a highly viscoelastic film, which has the capacity to withstand mechanical shocks during food storage. Thus, emulsions stabilized by proteins are more stable than those prepared with low molecular weight surfactants (Fennema, Damodaran & Parkin, 2010).

There are two ways of measuring these properties: emulsifying ability and emulsifying stability. Emulsifying ability is defined as the volume of oil that can be emulsified per gram of protein before emulsion inversion or collapse occurs (Kinsella & Melachouris, 1976). Emulsion stability refers to the ability of the protein to form an emulsion, which remains unchanged for a given duration of time, under specific conditions of time or temperature (Kinsella & Melachouris, 1976).

2. Tara gum (TG)

Tara gum, also known as Peruvian carob, is a powder with white or beige coloration obtained by grinding the endosperm of the *Caesalpinia spinosa tree*, which is originated from Peru and has been cultivated largely in the Chinese provinces of Yunnan and Sichuan. The major component of TG is galactomannan polysaccharides, consisting of a linear main chain (1-4) –β-D-mannopyranose units linked by (1-6) glycosidic bond with α-D-galactopyranose units (Figure 3). TG is characterized by being similar structure and functional properties with guar and locust gums (Sittikijyothin et al., 2005; Wu, Li, Cui, Eskin, & Goff, 2012).

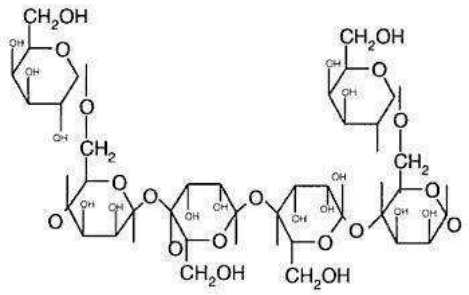

Fig 3. Chemical structure of TG. Source: Wu et al., 2012

Aqueous solutions of TG are neutral and highly viscous. TG is characterized by being soluble in cold water, but for complete solubility and maximum viscosity at a given concentration, heating is required. TG has high water retention capacity and

effective protective colloidal characteristics and its solutions exhibit a relatively low viscosity loss after heating to 120 °C. Therefore, it has great potential to be used in conjugation with proteins conferring these properties to proteins and thereby increasing their stability (Dea et al., 1977).

3. Protein-polysaccharide conjugates obtaining by Maillard reaction

Protein-polysaccharide conjugates obtained via the Maillard reaction consist of several glycosylated products and are synthesized under controlled conditions of temperature, water activity (a_w), pH and incubation time in order to prevent the reaction progression to produce compounds harmful to the health. In the Maillard reaction, the ε-amino group of the lysine residue present in the protein binds covalently to the carbonyl group of the polysaccharide (Fig. 4) (Kato, 2002; Silván, Assar, Srey, Dolores del Castillo, & Ames, 2011).

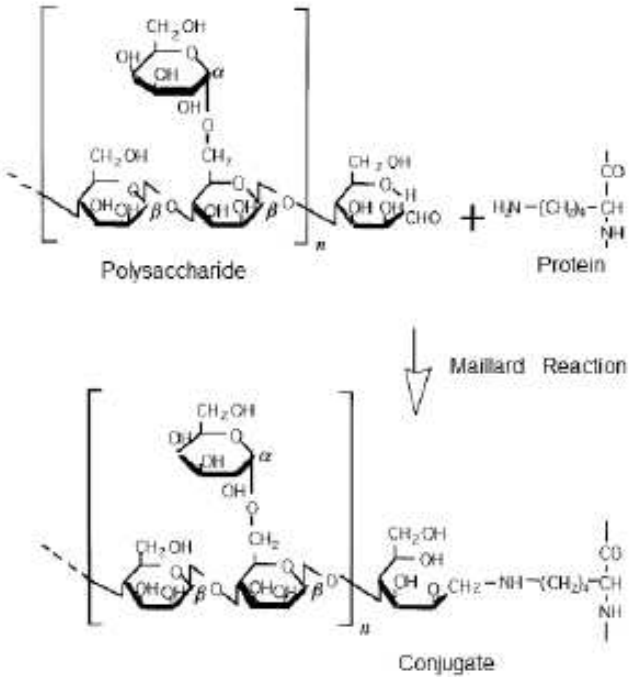

Fig.4. Schematic representation of protein-polysaccharide bond during Maillard reaction. Source: adapted from de Oliveira, Coimbra, de Oliveira, Zuñiga, & Rojas (2014)

Rate and mechanism of the Maillard reaction can be influenced by the temperature, activation energy, water activity (a_w) and pH. The activation energy varies between 10 and 160 kJ.mol^{-1}, therefore, energy in the form of heat is required for the Maillard reaction to occur and the increase in temperature results in high reaction rates (Damodaran, 2007). Water activity also has a high impact on the

activation energy, a_w values in the range of 0.3 to 0.70 increase the reaction velocity. At low values of a_w the Maillard reaction occurs slowly. Another factor that affects the reaction rate is pH, in which case the reaction rate is maximized at slightly alkaline pH (Damodaran, 2007). Fig. 5 presents a scheme of the structure of a protein-polysaccharide conjugate.

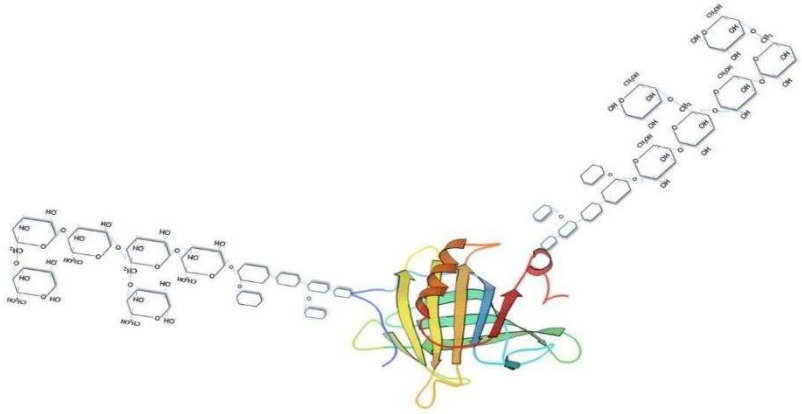

Fig. 5. Schematic representation of a protein-polysaccharide conjugate. Source: adapted from de Oliveira, Coimbra, de Oliveira, Zuñiga, & Rojas (2014).

The interactions between proteins and polysaccharides under specific conditions can promote the formation of hydrogels with different functional properties compared to those of a single polymer species (Damodaran, 2007). In addition to their role as protective backing for bioactive food ingredients, protein-polysaccharide conjugates are designed to exhibit the required functional attributes within the final product (e.g. optical properties, rheological properties, foaming, encapsulation properties and physical-chemistry stability)(McClements, 2015).

Other studies report that the conformational structure of the protein and the particular characteristics of the polysaccharides, such as hydrophobicity and viscosity have a high influence on the techno-functional properties of conjugates obtained via the Maillard reaction. The type of polysaccharide plays an important role in the protein-polysaccharide conjugation. Monosaccharides and disaccharides are characterized by being highly reactive, but the low reactivity of polysaccharides and the steric hindrance limit the progression of the Maillard reaction and this causes a decrease in posterior glycosylation reactions, preventing excessive color changes and polymerization of proteins (Niu, Jiang, Pan, & Zhai, 2011).

The hybrid biopolymer conjugates prepared from proteins and polysaccharides may have properties that combine the advantages of both building materials for using as nanocarriers for bioactive food ingredients (Jones & McClements, 2011). In addition, these conjugates not only exhibit excellent thermal stability and antimicrobial activity, but also decrease the allergenicity of some proteins (Li, Luo, & Feng, 2011).

3.1. Methods for obtaining protein-polysaccharide conjugates

Among the most widely used methods for obtaining protein-polysaccharide conjugates are the dry-heating or heating in aqueous solution. The first one is characterized for using the heating of a dry mixture of protein and polysaccharide in certain conditions of temperature and relative humidity. The second method consists of the utilization of a protein-polysaccharide mixture in a buffer solution, which is heated at a certain temperature.

3.1.1. Reaction in dry-heating conditions

The first step in the dry heating reaction is to prepare the protein-polysaccharide dispersion in the desired molar or mass ratio, depending on the type of protein and polysaccharide used. The mixture is then lyophilized or spray-dried. The conjugates are produced during the storage of lyophilized or dried powder at certain temperature conditions (40 - 80 °C), 60 °C being the most common. Relative humidity (RH) is also controlled during storage generally in the range of 65% to 79%. The reaction time for conjugate formation depends on the type and conformation of the protein, as well as the type of polysaccharide. The reaction can happen in hours or in weeks. Once the storage is complete, the synthesized conjugates are immediately frozen to stop the progression of the Maillard reaction (Akhtar & Dickinson, 2003; Aminlari, Ramezani, & Jadidi, 2005; Miralles, Martínez-Rodríguez, Santiago, van de Lagemaat, & Heras, 2007; Du et al., 2013).

3.1.2. Reaction with heating in aqueous solution

When the Maillard reaction occurs in aqueous solution, denaturation and polymerization of the protein may occur at elevated temperatures. In the presence of high concentrations of biopolymers, the produced glycosylation could increase, although this could also result in high denaturation and polymerization of the protein. The first step in obtaining conjugates by heating in aqueous solution is to prepare the

solution in the desired molar or mass ratio and adjusting the pH using a buffer. The solution is then subjected to heating at certain conditions of time and temperature. Finally, the conjugates are purified by chromatographic and frozen methods for their subsequent characterization (Zhu, Damodaran, & Lucey, 2008; Mu, Zhao, Zhao, Cui, & Liu, 2011; Niu et al., 2011; Zhuo et al., 2013).

3.2. Nanostructures from protein-polysaccharide conjugates

Nanostructures originating from protein-polysaccharide conjugates are characterized for promoting and/or enhancing and/or modifying techno-functional properties, such as gelling, emulsifying, stabilizing, antioxidant and antimicrobial properties. These properties are differentiated from those when one has the individual protein and polysaccharide or the conjugates without the formation of nanostructures (Weiss, Takhistov, & McClements, 2006). In addition to these functional technical properties, the nanostructures can be used for releasing bioactive compounds, polypeptides, vaccines, among others (Z. Liu et al., 2008).

These nanostructures are easy to prepare and present pH-responsive properties, offering reversible sites for binding and releasing compounds. In addition, low density and capacity for network formation offer more space and binding sites; the cross-linking property can prevent dissociation after dilution and the nanometer size can respond to stimuli from the medium immediately (Hu, Yu, & Yao, 2007).

3.3. Characterization techniques of nanostructures from protein-polysaccharide conjugates

Protein-polysaccharide nanostructures are widely characterized by dynamic light scattering (DLS), zeta potential (ζ), molecular fluorescence spectroscopy (FI), circular dichroism (CD), Raman spectroscopy, chromatographic techniques, differential scanning calorimetry, rheological measurements, and microscopy techniques. These techniques have been used together to obtain information on the determination of size, molar mass, particle shape, particle surface morphology, surface electrical charges of the nanostructure. They also determine the stability of secondary and tertiary structures in nanostructures as well as detection of the presence of structural components (Schillen, Brown, & Johnsen, 1994; Giroux, Houde, & Britten, 2010; Donato, Kolodziejcyk, & Rouvet, 2011; Medrano, Abirached, Moyna,

Panizzolo, & Añón, 2012). Table 2 shows several studies involving the formation of protein-polysaccharide conjugates using the different characterization techniques.

3.3.1. Dynamic light scattering

The dynamic light scattering technique (DLS) also known as photon correlation spectroscopy or quasi-elastic light scattering technique is generally used for the rapid determination of the size distribution profile of nano-sized particles, emulsions, colloids, suspensions or dispersion of polymers. The DLS measures the Brownian motion of the suspended particles and relates this to the size of the particles. The DLS technique uses a laser to analyze intensity fluctuations in scattered light (Gupta & Ghosh, 2014).

When a system is affected by the electromagnetic radiation, the electrons of the molecules of this system, which oscillate with the same frequency of the incident radiation, are polarized by induction of the electric field of the radiation. Thus, the molecules become secondary sources of radiation and scatter this incident light, which happens to be called scattered light. The size, shape and molecular interactions of the irradiated material can lead to changes in frequency, angular distribution, polarization and scattered light intensity. In this way, it is possible to obtain information about the structure and the molecular dynamics of the scattering medium from the characteristics of the scattered light of a given system. The choice of radiation type is based on the range of lengths of interest and on the interaction of radiation with matter (Poole & Owens, 2003).

This method has several advantages: the experiment is fast, almost automatic, cost-effective equipment, the possibility of analyzing samples containing distributions of many species and different molar masses (e.g. biomolecules such as proteins). In addition, it also determines the average particle size and polydispersity index (PDI) (Sundar, Kundu, & Kundu, 2010).

3.3.2. Zeta potential

The zeta potential is used to describe the electro-kinetic potential of colloidal systems (Mills, Cvitas, Homann, Kallay, & Kuchitsu, 1993). In the case of colloids, the zeta potential is a unit used for expressing the potential difference between the dispersion medium and the stationary fluid layer attached to the dispersed particle (Fig. 6). A value of 30 mV (positive or negative) is taken as the optimal value for

determining the electrostatic stability of the colloidal system, since it indicates the value that separates a low-load surface from a highly charged one (Preetz, Hauser, Hause, Kramer, & Mäder, 2010).

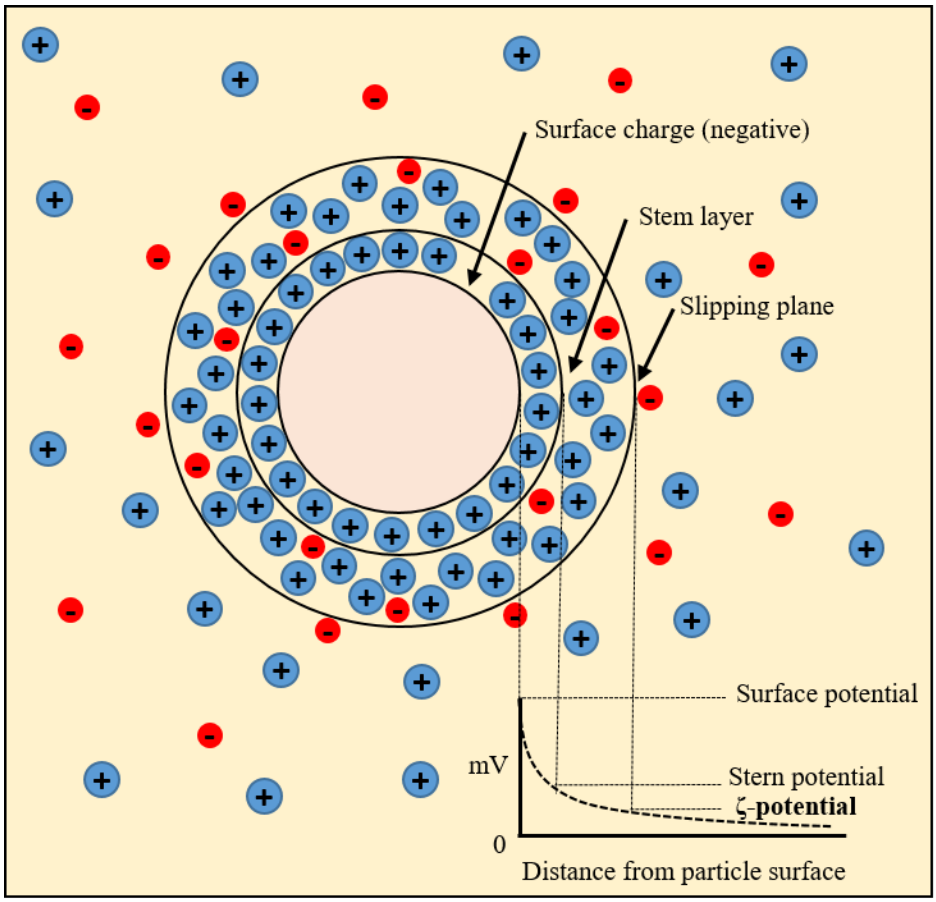

Fig. 6. Diagram showing the ionic concentration and potential difference as a function of distance from the charged surface of a particle suspended in a dispersion medium. Source: adapted from Malvern Instruments (2003).

The value of the zeta potential is related to the electrostatic stability of the dispersions, since there is a repulsion between molecules with similar charge in the dispersion. For small drops, a high zeta potential indicates good electrostatic stability, indicating no aggregation. When the zeta potential is low, the attraction exceeds the repulsion and this leads to the dispersion rupture leading to flocculation.

The main factors that influence the zeta potential of the nanoparticles are the presence of different surfactants, type of dispersant phase, presence of different particles, ionic strength, particle morphology and size, and pH (Simunkova et al., 2009).

Table 2. Formation of protein-polysaccharide conjugates using the different characterization techniques.

Characterization technique	System	Reaction conditions	Main results	Reference
Dynamic light scattering (DLS)	Lz-Pullulan	Dry-heating method. Lz/pullulan mixture, 1:2, 1:4, 1:6, 1:8, 1:10, 1:12 mass ratio, pH 7. The mixtures were incubated at 60 °C, 79 % RH for 1, 2, 3, 4, 5, 6 and 7 days.	Mean size of conjugate was 16.51 nm, which was 3.5-fold to the native lysozyme.	Sheng et al., 2017
	WPI-SBP	Dry-heating method. WPI/SBP mixture, 3:1, 2:1, 1: 1 mass ratio, pH 6.75. The mixtures were incubated at 60 °C, 79 % RH for 72 h.	Results showed that the mean size of the emulsion particles using the conjugates was lower than when protein was used as a stabilizer.	Qi et al., 2017
Zeta potential	CPI-GA	Heating in solution method. CPI-GA mixture, 2:1 mass ratio, pH 1-7. The mixture was heated at 90 °C for 15 min.	Zeta potential of conjugate solution to more acidic pH (pH 3.8) compared to the CPI and mixture solutions.	Safoura et al., 2017
	β-lg-Pectin	Dry-heating method. β-lg/pectin mixture, 1: 2 mass ratio, pH 7. The mixtures were incubated at 80 °C, 79 % RH for 1.5 to 72 h.	The reaction time did not significantly affect the zeta potential values.	Schmidt et al., 2016
Differential scanning calorimetry(DSC)	WPI-Maltodextrin	Dry-heating method. WPI/Maltodextrin mixture, 1: 1 mass ratio, pH 4, 5, 6, and 7. The mixtures were incubated at 80 °C, 65 % RH for 1., 2 and 4 h.	pH increase caused a rise in T_d and reduction of ΔH_d of the conjugates.	Wang & Zhong, 2014a
	WPI-Maltodextrin	Dry-heating method. WPI/Maltodextrin mixture, 1: 1 mass ratio, pH 6. The mixtures were incubated at 80 °C, 65 % RH for 2 h.	Increase in co-solutes concentration caused a rise in T_d and reduction of ΔH_d of the conjugates.	Wang & Zhong, 2014b

Characterization technique	System	Reaction conditions	Main results	Reference
Transmission electronic microscopy (TEM)	BSA-CFG	Heating in solution method. BSA/CFG mixture, 10:1, 4:1, 1:1, 1:4 mass ratio, pH 6. The mixtures were heated at 35°C in water bath for 4 h.	Conjugates showed spherical shape with mean diameter between 16.9 and 32.1 nm.	Liu et al., 2017
Scanning electronic microscopy (SEM)	Sodium caseinate-Lactose	Heating in solution method. Sodium caseinate/lactose mixture, 1:1, 1:2, 1:3, 1:4, 2:1, 3:1, 4:1 mass ratio, pH 7.5, 8, 9, 10 and 11. The mixtures were heated at 80°C in water bath for 30 min.	Conjugates were uniform in size and with relatively smooth surfaces.	Li et al., 2017
	BSA-CFG	Heating in solution method. BSA/CFG mixture, 10:1, 4:1, 1:1, 1:4 mass ratio, pH 6. The mixtures were heated at 35°C in water bath for 4 h.	Conjugates showed smooth area and this was attributed to the intramolecular conjugation of CFG or BSA.	Liu et al., 2017
Confocal microscopy	WPI-Maltodextrin-Lactose	Dry-heating method. WPI/Maltodextrin mixture (1:2 mass ratio) and Maltodextrin/lactose (1:1, 1:2, 1:4, 1:6, 1:10 molar ratio), pH 7. The mixtures were incubated at 80 °C, 79 % RH for 3 h.	Droplets were well dispersed and still separated from each other after 4 weeks and the mean diameter was less than 5000 nm.	Ding et al., 2017
	WPH-Maltodextrin	Heating in solution method. WPH/maltodextrin mixture, 1:1 mass ratio, pH 8.2. The mixtures were heated at 90°C in water bath for 8 h.	Microstructural analysis of the emulsions showed that all samples had fine and uniformly distributed oil droplets immediately post homogenization.	Drapala et al., 2016

Characterization technique	System	Reaction conditions	Main results	Reference
Atomic force microscopy (AFM)	WPI-Maltodextrin	Dry-heating method. WPI/Maltodextrin mixture, 1: 1 mass ratio, pH 6. The mixtures were incubated at 80 °C, 65 % RH for 2 h.	The addition of high concentrations of D-glucose reduced the irregularity of aggregate morphology, eventually resulting in uniform particles of 5 nm.	Wang & Zhong, 2014b
Molecular fluorescence spectroscopy	WPI-Glucose	Dry-heating method. WPI/glucose mixture, 1: 1 mass ratio, pH 7. The mixtures were incubated at 60 °C, 79 % RH for 1, 4 and 7 days.	All of the conjugates exhibited higher fluorescence intensity than the intact protein WPI, and a marked blue shift in the maximum fluorescence intensity was observed when increasing heating time.	Q. Liu et al., 2014
	β-lg-Dextran, α-la-Dextran and BSA-Dextran	Dry-heating method. β-lg/dextran, α-la/dextran and BSA/dextran mixtures, 1: 1 mass ratio, pH 7. The mixture were incubated at 60 °C, 0.44a_w for 12, 24, 36, 48, 60, 72 and 96 h.	Glycosylation with dextran lowered the fluorescence intensity of β-lg, which has been attributed to a shielding effect of the polysaccharide chain.	Jímenez-Castaño, Villamiel, & López-Fandiño 2007
Circular dichroism	β-lg-FOS	Dry-heating method. β-lg-FOS mixture, 1: 0, 1:1, 1:2, 1:4, 1:6, 1:8 and 1:10 mass ratio, pH 7. The mixture were incubated at 50 °C, 79 % RH for 24 h.	The broad negative maximum and the blue shift show that the β-sheet regions were changed by conjugation with FOS	Chamani et al., 2005

Where: Lz: Lysozyme; WPI: Whey protein isolate; WPH: Whey protein hydrolyzed; SBP: Sugar beet pectin; CPI: Canola protein isolate; CFG: Corn fiber gum.

The zeta potential is calculated indirectly through electrophoretic mobility. For determining its value, a system is constituted by a cuvette with two electrodes, where the dispersion is inserted and an electric field is applied. The particles with liquid electric charge will move towards the opposite charge electrode at a certain velocity (electrophoretic mobility)(Honary & Zahir, 2013). The zeta potential is related to electrophoretic mobility and given by Henry's equation (equation 1).

$$U_E = \left(\frac{2\varepsilon\zeta}{3\eta}\right)[f(kR)] \quad (1)$$

Where: U_E is the electrophoretic mobility, ε and η are the dielectric constant and the viscosity of the solvent, respectively, ζ is the zeta potential and $f(kR)$, the Henry function.

3.3.3. Differential scanning calorimetry (DSC)

DSC is a technique that involves the study of heat and mass changes as a function of temperature. Along with the sample, a standard reference is also used to correlate observed changes to the nanoparticle samples. During the analysis, the measurements corresponding to the sample and the standard reference in terms of their mass and heat changes are registered at the same temperature. Several of these measurements are observed at increasing temperatures. The specific temperature in which any drastic thermal or mass changes occur is observed, and this provides a complete idea about the nature of the nanoparticle, its melting range, purity, and homogeneity (Venturini et al., 2011).

This technique provides qualitative and quantitative data on exothermic (heat energy release) and endothermic processes (heat energy absorption), allowing the gathering of information related to changes in physical and chemical properties, such as characteristic temperatures (melting, crystallization, glass transition), enthalpies of phase transition and reaction and thermal and oxidative stability and reaction kinetics (Ionashiro, 2004).

DSC can be used to characterize different compounds, such as proteins. Areas of application extend from the scientific to the industrial domain, with particular importance in the pharmaceutical, cosmetic and food industries, either in the research and development phase of a process or product, or in the quality control phase of raw materials and products. In addition, DSC analysis also indicate the nature of

incorporated nutraceuticals and whether they are in intact or their degraded form (Venturini et al., 2011).

3.3.4. Fluoresce molecular spectroscopy (FI)

Fluorescence spectroscopy is widely used for the study of conformational changes in proteins, based on the emission of electromagnetic radiation due to electronic transitions between excited electronic states and lower energy states. Proteins contain intrinsic chromophores, the amino acid residues tryptophan, tyrosine and phenylalanine, whose fluorescence is highly specific and sensitive to the environment in which they are found. Small conformational changes involving, in particular, tryptophan, and/or their surrounding areas, induce distinct responses in the fluorescence emission, quantum yield, or emission peak shift (Lakowicz & Maliwal, 1985; Skoog, Holler, & Crouch, 2007).

This occurs because indole, tryptophan and its derivatives are very sensitive to the polarity of the solvent and feel their general and specific effects. Thus, the emission spectra of tryptophan residues reflect the polarity of their environment. On the other hand, in a protein, the emission of fluorescence is the sum of the contributions of their individual fluorophores, which depend on the microenvironment of each residue. Minor changes in this microenvironment are revealed by fluorescence. Therefore, this technique is able to study the occurrence of local conformational changes, that is, at the tertiary level, especially in the microenvironment of aromatic amino acid residues, allowing the inference of the microhabitat of these residues (Lucca, Hansen, & Oliva, 2006).

3.3.5. Circular Dichroism (CD)

The DC spectroscopy allows analyzing the secondary and tertiary structure of proteins, the structural changes in them, the stability of the protein, as well as the integrity and their folds (Kelly & Price, 2000; Lucca et al., 2006). This technique is based on the determination of the difference in the absorbance of circularly polarized light on the left and right as a function of the wavelength. The ultraviolet (UV) region between 190 and 260 nm corresponds to the absorption point of the amide bonds of the peptide chain of the protein; therefore, the obtained DC spectrum is analyzed in terms of secondary structure. Each protein and/or peptide conformation (α-helix, β-sheet, β-loop and randon coil) presents a typical spectrum of DC. The DC spectrum

near the UV region (260 to 320 nm) reflects the aromatic amino acid chains and provides information on the protein tertiary structure (Harding & Chowdhry, 2001).

The CD can be used to detect conformational changes of macromolecules; composition of chiral mixtures; interaction of these macromolecules with other smaller molecules, especially asymmetric (chiral) molecules. Among the advantages in the use of this technique, are:

- Simple and fast experiments;
- Full recovery of the sample;
- The analysis is done in solution. This detail is important because, in the crystallization process may occur a change in the structure of the molecule, especially in biological systems. In aqueous phase, there is a very close reproduction to what is the reality of biological systems "in vivo" (Corrêa & Ramos, 2009).

3.3.6. Transmission electronic microscopy (TEM)

Transmission electron microscopy is the method of analysis of any particle for the range of nanometers. An electron beam is passed through the sample to be analyzed. An image is formed by the interaction of the electrons with the sample being analyzed, which is enlarged and then projected onto an image.

The main disadvantage of this type of microscopy is the sample preparation technique, which is extensive and makes it a time-consuming process. However, in the case of nanoemulsions, TEM studies help to know the morphology of emulsions. Thus, it allows determining the effect of the nanoemulsion formation method on the shape and structure of the particles droplets. The imaging principle involves combining bright field visualization with corresponding magnification, especially for small particles. This property also helps to perform the diffraction and estimation of selected areas of a nanoemulsion and its evaluation of the particle morphology (Gupta & Ghosh, 2014).

A modern transmission microscope has five or six magnetic lenses and several electromagnetic deflection coils and apertures located along the path of the electron beam. Among these components, there are three with major importance with respect to the electronic diffraction phenomena: objective lens, objective aperture and selective diffraction aperture. The function of the projector lens is only the production

of a parallel beam and sufficient incident intensity on the surface of the sample. Electrons leave the sample on the lower surface with a distribution of intensity and direction controlled mainly by the diffraction laws imposed by the crystalline arrangement of the atoms in the sample. Then, the objective lens form the first image of this angular distribution of the diffracted electron beams. After this very important objective lens process, the remaining lenses only serve to augment the image or diffraction pattern for future viewing on the screen or on the photographic plate (Reimer & Kohl, 2008).

3.3.7. Atomic force microscopy (AFM)

Atomic force microscopy has recently been developed for imaging purposes (Luykx, Peters, van Ruth, & Bouwmeester, 2008). A very high resolution can be achieved through the AFM technique, due to the small, precise and infinitesimal details as individual atoms or molecules that have dimensions of a few nanometers. This technique relies on the rapid scanning of a nanometer-sized sharp probe under a compound that is previously immobilized on a defined surface of mica or glass. A piezoelectric system, which shifts at the x, y, and z positions, monitors the scanning of the sample surface, by varying the applied voltage. Therefore, a high-resolution three-dimensional image is obtained. Using AFM, liposomes, bioactive compounds encapsulated in proteins or carbohydrates and other nanometric forms can be visualized (Luykx et al., 2008). In addition, the structure, morphology and nature of nanostructures can also be studied using AFM. However, the difficulty found by using AFM is that no particle of a soft or viscous nature can be analyzed.

4. Final considerations

Maillard reaction under controlled conditions of temperature and relative humidity is one of the few methods that allow covalent bonds between proteins and polysaccharides without the formation of compounds detrimental to health, since this reaction is carried out without the addition of toxic compounds. In addition, protein glycosylation via the Maillard reaction can improve the techno-functional properties of proteins and has potential for use in matrices for controlled release of bioactive agents.

The objective of this review on the preparation of nanostructures formed by protein-polysaccharide conjugates is to explore the properties of these molecules by

means of structure control, interface stability and the integration of these nanostructures at atomic, molecular and supramolecular levels. The preparation of nanostructures from the conjugates, the control of the size, morphology and structure of the nanoparticles are still subject to a series of difficulties that have to be overcome to develop new functional products based on protein nanoparticles, therefore, new research is necessary to determine the feasibility of industrial applications of nanostructured conjugates obtained through the Maillard reaction.

5. References

Adjonu, R., Doran, G., Torley, P., & Agboola, S. (2014). Whey protein peptides as components of nanoemulsions: A review of emulsifying and biological functionalities. *Journal of Food Engineering*, *122*, 15–27. https://doi.org/10.1016/J.JFOODENG.2013.08.034

Akhtar, M., & Dickinson, E. (2003). Emulsifying properties of whey protein–dextran conjugates at low pH and different salt concentrations. *Colloids and Surfaces B: Biointerfaces*, *31*(1–4), 125–132. https://doi.org/10.1016/S0927-7765(03)00049-3

Al-Hakkak, J., & Al-Hakkak, F. (2010). *Journal of food engineering. Journal of Food Engineering* (Vol. 100). Elsevier Science Pub. Co. Retrieved from https://www.cabdirect.org/cabdirect/abstract/20103170180

Alahdad, Z., Ramezani, R., Aminlari, M., & Majzoobi, M. (2009). Preparation and Properties of Dextran Sulfate−Lysozyme Conjugate. *Journal of Agricultural and Food Chemistry*, *57*(14), 6449–6454. https://doi.org/10.1021/jf900246b

Álvarez, C., García, V., Rendueles, M., & Díaz, M. (2012). Functional properties of isolated porcine blood proteins modified by Maillard's reaction. *Food Hydrocolloids*, *28*(2), 267–274. https://doi.org/10.1016/J.FOODHYD.2012.01.001

Alves, J. G. L. F., Brenneisen, J., Ninni, L., Meirelles, A. J. A., & Maurer, G. (2008). Aqueous Two-Phase Systems of Poly(ethylene glycol) and Sodium Citrate: Experimental Results and Modeling. *Journal of Chemical & Engineering Data*, *53*(7), 1587–1594. https://doi.org/10.1021/je800137f

Aminlari, M., Ramezani, R., & Jadidi, F. (2005). Effect of Maillard-based conjugation

with dextran on the functional properties of lysozyme and casein. *Journal of the Science of Food and Agriculture*, *85*(15), 2617–2624. https://doi.org/10.1002/jsfa.2320

Araújo, J. M. A. (2011). Proteínas. In *Química de Alimentos.* (5th ed., pp. 380–415). Viçosa: UFV.

Boaglio, A., Bassani, G., Picó, G., & Nerli, B. (2006). Features of the milk whey protein partitioning in polyethyleneglycol-sodium citrate aqueous two-phase systems with the goal of isolating human alpha-1 antitrypsin expressed in bovine milk. *Journal of Chromatography B*, *837*(1–2), 18–23. https://doi.org/10.1016/j.jchromb.2006.03.049

Bromley, E. H., Krebs, M. R. H., & Donald, A. M. (2005). Aggregation across the length-scales in beta-lactoglobulin. *Faraday Discussions*, *128*, 13–27. Retrieved from http://www.ncbi.nlm.nih.gov/pubmed/15658764

Cerqueira, M. A., Pinheiro, A. C., Souza, B. W. S., Lima, A. M. P., Ribeiro, C., Teixeira, J. A., Moreira, R. A., Coimbra, M. A., Gonçalves, M. P., & Vicente, A. A (2009). Extraction, purification and characterization of galactomannans from non-traditional sources. *Carbohydrate Polymers*, *75*(3), 408-414. https://doi.org/10.1016/j.carbpol.2008.07.036

Chamani, J., Moosavi-Movahedi, A. A., & Hakimelahi, G. H. (2005). Structural changes in ??-lactoglobulin by conjugation with three different kinds of carboxymethyl cyclodextrins. *Thermochimica Acta*, *432*(1), 106–111. https://doi.org/10.1016/j.tca.2005.04.014

Chatterton, D. E. W., Smithers, G., Roupas, P., & Brodkorb, A. (2006). Bioactivity of β-lactoglobulin and α-lactalbumin—Technological implications for processing. *International Dairy Journal*, *16*(11), 1229–1240. https://doi.org/10.1016/J.IDAIRYJ.2006.06.001

Chrysina, E. D., Brew, K., & Acharya, K. R. (2000). Crystal structures of apo- and holo-bovine alpha-lactalbumin at 2. 2-A resolution reveal an effect of calcium on inter-lobe interactions. *J.Biol.Chem.*, *275*, 37021–37029. https://doi.org/10.2210/PDB1F6S/PDB

Corrêa, D. H. A., & Ramos, C. H. I. (2009). The use of circular dichroism spectroscopy

to study protein folding , form and function. *African Journal of Biochemistry Research*, *3*(5), 164–173.

Corzo-Martínez, M. C., Sánchez, C. C., Moreno, F. J., Patino, J. M. R., and Villamiel, M. (2012). Interfacial and foaming properties of bovine b-lactoglobulin: Galactose Maillard Conjugates. *Food Hydrocolloids*, *27*, 438–447.

Damodaran, S. (2007). Amino acids, peptides, and proteins. In *Fennema's Food Chem* (4th ed., pp. 247–329). Boca Raton: CRC Press.

de Oliveira, F. C., Coimbra, J. S. dos R., de Oliveira, E. B., Zuñiga, A. D. G., & Rojas, E. E. G. (2016). Food Protein-polysaccharide Conjugates Obtained via the Maillard Reaction: A Review. *Critical Reviews in Food Science and Nutrition*, *56*(7), 1108–1125. https://doi.org/10.1080/10408398.2012.755669

De Wit, J. . (2001). *Lecturer's Handbook on Whey and Whey Products* (1st ed.). Belgium: European Whey Products Association.

Dea, I. C. M., Morris, E. R., Rees, D. A., Welsh, E. J., Barnes, H. A., & Price, J. (1977). Associations of like and unlike polysaccharides: Mechanism and specificity in galactomannans, interacting bacterial polysaccharides, and related systems. *Carbohydrate Research*, *57*, 249–272. https://doi.org/10.1016/S0008-6215(00)81935-7

Ding, R., Valicka, E., Akhtar, M., & Ettelaie, R. (2017). Insignificant impact of the presence of lactose impurity on formation and colloid stabilising properties of whey protein–maltodextrin conjugates prepared via Maillard reactions. *Food Structure*, *12*, 43–53. https://doi.org/10.1016/j.foostr.2017.02.004

Donato, L., Kolodziejcyk, E., & Rouvet, M. (2011). Mixtures of whey protein microgels and soluble aggregates as building blocks to control rheology and structure of acid induced cold-set gels. *Food Hydrocolloids*, *25*(4), 734–742. https://doi.org/10.1016/J.FOODHYD.2010.08.020

Drapala, K. P., Auty, M. A. E., Mulvihill, D. M., & O'Mahony, J. A. (2016). Performance of whey protein hydrolysate–maltodextrin conjugates as emulsifiers in model infant formula emulsions. *International Dairy Journal*, *62*, 76–83. https://doi.org/10.1016/j.idairyj.2016.03.006

Du, Y., Shi, S., Jiang, Y., Xiong, H., Woo, M. W., Zhao, Q., … Sun, W. (2013). Physicochemical properties and emulsion stabilization of rice dreg glutelin conjugated with κ-carrageenan through Maillard reaction. *Journal of the Science of Food and Agriculture*, *93*(1), 125–133. https://doi.org/10.1002/jsfa.5739

Fagani, R. (2016). Novas alternativas para o soro de leite. Retrieved June 17, 2018, from http://www.milkpoint.com.br/industria/radar-tecnico/leite-fluido/novas-alternativas para-o-soro-de-leite-97611n.aspx

Fennema, O. R., Damodaran, S., Parkin, K. L. (2010). *Química de Alimentos de Fennema*. (4, Ed.). Artmed.

Fidelis, P. C. (2011). *Desenvolvimento de um adsorvente contínuo supermacroporoso de troca catiônica para recuperação de lactoferrina de soro de leite*. Universidade Federal de Viçosa.

Giroux, H. J., Houde, J., & Britten, M. (2010). Preparation of nanoparticles from denatured whey protein by pH-cycling treatment. *Food Hydrocolloids*, *24*(4), 341–346. https://doi.org/10.1016/J.FOODHYD.2009.10.013

Graveland-Bikker, J. F., & de Kruif, C. G. (2006). Unique milk protein based nanotubes: Food and nanotechnology meet. *Trends in Food Science & Technology*, *17*(5), 196–203. https://doi.org/10.1016/J.TIFS.2005.12.009

Gupta, S. Sen, & Ghosh, M. (2014). Preparation and characterisation of protein based nanocapsules of bioactive lipids. *Journal of Food Engineering*, *121*, 64–72. https://doi.org/10.1016/J.JFOODENG.2013.08.013

Haque, Z; Kito, M. (1983). Lyophilization of αs1-casein. 2. Conformational and functional effects. *J Agric Food Chem*, *31*(6), 1231–1237.

Harding, S. E. (Stephen E. ., & Chowdhry, B. Z. (2001). *Protein-ligand interactions, structure and spectroscopy : a practical approach*. Oxford University Press. Retrieved from https://books.google.com.br/books/about/Protein_ligand_Interactions_Structure_an.html?id=O0Q7J704Zv4C&redir_esc=y

Hettiarachchy, N. S., Ziegler, G. D. (1994). *Protein Functionality in Food Systems*. (M. Dekker, Ed.).

Honary, S., & Zahir, F. (2013). Effect of Zeta Potential on the Properties of Nano-Drug Delivery Systems - A Review (Part 1). *Tropical Journal of Pharmaceutical Research*, *12*(2), 255–264. https://doi.org/10.4314/tjpr.v12i2.19

Hu, J., Yu, S., & Yao, P. (2007). Stable Amphoteric Nanogels Made of Ovalbumin and Ovotransferrin via Self-Assembly. https://doi.org/10.1021/la063419x

Ionashiro, M. G. (2004). *Fundamentos da termogravimetria, análise térmica diferencial, calorimetria exploratória diferencial*. Araraquara: Giz Editorial.

Jara, F., & Pilosof, A. M. R. (2011). Partitioning of α-lactalbumin and β-lactoglobulin in whey protein concentrate/hydroxypropylmethylcellulose aqueous two-phase systems. *Food Hydrocolloids*, *25*(3), 374–380. https://doi.org/10.1016/J.FOODHYD.2010.07.003

Jiménez-Castaño, L., Villamiel, M., & López-Fandiño, R. (2007). Glycosylation of individual whey proteins by Maillard reaction using dextran of different molecular mass. *Food Hydrocolloids*, *21*(3), 433–443. https://doi.org/10.1016/j.foodhyd.2006.05.006

Jones, O. G., & McClements, D. J. (2011). Recent progress in biopolymer nanoparticle and microparticle formation by heat-treating electrostatic protein–polysaccharide complexes. *Advances in Colloid and Interface Science*, *167*(1–2), 49–62. https://doi.org/10.1016/J.CIS.2010.10.006

Kamau, S. M., Cheison, S. C., Chen, W., Liu, X.-M., & Lu, R.-R. (2010). Alpha-Lactalbumin: Its Production Technologies and Bioactive Peptides. *Comprehensive Reviews in Food Science and Food Safety*, *9*(2), 197–212. https://doi.org/10.1111/j.1541-4337.2009.00100.x

Kasran, M., Cui, S. W., & Goff, H. D. (2013). Emulsifying properties of soy whey protein isolate–fenugreek gum conjugates in oil-in-water emulsion model system. *Food Hydrocolloids*, *30*(2), 691–697. https://doi.org/10.1016/J.FOODHYD.2012.09.002

Kato, A. (2002). Industrial applications of Millard-type protein– polysaccharide conjugados. *Food Science and Technology Research, 8*, 193–199.

Kelly, S. M., & Price, N. C. (2000). The use of circular dichroism in the investigation

of protein structure and function. *Current Protein & Peptide Science*, *1*(4), 349–84. Retrieved from http://www.ncbi.nlm.nih.gov/pubmed/12369905

Kilara, A., Vaghela, M. N. (2000). *Proteins in food Processing* (1st ed.). Cambridge: Woodhead Limited Publishing.

Kinsella, J. E., & Melachouris, N. (1976). Functional properties of proteins in foods: A survey. *C R C Critical Reviews in Food Science and Nutrition*, *7*(3), 219–280. https://doi.org/10.1080/10408397609527208

Ko, S., & Gunasekaran, S. (2006). Preparation of sub-100-nm β-lactoglobulin (BLG) nanoparticles. *Journal of Microencapsulation*, *23*(8), 887–898. https://doi.org/10.1080/02652040601035143

Lakowicz, J. R., & Maliwal, B. P. (1985). Construction and performance of a variable-frequency phase-modulation fluorometer. *Biophysical Chemistry*, *21*(1), 61–78. Retrieved from http://www.ncbi.nlm.nih.gov/pubmed/3971026

Li, J., Shaoyong Yu, Ping Yao, * and, & Jiang, M. (2008). Lysozyme−Dextran Core−Shell Nanogels Prepared via a Green Process. https://doi.org/10.1021/LA702785B

Li, K., Woo, M. W., Patel, H., & Selomulya, C. (2017). Enhancing the stability of protein-polysaccharides emulsions via Maillard reaction for better oil encapsulation in spray-dried powders by pH adjustment. *Food Hydrocolloids*, *69*, 121–131. https://doi.org/10.1016/j.foodhyd.2017.01.031

Li, Y., Zhong, F., Ji, W., Yokoyama, W., Shoemaker, C. F., Zhu, S., & Xia, W. (2013). Functional properties of Maillard reaction products of rice protein hydrolysates with mono-, oligo- and polysaccharides. *Food Hydrocolloids*, *30*(1), 53–60. https://doi.org/10.1016/J.FOODHYD.2012.04.013

Li, Z., Luo, Y., & Feng, L. (2011). Effects of Maillard reaction conditions on the antigenicity of α-lactalbumin and β-lactoglobulin in whey protein conjugated with maltose. *Eur. Food Res. Technol*, *233*, 387-394. https://doi.org/ 10.1007/s00217-011-1532-7

Liu, Q., Kong, B., Han, J., Sun, C., & Li, P. (2014). Structure and antioxidant activity of whey protein isolate conjugated with glucose via the Maillard reaction under

dry-heating conditions. *Food Structure*, *1*(2), 145–154. https://doi.org/10.1016/j.foostr.2013.11.004

Liu, J., Ru, Q., & Ding, Y. (2012). Glycation a promising method for food protein modification: Physicochemical properties and structure, a review. *Food Research International*, *49*(1), 170–183. https://doi.org/10.1016/J.FOODRES.2012.07.034

Liu, Y., Yadav, M. P., Chau, H. K., Qiu, S., Zhang, H., & Yin, L. (2017). Peroxidase-mediated formation of corn fiber gum-bovine serum albumin conjugates: Molecular and structural characterization. *Carbohydrate Polymers*, *166*, 114–122. https://doi.org/10.1016/j.carbpol.2017.02.069

Liu, Y., Zhao, G., Zhao, M., Ren, J., & Yang, B. (2012). Improvement of functional properties of peanut protein isolate by conjugation with dextran through Maillard reaction. *Food Chemistry*, *131*(3), 901–906. https://doi.org/10.1016/J.FOODCHEM.2011.09.074

Liu, Z., Jiao, Y., Wang, Y., Zhou, C., & Zhang, Z. (2008). Polysaccharides-based nanoparticles as drug delivery systems. *Advanced Drug Delivery Reviews*, *60*(15), 1650–1662. https://doi.org/10.1016/J.ADDR.2008.09.001

Loch, J., Polit, A., Gorecki, A., Bonarek, P., & Kurpieswska, K. (2011). Two modes of fatty acid binding to bovine beta-lactoglobulin-crystallographic and spectroscopic studies. *J. Mol. Recongnit, 24,* 341-349. https://doi.org/ 10.2210/PDB3NPO/PDB

Lucca, R. S., Hansen, D., & Oliva, M. L. V. (2006). Estudo Espectroscópicos de inibidores de serinoproteinases isoladas de sementes de Bauhinia bauhinioides: Estimativa de estrutura secundária e estudos de pH. *Varia Scientia*, *5*, 97–112.

Luykx, D. M. A. M., Peters, R. J. B., van Ruth, S. M., & Bouwmeester, H. (2008). A Review of Analytical Methods for the Identification and Characterization of Nano Delivery Systems in Food. *Journal of Agricultural and Food Chemistry*, *56*(18), 8231–8247. https://doi.org/10.1021/jf8013926

Maganha, M. (2006). Guia técnico ambiental da indústria de produtos lácteos. Retrieved November 28, 2017, from http://www.cetesb.sp.gov.br

Malvern Instruments ltd. (2003). Manual, Zetasizer Nano Series Uses. Retrived

August 22, 2018, from https://www.malvern.com/br/products

Martinez-Alvarenga, M. S., Martinez-Rodriguez, E. Y., Garcia-Amezquita, L. E., Olivas, G. I., Zamudio-Flores, P. B., Acosta-Muniz, C. H., & Sepulveda, D. R. (2014). Effect of Maillard reaction conditions on the degree of glycation and functional properties of whey protein isolate – Maltodextrin conjugates. *Food Hydrocolloids*, *38*, 110–118. https://doi.org/10.1016/J.FOODHYD.2013.11.006

McClements, D. J. (2015). Encapsulation, protection, and release of hydrophilic active components: Potential and limitations of colloidal delivery systems. *Advances in Colloid and Interface Science*, *219*, 27–53. https://doi.org/10.1016/J.CIS.2015.02.002

Medrano, A., Abirached, C., Moyna, P., Panizzolo, L., & Añón, M. C. (2012). The effect of glycation on oil–water emulsion properties of β-lactoglobulin. *LWT - Food Science and Technology*, *45*(2), 253–260. https://doi.org/10.1016/j.lwt.2011.06.017

Mills, I., Cvitas, T., Homann, K., Kallay, N., & Kuchitsu, K. (1993). *IUPAC Quantities, Units, and Symbols in Physical Chemistry* (2nd ed.). Oxford: Blackwell Publishing and the Institute of Food Technologists.

Miralles, B., Martínez-Rodríguez, A., Santiago, A., van de Lagemaat, J., & Heras, A. (2007). The occurrence of a Maillard-type protein-polysaccharide reaction between β-lactoglobulin and chitosan. *Food Chemistry*, *100*(3), 1071–1075. https://doi.org/10.1016/j.foodchem.2005.11.009

Morr, C. V.; Foegeding, E. A. (1990). Composition and functionality of commercial whey and milk protein concentrates and isolates: a status report. *Food Technology*, *44*, 100–112.

Mu, L., Zhao, H., Zhao, M., Cui, C., & Liu, L. (2011). Physicochemical Properties of Soy Protein Isolates-Acacia Gum Conjugates. *Czech J. Food Sci*, *29*(2), 129–136. Retrieved from https://www.agriculturejournals.cz/publicFiles/51856.pdf

Niu, L.-Y., Jiang, S.-T., Pan, L.-J., & Zhai, Y.-S. (2011). Characteristics and functional properties of wheat germ protein glycated with saccharides through Maillard reaction. *International Journal of Food Science & Technology*, *46*(10), 2197–2203. https://doi.org/10.1111/j.1365-2621.2011.02737.x

Oliveira, A. S. de, Campos, J. M. de S., Valadares Filho, S. de C., Assis, A. J. de, Teixeira, R. M. A., Valadares, R. F. D., … Oliveira, G. S. de. (2007). Substituição do milho por casca de café ou de soja em dietas para vacas leiteiras: consumo, digestibilidade dos nutrientes, produção e composição do leite. *Revista Brasileira de Zootecnia*, *36*(4 suppl), 1172–1182. https://doi.org/10.1590/S1516-35982007000500026

Oliver, C. M., Melton, L. D., & Stanley, R. A. (2006). Creating Proteins with Novel Functionality via the Maillard Reaction: A Review. *Critical Reviews in Food Science and Nutrition*, *46*(4), 337–350. https://doi.org/10.1080/10408690590957250

Onwulata, C., Huth, J. (2008). *Whey Processing, Functionality and Health Benefits* (1st ed.). EUA: Blackwell Publishing and the Institute of Food Technologists.

Permyakov, E. A., & Berliner, L. J. (2000). alpha-Lactalbumin: structure and function. *FEBS Letters*, *473*(3), 269–74. Retrieved from http://www.ncbi.nlm.nih.gov/pubmed/10818224

Pinheiro Alves, M., De Oliveira Moreira, R., Henrique Rodrigues Júnior, P., Carla de Freitas Martins, M., Tuler Perrone, Í., & Fernandes de Carvalho, A. (2014). SORO DE LEITE: TECNOLOGIAS PARA O PROCESSAMENTO DE COPRODUTOS. *Revista Do Instituto de Laticínios CâNdido Tostes*, *69*(3), 212. https://doi.org/10.14295/2238-6416.v69i3.341

Pirestani, S., Nasirpour, A., Keramat, J., Desobry, S., & Jasniewski, J. (2016). *Effect of glycosylation with gum Arabic by Maillard reaction in a liquid system on the emulsifying properties of canola protein isolate*. *Carbohydrate Polymers*. Elsevier Ltd. https://doi.org/10.1016/j.carbpol.2016.11.044

Poole, C. P., & Owens, F. J. (2003). *Introduction to nanotechnology*. Wiley.

Poppi; F.A., Costa; M.R., de Rensis; C.M.V.B., Sivieri, K. (2010). Soro de Leite e Suas Proteínas: Composição e Atividade FuncionaL. *Unopar Científica*, *14 (2)*, 31–37.

Preetz, C., Hauser, A., Hause, G., Kramer, A., & Mäder, K. (2010). Application of atomic force microscopy and ultrasonic resonator technology on nanoscale: Distinction of nanoemulsions from nanocapsules. *European Journal of*

Pharmaceutical Sciences, *39*(1–3), 141–151. https://doi.org/10.1016/J.EJPS.2009.11.009

Reimer, L., & Kohl, H. (Helmut). (2008). *Transmission electron microscopy : physics of image formation*. Springer.

Sanmartín, E., Arboleya, J. C., Villamiel, M., & Moreno, F. J. (2009). Recent Advances in the Recovery and Improvement of Functional Proteins from Fish Processing By-Products: Use of Protein Glycation as an Alternative Method. *Comprehensive Reviews in Food Science and Food Safety*, *8*(4), 332–344. https://doi.org/10.1111/j.1541-4337.2009.00083.x

Schillen, K., Brown, W., & Johnsen, R. M. (1994). Micellar Sphere-to-Rod Transition in an Aqueous Triblock Copolymer System. A Dynamic Light Scattering Study of Translational and Rotational Diffusion. *Macromolecules*, *27*(17), 4825–4832. https://doi.org/10.1021/ma00095a025

Schmidt, U. S., Pietsch, V. L., Rentschler, C., Kurz, T., Endreß, H. U., & Schuchmann, H. P. (2016). Influence of the degree of esterification on the emulsifying performance of conjugates formed between whey protein isolate and citrus pectin. *Food Hydrocolloids*, *56*, 1–8. https://doi.org/10.1016/j.foodhyd.2015.11.015

Sgarbieri, V. C. (2005). Structural and Physicochemical Properties of Milk Proteins. *Brazilian Journal of Food Technologies*, *8*, 43–56.

Silván, J. M., Assar, S. H., Srey, C., Dolores del Castillo, M., & Ames, J. M. (2011). Control of the Maillard reaction by ferulic acid. *Food Chemistry*, *128*(1), 208–213. https://doi.org/10.1016/j.foodchem.2011.03.047

Simunkova, H., Pessenda-Garcia, P., Wosik, J., Angerer, P., Kronberger, H., & Nauer, G. E. (2009). The fundamentals of nano- and submicro-scaled ceramic particles incorporation into electrodeposited nickel layers: Zeta potential measurements. *Surface and Coatings Technology*, *203*(13), 1806–1814. https://doi.org/10.1016/J.SURFCOAT.2008.12.031

Sittikijyothin, W., Torres, D., & Gonçalves, M. P. (2005). Modelling the rheological behaviour of galactomannan aqueous solutions. *Carbohydrate Polymers*, *59*(3), 339–350. https://doi.org/10.1016/J.CARBPOL.2004.10.005

Skoog, D. A., Holler, F. J., & Crouch, S. R. (2007). *Principles of instrumental analysis*.

Spencer, W. J., Binette, A., Ward, T. L., Davis, L. D. R., Blais, D. R., Harrold, J., … Altosaar, I. (2010). Alpha-Lactalbumin in Human Milk Alters the Proteolytic Degradation of Soluble CD14 by Forming a Complex. *Pediatric Research*, *68*(6), 490–493. https://doi.org/10.1203/PDR.0b013e3181f70f21

Spotti, M. J., Perduca, M. J., Piagentini, A., Santiago, L. G., Rubiolo, A. C., & Carrara, C. R. (2013). Gel mechanical properties of milk whey protein–dextran conjugates obtained by Maillard reaction. *Food Hydrocolloids*, *31*(1), 26–32. https://doi.org/10.1016/J.FOODHYD.2012.08.009

Sun, W.-W., Yu, S.-J., Yang, X.-Q., Wang, J.-M., Zhang, J.-B., Zhang, Y., & Zheng, E.-L. (2011). Study on the rheological properties of heat-induced whey protein isolate–dextran conjugate gel. *Food Research International*, *44*(10), 3259–3263. https://doi.org/10.1016/J.FOODRES.2011.09.019

Sundar, S., Kundu, J., & Kundu, S. C. (2010). Biopolymeric nanoparticles. *Science and Technology of Advanced Materials*, *11*(1), 014104. https://doi.org/10.1088/1468-6996/11/1/014104

Usui, M., Tamura, H., Nakamura, K., Ogawa, T., Muroshita, M., Azakami, H., … Kato, A. (2004). Enhanced bactericidal action and masking of allergen structure of soy protein by attachment of chitosan through Maillard-type protein-polysaccharide conjugation. *Nahrung/Food*, *48*(1), 69–72. https://doi.org/10.1002/food.200300423

Venturini, C. G., Jäger, E., Oliveira, C. P., Bernardi, A., Battastini, A. M. O., Guterres, S. S., & Pohlmann, A. R. (2011). Formulation of lipid core nanocapsules. *Colloids and Surfaces A: Physicochemical and Engineering Aspects*, *375*(1–3), 200–208. https://doi.org/10.1016/J.COLSURFA.2010.12.011

Wang, W., & Zhong, Q. (2014a). Improved thermal stability of whey protein-maltodextrin conjugates at pH 5.0 by d-Glucose, sucrose, d-cellobiose, and lactose. *Food Hydrocolloids*, *41*, 257–264. https://doi.org/10.1016/j.foodhyd.2014.04.025

Wang, W., & Zhong, Q. (2014b). Properties of whey protein-maltodextrin conjugates as impacted by powder acidity during the Maillard reaction. *Food Hydrocolloids*,

38, 85–94. https://doi.org/10.1016/j.foodhyd.2013.11.018

Weiss, J., Takhistov, P., & McClements, D. J. (2006). Functional Materials in Food Nanotechnology. *Journal of Food Science*, *71*(9), R107–R116. https://doi.org/10.1111/j.1750-3841.2006.00195.x

Wijaya, W., Van der Meeren, P., & Patel, A. R. (2017). Cold-set gelation of whey protein isolate and low-methoxyl pectin at low pH. *Food Hydrocolloids*, *65*, 35–45. https://doi.org/10.1016/J.FOODHYD.2016.10.037

Wong, D. W. S., Camirand, W. M., Pavlath, A. E., Parris, N., & Friedman, M. (1996). Structures and functionalities of milk proteins∗ . *Critical Reviews in Food Science and Nutrition*, *36*(8), 807–844. https://doi.org/10.1080/10408399609527751

Wu, Y., Li, W., Cui, W., Eskin, N. A. M., & Goff, H. D. (2012). A molecular modeling approach to understand conformation–functionality relationships of galactomannans with different mannose/galactose ratios. *Food Hydrocolloids*, *26*(2), 359–364. https://doi.org/10.1016/J.FOODHYD.2011.02.029

Zhu, D., Damodaran, S., & Lucey, J. A. (2008). Formation of Whey Protein Isolate (WPI)−Dextran Conjugates in Aqueous Solutions. *Journal of Agricultural and Food Chemistry*, *56*(16), 7113–7118. https://doi.org/10.1021/jf800909w

Zhuo, X.-Y., Qi, J.-R., Yin, S.-W., Yang, X.-Q., Zhu, J.-H., & Huang, L.-X. (2013). Formation of soy protein isolate-dextran conjugates by moderate Maillard reaction in macromolecular crowding conditions. *Journal of the Science of Food and Agriculture*, *93*(2), 316–323. https://doi.org/10.1002/jsfa.5760

ARTICLE 1

Nanostructured systems formed from conjugates of α-lactalbumin and tara gum

ABSTRACT

Nanostructures from conjugates of α-lactalbumin and tara gum were obtained via heat-gelation process with pH adjustment. The conjugates were produced by Maillard reaction using the dry-heating method and they were characterized by browning index (*BI*) and percentage of free amino groups (*% FAG*). Nanostructured systems were characterized by (*i*) dynamic light scattering, zeta potential, circular dichroism, and intrinsic fluorescence to evaluate the structures, (*ii*) differential scanning calorimetry to investigate the thermal behavior, (*iii*) transmission electron microscopy and atomic force microscopy to evaluate the morphology, and (*iv*) foaming ability and emulsifying stability to determine if the systems exhibit technological functionalities. The most appropriate time of conjugation was 2 days. The spray-dried and lyophilized mixtures presented different values of *BI* and *% FAG* ($p < 0.05$). Nanostructures with average sizes lower than 300 nm were formed under different process conditions. Analyses of circular dichroism and intrinsic fluorescence showed conformational changes in the nanostructures, mainly a decrease in the α-helix content. The thermal stability of the α-lactalbumin was improved by the effect of glycosylation showing a temperature denaturation of 63.6 °C (pure protein) and 67.5 °C (nanostructures). Treatment at 50 °C, pH 9.2, and 15 min showed foaming and emulsifying stabilities compared to the control. The characteristics presented by the studied systems pointed out their feasibility to be used in the food industry.

Keywords: Maillard reaction, glycosylation, conjugates, emulsifying stability, foaming ability.

1. Introduction

Whey proteins are a class of compound used in the nanotechnology and food industries due to their techno-functional properties (solubility, foaming ability, emulsification, film formation, and gelification), high nutritional values, superior bioavailability, and for being recognized as a safe nutritional ingredient (Adjonu, Doran, Torley, & Agboola, 2014; Yi, Fan, Yokoyama, Zhang, & Zhao, 2016). These proteins can form aggregate whose particle sizes are easily monitored. Moreover, they have the ability to combine polysaccharides and bioactive compounds among other materials (Ramos et al., 2014; Yi, Fan, Yokoyama, Zhang, & Zhao, 2016).

However, usual industrial process conditions such as high temperatures, prolonged heating times, salt concentration (ionic strength), organic solvents and proteolytic agents affect the stability of whey proteins, resulting in flocculation and aggregation process. In addition, the net electrical charge of the whey protein surface is reduced when the pH is close to their isoelectric point (IP), which leads to aggregation and instability of proteins and, consequently, reduces their application in food matrices (Yi, Fan, Zhang, et al., 2016b; Saraiva et al., 2017).

Conjugation of whey protein with polysaccharides through the Maillard reaction can enhance the protein stability at certain environmental conditions and intensify their techno-functional properties (Sanmartín, Arboleya, Villamiel & Moreno, 2009; Álvarez, García, Rendueles, & Díaz, 2012; Corzo-Martínez, Sánchez, Moreno, Patino, & Villamiel, 2012; Spotti et al., 2013). Systems of whey protein with maltodextrins proved to be resistant to aggregation after grafting (Wang & Zhong, 2014a) and conjugates of isolated whey protein with red seaweed revealed better foaming stability (Chiu, Chen, & Chang, 2009).

In the Maillard reaction, the protein and the polysaccharide are linked by a covalent bond between the ε-amino group of the lysine residues, and the carbonyl group of the polysaccharides (Kato, 2002; J. Liu, Ru, & Ding, 2012; Markman & Livney, 2012). This process occurs under controlled conditions of time, temperature, and relative humidity, without the use of chemical agents.

The second most abundant whey protein is the α-1actalbumin, a globular and monomeric protein composed by 123 amino acids, with 4 disulfide bonds, molar mass of about 14 kDa and isoelectric point equal to 4.4. This protein has 13 potentially

reactive amino groups, including the amino terminal group (Gu, Matsumura, Yamaguchi, & Mori, 2001; Livney, 2010; Delavari et al., 2015).

Among the diverse polysaccharides present on the market, the tara gum (TG) is a food additive that can be used as a thickener and stabilizer to alter the consistency and viscosity of food products (Sittikijyothin, Torres, & Gonçalves, 2005). In addition, tara gumcould be applied in the formation of gels, films and coatings with other polysaccharides and/or proteins (Cerqueira et al., 2009). The literature reports the physical-chemical and structural behavior of the tara gum (Cerqueira et al., 2009; Jiménez-Castaño et al., 2007; Sittikijyothin, Torres, & Gonçalves, 2005), however, research involving conjugation of whey proteins with tara gum are scarce.

In this context, we hypothesize that α-lactalbumin glycosylated with tara gum will improve the protein stability under different process condition. Therefore, the formation and characterization of nanostructured systems produced with α-la-TG conjugates were performed in this research.

2. Material and methods

Powder of α-lactalbumin (α-la; 95 % protein, 90 % of which is α-la) was kindly donated by Davisco Food International, Inc. (Eden Prairie, MN, USA). Tara gum (TG) was purchased from GastronomyLab (Brasilia, Brazil). Both chemicals were used as furnished without further purification. All other chemicals were of analytical grade and also used without further purification. Deionized water (Millipore Co., MA, USA) was used in all the experiments.

2.1. Preparation of α-la-TG conjugates

Individually dispersions of α-la and TG were prepared at 2 $mg \cdot mL^{-1}$ concentration. Mixtures of α-la+TG were formed by adding dispersions of α-la and TG (1:1, w/w) and stirring the mixtures at 25 $\pm$ 0.1 °C for 12 h (Kato, 2002). Two drying methods for mixture dehydration were tested, the lyophilization (L) and the spray dry (SD) methods. In the first one, the mixtures were frozen at -55 ºC for 5 h (Ultra freezer, Terroni, Brazil) and lyophilized (Lyophilizer LS 3000, Terroni, SP, Brazil) by a first drying step at -45 °C and pressure of 400 mTorr during 40 h, followed by a secondary drying step at 20 °C and pressure of 200 mTorr during 8 h. In the second method, the mixtures were spray-dried (Mini-Spray Dryer model B-290, Büchi Laboratoriums-Technik, Flawil, Switzerland) by using inlet temperature (T_{inlet}) of 160 °C, outlet

temperature (T_{outlet}) of 90 °C, air flowrate (F_{air}) of 40 $m^3 \cdot h^{-1}$, and feeding rate (F_r) of 250 $mL \cdot h^{-1}$ (Wang & Zhong, 2014b). Mass of 0.250 g of lyophilized, and/or spray-dried mixture powder was incubated at 60 °C and 79 % of relative humidity in a desiccator (approx. 0.8 L volume). Relative humidity was maintained constant by using saturated KBr (Vetec, RJ, Brazil) solution. Each system required 3 h to reach the equilibrium condition (60 °C and 79 % RH). After this interval, the heating time was immediately recorded, then samples were collected during 9 days (at the days 1, 2, 3, 5, 7, and 9) and they were kept refrigerated (4 ºC) until analysis.

2.2. Conjugate characterization

Browning index (*BI*) and percentage the free primary amino groups (*% FAG*) of systems were evaluated in order to determine the most appropriate incubation time to obtain the conjugates.

2.2.1. Browning index determination

The extent of the Maillard reaction of the α-la-TG conjugate powders (L or SD) was monitored by means of the brown color appearance using a colorimeter (Chroma Meter CR-300 series, Konica Minolta Sensing, Inc., USA). The CIE Lab system defined in rectangular coordinates (L^*, a^*, b^*), with diffuse illumination/0° was applied and then the browning index (*BI*) was calculated according to Equations (1) and (2) (Martinez-Alvarenga et al., 2014).

$$BI = \frac{100(x - 0.31)}{0.172} \quad (1)$$

$$x = \frac{a + 1.75\,(L)}{5.645(L) + a - 3.012(b)} \quad (2)$$

Where *L*, *a*, and *b* are, respectively, the values of lightness, of green–red and of blue–yellow color components obtained in the colorimeter, *BI* is the browning index, and *x* is the value obtained in Equation (2). Mixture (L or SD) of α-la+TG without heat treatment was used as control.

2.2.2. Free amino groups detection

The degree of modification of the primary amino groups was measured indirectly using a colorimetric assay based on the reaction between o-phthalaldehyde (OPA, Sigma-Aldrich, Austria) and the primary amine group (-NH_2) in proteins (OPA technique)

(Vigo, Malec, Gomez, & Llosa, 1992; Sun et al., 2011). A volume of 200 μL of α-la-TG conjugate dispersion (2 mg·mL^{-1}) prepared with L or SD powder was mixed with 800 μL of 0.1 mol·L^{-1}sodium tetraborate buffer solution (Fmaia, São Paulo, Brazil), 100 μL of 20 % (w/v) sodium dodecyl sulfate (SDS) (USB, Cleveland, USA), and 100 μL 2-mercaptoethanol (Vetec, RJ, Brazil). Then, the systems were subjected to heating in a thermostatic bath (Tecnal, Sao Paulo, Brazil) at 90 °C for 5 min. OPA reagent was prepared immediately before use: 80 mg of OPA was dissolved in 2 mL of pure ethanol (Sigma-Aldrich, St. Louis, USA) and added 50 mL of 0.1 mol·L^{-1} sodium tetraborate buffer solution (pH 9.85), 0.2 mL of 2-mercaptoethanol (Vetec, RJ , Brazil), and 5 mL of 20 % (w/v) SDS. The reagent was made up to 100 mL with deionized water. Conjugate dispersion (100 μL) was mixed with 2 mL of OPA reagent and the resulted mixture was stirred in vortex (Phoenix, São Paulo, Brazil). Absorbance of systems was measured at 340 nm (Spectrophotometer Care 50 Probe, Varian, Japan). The decrease in free amino groups (*FAG*) of conjugates was calculated using pure α-la dispersion, without incubation stage, as control and reference (100 %), by means of Equation (3):

$$FAG\ (\%) = \frac{A_C}{A_{\alpha-\mathrm{la}}} * 100 \qquad (3)$$

Where A_C is the conjugate absorbance and $A_{\alpha-\mathrm{la}}$ is the α-la control absorbance.

2.3. Production of nanostructured α-la-TG conjugates

The heat-gelation process with pH adjustment was used to produce nanostructures from α-la-TG conjugates (Li, Yu, Yao, & Jiang, 2008). Dispersions of 2 mg·mL^{-1} from α-la-TG conjugates (L or SD) were prepared, pH value was adjusted using HCl (Vetec, RJ, Brazil) (0.1 mol·L^{-1}) or NaOH (Vetec, St. Louis, USA) (0.1 mol·L^{-1}). The systems were subjected to heating in a thermostatic bath (TE-184, Tecnal, Brazil). The dispersions containing the formed nanostructures were immediately cooled in an ice bath and kept at 4 °C until their characterization. Different values of pH, temperatures and heating times (Table 1) were evaluated following a central composite design (CCD) in order to evaluate the combined effect of these variables on the particle size of α-la-TG nanostructures, with 2^3 factorial and star design with three central points as shown in Table 2. The values of pH and temperature were defined according to the

isoelectric point (pI 4.4) and the denaturation temperature (63 °C) of pure α-la in aqueous solution, respectively as suggested by Teófilo & Ferreira (2006).

Table 1. Uncoded and coded levels of independent variables used in the CCD

Independent variable	Coded and uncoded levels				
	-α	-1	0	1	+α
Temperature (°C)	39.8	50	65	80	90.2
pH	2.1	3.9	6.5	9.2	11
Time (min)	4.8	15	30	45	55.2

2.4. Characterization of the nanostructures

2.4.1. Dynamic light scattering (DLS) analysis

DLS measurements of 2 mg·mL^{-1} α-la-TG (L or SD) nanostructured dispersions were used in order to determine the mean hydrodynamic diameter of their particles (Z-average). Experimental runs in triplicate were conducted at (25.0 $\pm$ 0.1) °C in polystyrene cuvettes by using a particle size instrument (Zetasizer Nano ZS, Malvern Instruments Ldt, United Kingdom) equipped with an avalanche photodiode detector, a digital correlator (TurboCor), and a helium–neon (HeNe) laser (4 mW and 632.8 nm) as source of linearly polarized light. The scattered intensity was measured under a 173° detection angle with respect to the source. The autocorrelation function was analyzed by the CONTIN algorithm to determine the size distribution (in nanometers). Dispersions of pure α-la and of α-la+TG mixture (without heat treatment) were used as control.

2.4.2. ζ-potential analysis

ζ-potential measurements of 2 mg·mL^{-1} α-la-TG nanostructured suspensions were performed in triplicate using the technique of laser doppler micro electrophoresis to determinate the net surface electrical charge of the nanostructures. The experimental runs were conducted at (25.0 ± 0.1) °C in disposable folded capillary cuvettes by using an apparatus (Zetasizer Nano ZS, Malvern Instruments Ldt, United Kingdom) equipped with a HeNe laser (4 mW). Dispersions of pure α-la and of α-la+TG mixture (without heat treatment) were used as control.

Table 2. Central composite design with decoded values of three variables (temperature, pH, time) with three central points (treatments 15, 16, and 17).

Treatment	Temperature (°C)	pH	Time (min)
1	50.0	3.9	15.0
2	50.0	3.9	45.0
3	50.0	9.2	15.0
4	50.0	9.2	45.0
5	80.0	3.9	15.0
6	80.0	3.9	45.0
7	80.0	9.2	15.0
8	80.0	9.2	45.0
9	39.8	6.5	30.0
10	90.2	6.5	30.0
11	65.0	2.1	30.0
12	65.0	11.0	30.0
13	65.0	6.5	4.8
14	65.0	6.5	55.2
15	65.0	6.5	30.0
16	65.0	6.5	30.0
17	65.0	6.5	30.0

2.4.3. Molecular fluorescence spectroscopy analysis

Fluorimetry measurements of 2 $mg \cdot mL^{-1}$ α-la-TG nanostructured suspensions were obtained in order to determinate conformational changes in the structures. The experimental runs were conducted at (25.0 ± 0.1) °C by using a spectrofluorometer (ISS, K2, USA), at wavelength ranging from 290 to 450 nm, quartz cuvettes of 10 mm path length (Hellma Analytics, Germany), and with tryptophan (Trp) and tyrosine (Tyr) excitation source of 285 nm (Taheri-Kafrani et al., 2011). Spectra were baseline-corrected by subtracting blank spectra (Milli-q water). Dispersions of pure α-la and α-la+TG mixture (without heat treatment) were used as control.

2.4.4. Circular dichroism (CD) spectroscopy

CD measurements of 2 $mg \cdot mL^{-1}$ α-la-TG nanostructured dispersions were determined in order to assess modifications in the secondary structure of the particles. The experimental runs were conducted at (25.0 $\pm$ 0.1) °C by using a spectropolarimeter (Jasco Corporation, J-810, Japan), equipped with a temperature controller (Jasco Corporation, Peltier PFD 425S, Japan) coupled to a thermostatic bath (Julabo, AWC 100, Germany), in quartz cuvettes of 10 mm path length (Hellma Analytics, Germany),

at wavelength ranging from 190 to 260 nm, under constant nitrogen rate. Each spectrum was obtained by averaging ten consecutive measurements and was baseline-corrected by subtracting blank spectra (Milli-q water). Dispersions of pure α-la (without heat treatment) were used as control. CD data were normalized to mean residual molar ellipticity, applying Equation (4):

$$[\theta] = \frac{\theta \cdot 100 \cdot MM}{aa \cdot c \cdot l} \quad (4)$$

Where θ is the CD signal (degree), *MM* is the protein molar mass (kDa), *aa* is the number of amino acid residues, *c* is the protein concentration ($mg \cdot mL^{-1}$), and *l* is the optical path of the cuvette (cm). Deconvolution of the residual molar ellipticity data of the systems was performed by means of the CONTIN/LL - Reference 4 analysis method, according to Sreerama & Woody (2000).

2.4.5. Stability of α-la-TG nanostructures during storage

Nanostructured systems presenting mean hydrodynamic diameters varying between 10 and 300 nm (Uskoković, 2007) were selected to carry out stability analysis of particle size over 45 days, at 4 °C. Nanostructure sizes were measured at 1, 3, 10, 22, 30, and 45 days of storage.

2.5. Techno-functional properties of α-la-TG nanostructures

Foaming ability and emulsifying stability were evaluated for systems, which present the most stable distribution of particle size during storage.

2.5.1. Foaming ability

In order to evaluate the foaming ability of the systems, aliquots (15 mL) of nanostructured suspensions ($2\ mg \cdot mL^{-1}$) were added in a beaker (50 mL) and then homogenized (Ultra turrax, IKA, DI 25 Basic, Germany) during 72 s, at 13,500 rpm. Dispersions of pure α-la and α-la+TG mixture (without heat treatment) were used as control. The increase of the volume was determined by measuring the total volume and the foam volume, immediately after homogenization, according to Equation (5):

$$VI\ (\%) = \frac{B - A}{A} * 100 \quad (5)$$

Where *VI* is the volume increase (%), *A* is the initial volume of samples before agitation (mL), and *B* is the final volume of samples after agitation (mL).

Foam stability (*FS*) was measured immediately after stirring. The change in foam volume was calculated after agitation and at 5 min intervals up to 120 min. Equation (6) was used to determinate the foam stability (%):

$$FS\ (\%) = \frac{V_{ft}}{V_{f0}} * 100 \quad (6)$$

Where V_{f0} is the foam volume (mL) of samples at time 0 and V_{ft} is the foam volume (mL) of samples after time *t*. Experiments were done in triplicate.

2.5.2. Emulsifying stability

To evaluate the emulsifying stability of α-la-TG nanostructures, the emulsion stability index (*ESI*) was calculated according to McClements (2005). Oil-in-water emulsion (15 % w/w) was prepared adding 0.91 g of soy oil and 5.17 g of α-la-TG nanostructure dispersions (2 mg·mL^{-1}). The mixture was kept in agitation (Ultra Turrax, IKA, DI 25 Basic, Germany) at 13,500 rpm for 1 min, at 25 °C; after that, it was immediately homogenized (Ultrason Unique homogenizer, DES500, Brazil) at amplitude of 40 % and a power of 300 W for 1 min in ice-water bath. The oil droplet size (Z-average) of the emulsions was measured (Malvern Instruments Inc., Zetasizer Nano ZS, UK) at 0, 30 and 60 min after the formation of emulsions. Equation (7) was used to calculate *ESI*:

$$ESI = \frac{d(0)}{d(t) - d(0)} \quad (7)$$

Where $d(0)$ is the initial mean droplet diameter (nm) and $d(t)$ is the mean droplet diameter (nm) of the emulsion measured at time *t* (30 and 60 min). Pure α-la and α-la +TG mixture without heat treatment were used as control. Experiments were done in triplicate.

2.6. Thermal stability of α-la-TG nanostructures

The thermal behavior of α-la-TG nanostructures was determined by differential scanning calorimetry (DSC) measurements by using an apparatus (MicroCal VP-DSC, England) equipped with a thermal analysis system software (VP Viewer 2000-Origin 7). Aliquots of 500 μL of α-la-TG nanostructure suspension (2 mg·mL^{-1}) were degassed at 20 °C for 10 min before injection into the sample cell. A ramping of 1.5 °C·min^{-1} was used to increment the temperature from 20 to 97 °C. The denaturation

temperature (T_d) and the change in denaturation enthalpy (ΔH_d) were determined using a non-2-state model (MicroCal, England). DSC thermograms were baseline-corrected by subtracting blank thermogram (Milli-q water). Suspensions of pure α-la and of α-la+TG mixture (without heat treatment) were used as control.

2.7. Morphological characterization of α-la-TG nanostructures

2.7.1. Atomic force microscopy (AFM) analysis

Systems used in the AFM analysis were prepared by drying α-la-TG nanostructure dispersions on a freshly cleaved mica surface inside a desiccator containing dried silica gel, at room temperature for 24 h. Nanostructure images formed in a scan area of 10 x 10 μm for each sample were acquired in tapping mode (atomic force microscopy Universal SPM SystemNtegra Prima/NT-MDT).

2.7.2. Transmission electronic microscopy (TEM) analysis

Systems used in the TEM analysis were prepared by drying α-la-TG nanostructure dispersions at room temperature for 24 h. A drop of the dispersion was deposited onto 200 mesh copper grids coated with thin films of Formvare carbon (Koch Electron Microscopy, Brazil). The samples were then negatively stained with uranyl acetate (2 % w/w) (Merck, Germany) for 15 s. Images of α-la-TG nanostructures was obtaining on the equipment (transmission electron microscopy Zeiss, 43 model 109, Oberkochen, Germany) with accelerating voltage of 80 kV.

2.8. Data analysis

In aiming to select the most appropriate incubation time to form nanostructured α-la-TG conjugates, significant differences among means of both variables the browning index and the percentage of free amino groups were evaluated by means of the Tukey HSD test with $p < 0.05$ using the *Statistica* 10® software. Data were expressed as mean ± standard deviation. Normal probability plots were constructed by using *Statistica* 10® software. Through the DLS analysis, the most appropriate conditions for obtaining the nanostructures were determined. Data of techno-functional properties and stability during storage were evaluated using the analysis of variance (ANOVA) and the Tukey and Dunnett tests ($p < 0.05$) with the *Statistica* 10® software, respectively.

3. Results and discussion

3.1. Characterization of lyophilized (L) and spray-dried α-la-TG conjugates

3.1.1. Browning index and percentage of free amine groups

Appearance of brown color and reduction on the percentage of free amine groups of proteins are clear indicators of the development of the Maillard reaction (de Oliveira, Coimbra, de Oliveira, Zuñiga, & Rojas, 2014; Wooster & Augustin, 2007). Color development and the percentage of free amino groups (*% FAG*) were measured by using the Browning Index (*BI*) and OPA method, respectively.

The results of *BI* and *% FAG* observed for the conjugates composed of α-la-TG (L) and α-la-TG (SD) are shown in Fig. 1.

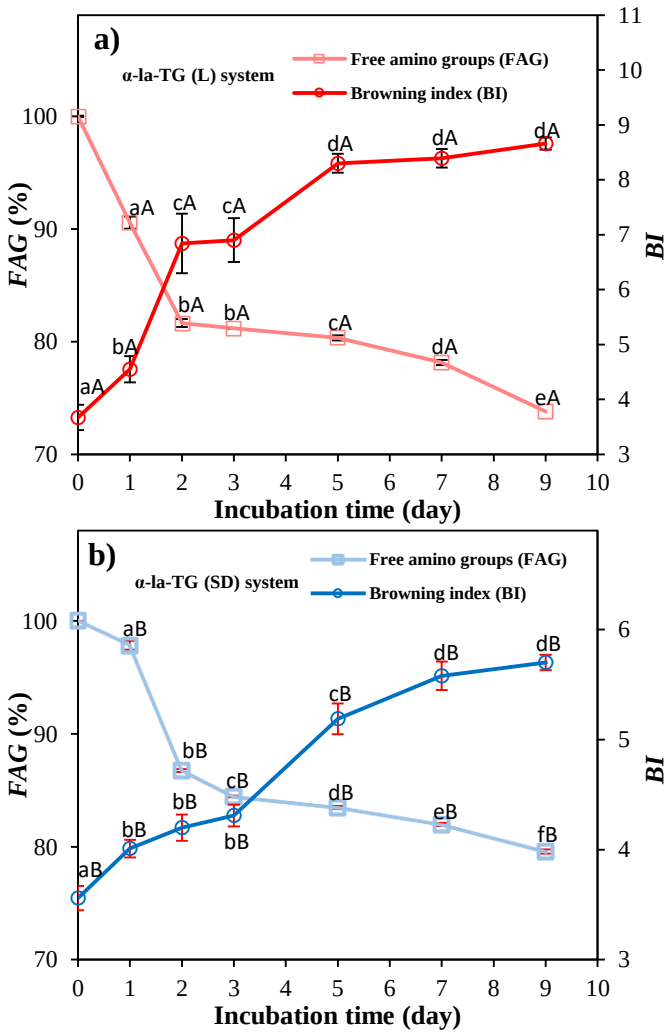

Fig. 1. Browning Index (*BI*) and percentage of free amine groups (% *FAG*) for (a) α-la-TG (L) and (b) α-la-TG (SD) systems. Values with the same lower-case letter in each line are not different by Tukey test ($p > 0.05$). Values with the same upper-case letter for e each day and the same response are not different by Tukey test ($p > 0.05$). The measurements were done in triplicate

The increment of *BI* with the increase of incubation time was statistically different (p <0.05) for all systems studied when the control is taken as reference. The major brown color was noticed at 9 days of dry-heating according to Fig. 1 and Fig 2.

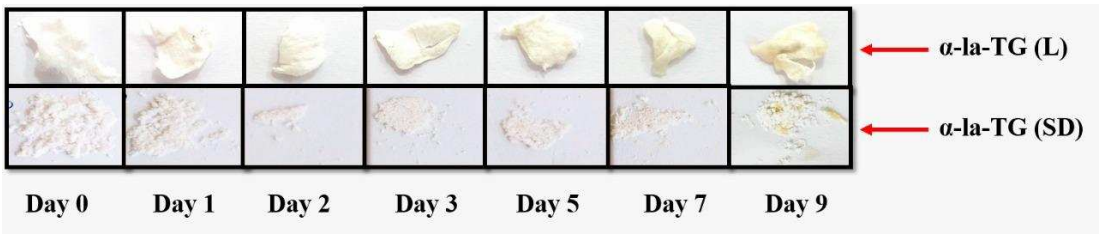

Fig. 2. Images of α-la-TG (L) and α-la-TG (SD) systems in different days of dry-heating.

These color differences between heating times may give evidence of some transitions of stages of Maillard reaction from the initial stage to the advanced or final stage, in which the production of brown-colored compounds known as melanoidins takes place (de Oliveira et al., 2014). Martinez-Alvarenga et al. (2014) studying whey protein isolate (WPI)-maltodextrin conjugates, reported values of *BI* varying from 5.14 (control) to 30.87 (3 days of heating). Similar tendency was observed in our study.

Progress of the Maillard reaction can also be studied by evaluating the percentage of free amino groups (*% FAG*) since the color changes may be associated with caramelization reaction and/or Maillard reaction (Randhir, Kwon, & Shetty, 2008).

Fig. 1 also revealed the decrease of *% FAG* with the increment of heating time. The lowest value of % *FAG* was observed for the highest heating time (9 days). These results were expected because the progress of Maillard reactions increases with the increment of the reaction time (Spotti et al., 2013). Wooster & Augustin (2007) studying WPI-Dextran conjugates reported a similar behavior tendency for *% FAG*.

The increment of *BI* and the decrease of *% FAG* is an indicative of the occurrence of conjugation between α-la and tara gum. With these results, the appropriate time of conjugation for the α-la-GT (L) and α-la-GT (SD) systems was 2 days because in larger reaction times with higher *BI* values and lower *% FAG* values (Fig. 1), the glycosylation reaction may occur simultaneously with the formation of final products of the Maillard reaction, which may cause damages to human health.

The effect of the use of the unit operations lyophilization (L) and spray dry (SD) on the conjugation reaction was also evaluated. Values of *BI* and *% FAG* for α-la-TG (SD) system were statistically different ($p < 0.05$) as compared with the values for α-la-TG (L) system, indicating that the progress of the Maillard reaction was lower in spray-dried mixtures. Probably, the high air temperatures (160 to 210 °C) used in the spray dry operation can promote the partial unfolding of α-la, resulting in irreversible aggregation of this protein (Toro-Sierra, Schumann, & Kulozik, 2013). A partial protein denaturation phenomenon can occur at the air-water interface causing the exposition of the hydrophobic groups of partially unfolded proteins to the air. Consequently, the intermolecular interactions among the exposed hydrophobic groups promote self-association, resulting in protein aggregates (Donaldson, Boonstra, & Hammond, 1980; Fink, 1998; Lu, Tang, Xiong, Qing, & Sun, 2016). These agglomerates are found in a dry environment in which hydrophilic groups, such as lysine, are confined inside the interior of the molecule. Therefore, the number of exposed amine groups of lysine are reduced. This behavior and a reduction in the interfacial area of the system decrease the probability of occurrence of covalent bonds with the polysaccharide, resulting in a reduction in the Maillard reaction progress (de Oliveira et al., 2014). On the other hand, in the lyophilization operation, α-la maintains proportions of the protein native state, which is characterized by higher lysine number in the surface (see supplementary material, item 1), increasing the number of possible covalent bonds between protein and polysaccharide.

3.2. Production of nanostructures from α-la-TG conjugates

Conjugates of α-la-TG obtained under controlled conditions (60 ° C, 79 % RH and heating time of 2 days) showed an appropriate relationship between *BI* and *% FAG*. Nanostructures from this conjugates were produced by heat-gelation process, evaluating the effect of temperature, pH and heating time (Table 2).

3.3. Characterization of nanostructures from α-la-TG conjugates

3.3.1. Dynamic light scattering analysis (DLS)

Data of size of α-la-TG nanostructured systems and controls (Dispersions of pure α-la and of α-la+TG mixture without heat treatment and pH adjustment) are shown in Table 3. The main populations defined here refer to those with the highest percentage in size distribution by volume.

Table 3. Dynamic light scattering of (L) and (SD) α-la-TG nanostructures, α-la+TG mixture and native α-la protein at different process conditions.

Treatment	System		α-la-TG (L)			α-la-TG (SD)		
			D_h	VD (%)	PDI	D_h	VD (%)	PDI
1	50 °C, pH 3.9, 15'	Peak 1	1486	96.5		977.3	94.6	
		Peak 2	159.9	1.7	0.561	94.90	4.1	0.720
		Peak 3	5057	1.8		5590	1.3	
2	50 °C, pH 3.9, 45'	Peak 1	149.6	1.8		1054	76.7	
		Peak 2	1556	98.2	0.570	106.7	3.0	0.550
		Peak 3	-	-		29.2	20.3	
3	50 °C, pH 9.2, 15'	Peak 1	108.6	0.5	0.400	44.3	38.3	0.582
		Peak 2	6539	99.5		234.3	61.7	
4	50 °C, pH 9.2, 45'	Peak 1	736.8	62.1		528.4	24.5	
		Peak 2	72.3	25.2	0.800	290.1	73.3	0.516
		Peak 3	5358	12.7		4894	2.2	
5	80 °C, pH 3.9, 15'	Peak 1	1207	87.5		1121	95.3	
		Peak 2	4644	9.6	0.566	76.2	4.7	0.532
		Peak 3	128.6	2.9		-	-	
6	80 °C, pH 3.9, 45'	Peak 1	2068	94,7	0.659	1530	88.1	0.527
		Peak 2	413.9	5.3		5099	2.6	
7	80 °C, pH 9.2, 15'	Peak 1	4072	44.6		3675.6	44.7	
		Peak 2	866.3	38.1	1.000	768.6	55.3	0.611
		Peak 3	79.56	17.3		-	-	
8	80 °C, pH 9.2, 45'	Peak 1	289.5	50.5		721.0	75.0	
		Peak 2	64.40	38.8	0.657	94.2	15.7	0.982
		Peak 3	4343	10.7		5424	9.2	
9	39.8 °C, pH 6.5, 30'	Peak 1	1028	3.2		34.3	34.2	
		Peak 2	124.6	89.8	0.345	161.5	6.9	0.345
		Peak 3	4998	7		210.6	58.9	
10	90.2 °C, pH 6.5, 30'	Peak 1	820.6	8.1		65.3	11.0	
		Peak 2	75.10	3.1	0.868	970.5	63.5	0.902
		Peak 3	4912	88.8		4243	25.4	
11	65 °C, pH 2.1, 30'	Peak 1	32.75	36.5		1059	80.4	
		Peak 2	171.4	2.4	0.810	85.8	10.5	1.000
		Peak 3	1792	61.1		4062	9.0	
12	65 °C, pH 11, 30'	Peak 1	46.3	28.3	0.410	11453	92.9	0.632
		Peak 2	167.7	71.7		111.6	7.1	
13	65 °C, pH 6.5, 4.8'	Peak 1	2423	63.2		865.3	85.7	
		Peak 2	217	4.3	0.932	60.8	11.4	0.481
		Peak 3	22.4	32.5		4930	2.9	
14	65 °C, pH 6.5, 55.2'	Peak 1	46.9	42.2		1200	4.8	
		Peak 2	992.2	31.9	0.745	121.4	67.6	0.576
		Peak 3	3945	25.9		34.14	27.5	
15	65 °C, pH 6.5, 30' (CP)	Peak 1	940.8	40.2		1042	74.4	
		Peak 2	3445	45.5	0.675	104.2	17.1	0.623
		Peak 3	90.5	14.3		4551	8.5	
16	Pure α-la	Peak 1	9.3	79.1		-	-	-
		Peak 2	14.6	17.2	0.432	-	-	-
		Peak 3	56.7	3.7		-	-	-
17	α-la+TG mixture	Peak 1	1124	27.7		-	-	-
		Peak 2	4088	50.3	0.961	-	-	-
		Peak 3	80.8	22.0		-	-	-

D_h: hydrodynamic diameter; VD: volume distribution; PDI: polydispersity index

Table 3 revels for α-la-GT (L) nanostructures that the thermal treatments at 80 °C and 65 °C in systems with, respectively, pH 9.2 and 11, at heating time of 45 and 30 min presented particle size of main population equal to 289.5 and 167.7 nm. This indicates that: (*i*) at more alkaline pH value, the α-la protein acquired negative charges, which makes the electrostatic repulsion between the particles increase (Saraiva et al., 2017), and (*ii*) the presence of reactive amine groups in α-la molecule allow the covalent linkages of a multiple number of tara gum molecules to the protein, resulting in the increase of the average particle size of the glycosylated α-la (Sheng et al., 2017) when compared to the pure α-la mean diameter (9.3 nm). Yang, Chun, Kim, Choi, & Lee (2017) observed lysozyme-galactomannan nanostructures with mean size of 263 nm.

For α-la-GT (L) nanostructures at pH 3.9, a pH condition close to isoelectric point of the α-la protein (4.4 pI), at heating temperatures of 50 °C and 80 °C, and at heating times of 15 and 45 min, values of main population size were superior than 1000 nm. Thus, at pH 3.9, the net surface charge of the protein could be close to zero, inducing the formation of aggregates with increase in the mean diameter of the particles (Wong, Day, & Augustin, 2011).

For α-la-TG (SD) systems, at heat treatments of 50 °C, pH 9.2, and heating times of 15 and 45 min, the particle sizes of main populations were of 234.4 and 290 nm, respectively. These size values are close to those verified in α-la-TG (L) system, probably due to the influence of pH. At condition of acid pH (pH: 2.1 to 3.9), all treatments showed size mean values for the major populations greater than 1000 nm, which pointed out to the non-formation of nanostructures. Treatments using high temperature (80 to 90.2 °C) and high heating time (45 min) showed values in micrometric range.

These results suggest that in general, high temperature and longer heating time favored the formation of larger aggregates, corroborating to the reports of Ryan, Zhong, & Foegeding (2013) and Diniz et al. (2014).

The influence of different values of pH, temperature and heating time on the average size of the nanostructures was evaluated following the central rotational composite design. The regression analysis revealed that linear and quadratic coefficients and the interaction effects of the three factors evaluated were not significant (p >0.05).

According to the coefficient of determination, there was no model adjustment (see supplementary material).

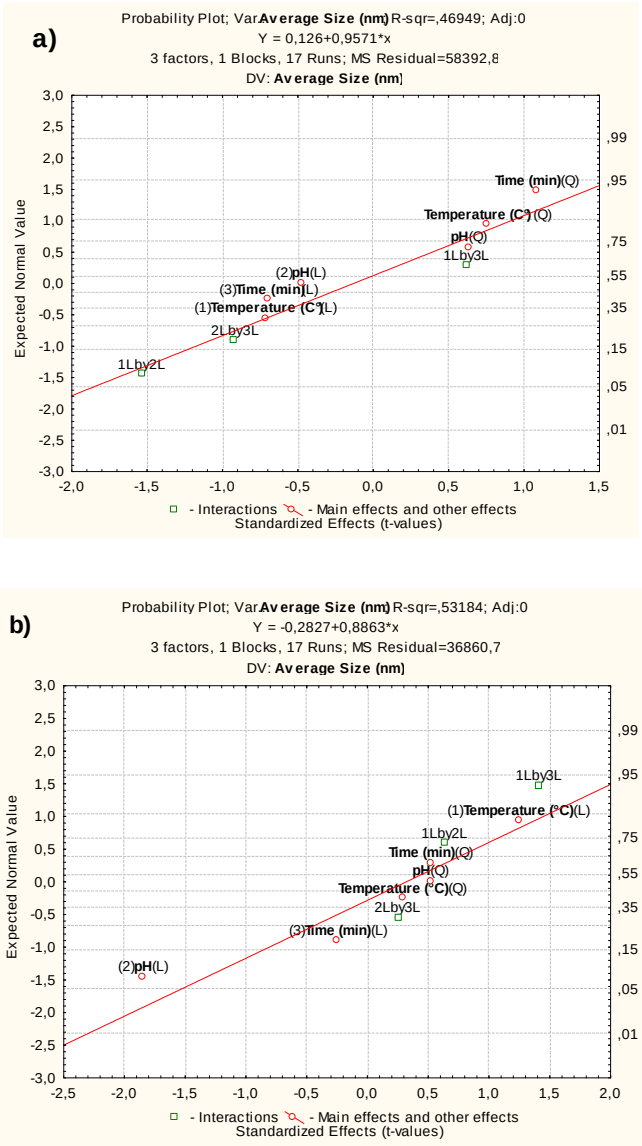

Fig. 3. Normal probability plots for (a) α-la-TG (L) system and (b) α-la-TG (SD) system.

Additionally, an alternative way to verify the influence of some selected factors on nanostructure mean diameters are plots of normal probability. The utilization of this type of graphs is because both the main effects (linear and quadratic) and the interaction effects are distributed according to a normal distribution centered at zero with σ^2 variance. In other words, the points representing such effects have to be concentrated over a straight line in the graph. However, if the graph points seem to deviate somewhat from the straight line, the data are not distributed in a normal way.

This behavior suggests the existence of significant effects that should be analyzed in detail (Levine, Berenson, & Stephan, 1998). Fig. 3 shows the normal probability plots for α-la-TG (L) and α-la-TG (SD) systems. Fig. 3a shows, for α-la-TG (L) system, distance among the straight line and the points representing the (*i*) linear effect of pH, (*ii*) the quadratic effect of the heating time, and (*iii*) the interaction between the linear effect of temperature and the heating time. This suggests that these effects are significantly different from zero and, therefore, they influence the nanostructure mean diameters. Fig. 3b shows, for the α-la-TG (SD) system, a linear effect of pH more noticeable.

3.3.2. ζ-potential analysis

The ζ-potential analysis is associated to the net surface charge of the system. Values of zeta potential of nanostructured α-la-TG (L) and α-la-TG (SD) systems and of controls (dispersions of pure α-la and α-la +TG mixture without heat treatment and pH adjustment) are shown in Table 4. Positive values of ζ-potential are observed for both nanostructured systems at conditions of pH values lower than the isoelectric point of α-la (4.4 pI). Conversely, treatments in with pH was higher than 4.4 led to negative values of ζ-potential, i.e., to negative charge of the net surface.

Table 4. Variation of zeta potential (mV) of native protein (α-la), α-la +TG mixture and the nanostructures in different conditions for the α-la-TG (L) and α-la-TG (SD) systems.

		Zeta potential (mV)	
Treatment	**System**	**α-la-TG (L)**	**α-la-TG (SD)**
1	50 °C, pH 3.9, 15'	-0.280	0.134
2	50 °C, pH 3.9, 45'	-0.012	0.244
3	50 °C, pH 9.2, 15'	-2.190	-7.460
4	50 °C, pH 9.2, 45'	-2.813	-6.285
5	80 °C, pH 3.9, 15'	-0.128	-0.611
6	80 °C, pH 3.9, 45'	-0.074	-0.167
7	80 °C, pH 9.2, 15'	-1.860	0.092
8	80 °C, pH 9.2, 45'	-3.765	-8.590
9	39.8 °C, pH 6.5, 30'	-3.333	-3.700
10	90.2 °C, pH 6.5, 30'	-5.935	-2.915
11	65 °C, pH 2.1, 30'	0.343	0.644
12	65 °C, pH 11, 30'	-3.940	-6.750
13	65 °C, pH 6.5, 4.8'	-1.955	0.045
14	65 °C, pH 6.5, 55.2'	-1.920	-4.065
15	65 °C, pH 6.5, 30'	-3.115	-3.780
16	Pure α-la	-5.690	
17	α-la+TG mixture	-4.320	

Treatments with pH values equal to 3.9, close to the pI of α-la, showed ζ-potential values close to zero, which can indicate that the net surface charge of nanostructures is near zero. Such phenomenon can result in low level of electric repulsion between the particles with an increase in their attraction that could increment aggregate formation. These results agree with the observed DLS data, at pH 3.9, of 1000 nm mean particle diameter.

For treatment 11 (65 °C, pH 2.1, 30') the ζ-potential value was close to zero for α-la-TG (L) and α-la-TG (SD) systems. This may be a consequence of conjugation of TG on the α-la surface. In addition, a decrease in the content of lysine residues after glycosylation reduces the ζ-potential values of nanostructures at pH below 4.4. Pirestani, Nasirpour, Keramat, Desobry, & Jasniewski (2016) observed a similar result in nanostructures from CPI-AG conjugates.

On the other hand, ζ-potential values for treatments at pH 6.5 were lower than α-la control (-11.69 mV). This was mainly attributed to the shielding effect of the TG layer outside the nanostructures, which was attached through the glycosylation reaction, leading to the remarkable decrease of ζ-potential. Lesmes & McClements (2012), Yi et al. (2016) and Fan, Yi, Zhang, Wen, & Zhao (2017) found similar behaviors in nanocomplexes from β-lg-Dextran, WPI-Dextran and α-la-Dextran conjugates respectively.

According to Riddick (1968), ζ-potential values between -30 and 30 mV indicate instability in the system. Values above 30 mV or below -30 mV indicate a high stability. In this study, all treatments showed ζ-potential values in the range of -30 and 30 mV for the α-la-TG (L) and α-la-TG (SD) systems. This result may be explained as follows. Tara gum is an uncharged polysaccharide, therefore, does not interact electrostatically with α-la, indicating that the system stability is not determined by electrostatic interactions but defined by hydrogen bonds and/or hydrophobic interactions (Chen et al., 2017). In addition, the steric hindrance provided by the hydrophilic TG molecules conjugated on α-la outside, leading to the decrease in ζ-potential.

3.3.3. Fluorescence spectroscopy

The intrinsic fluorescence spectra of pure α-la, α-la+TG mixture, and the nanostructures for α-la-TG (L) and α-la-TG (SD) systems are shown in Fig. 4 and 5, respectively.

In general, all treatments analyzed exhibited a marked blue shift in the maximum fluorescence intensity (FI) compared to the emission spectrum of pure α-la. This indicates that the surrounding chemical microenvironment of the chromophores tryptophan (Trp) and tyrosine (Tyr) became more apolar.

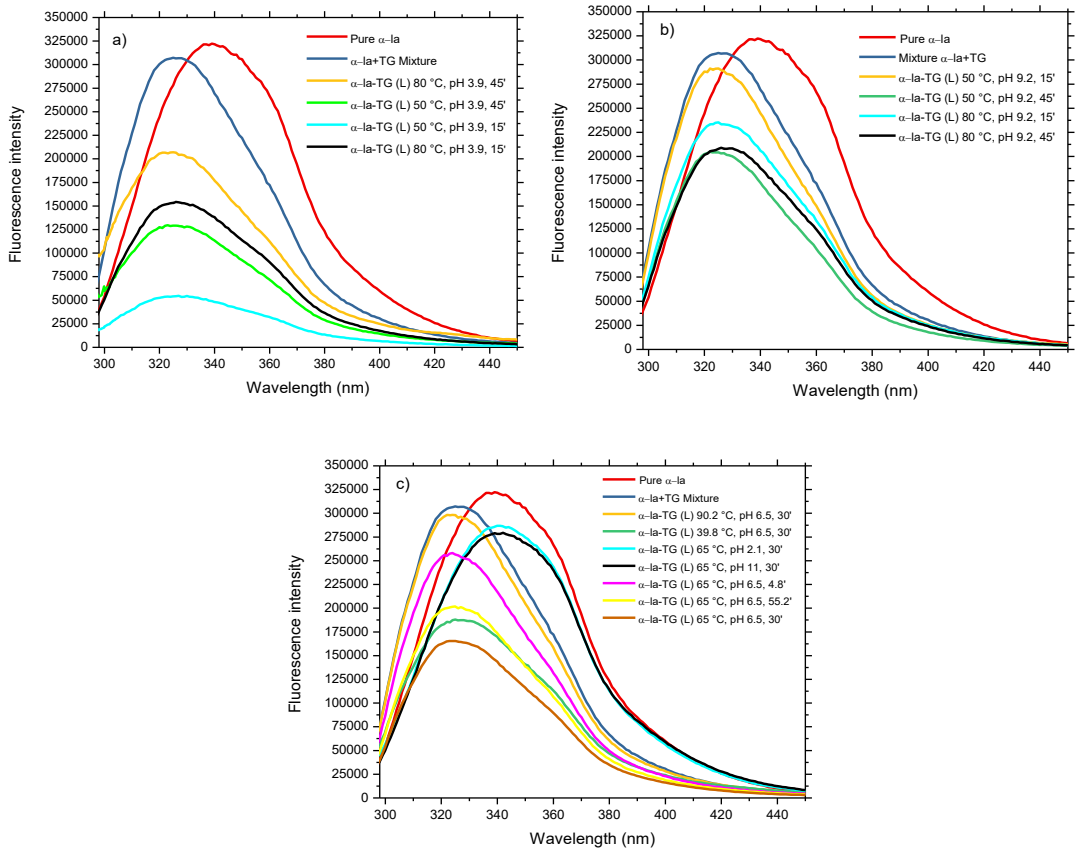

Fig. 4. Emission spectra of chromophores of pure protein (α-la), α-la+TG mixture and the nanostructures in different conditions for α-la-TG (L) system.

For treatments from α-la-TG (L) system, the maximum FI had a decrease in value compared to the controls (α-la) (Fig. 4a-b-c). This indicates that the tryptophan and tyrosine residues in α-la were confined to a more hydrophobic region, which was due to several polysaccharide molecules that were linked to the α-la through of the conjugation reaction. Therefore, the hydrophobicity of these conjugates became stronger (Liu, Ma, McClements, & Gao, 2016). Jiménez-Castaño, Villamiel, & López-Fandiño (2007) and Qiu et al. (2018) found similar behaviors in β-lg-dextran and casein-carrageenan conjugates, respectively.

Nanostructures from α-la-TG (L) system produced at pH 3.9 (Fig. 4a) showed values of maximum FI lower than other treatments (Fig. 4b-c). This may have occurred due to the fact that pH value of these treatments is close to IP of the α-la, therefore, aggregation process occurs and the Trp and Tyr residues are more hidden within the aggregate (Saraiva et al., 2017). On the other hand, treatments with high temperatures of heating (80 °C and 90.2 °C) showed maximum FI values higher than other treatments. This suggests that due to temperature increase, more molecules of the chromophores were exposed to the solvent indicating the possible unfolding of the protein. Similar results were obtained by Koch, Emin, & Schuchmann (2017) who studied WPI-Pectin conjugates.

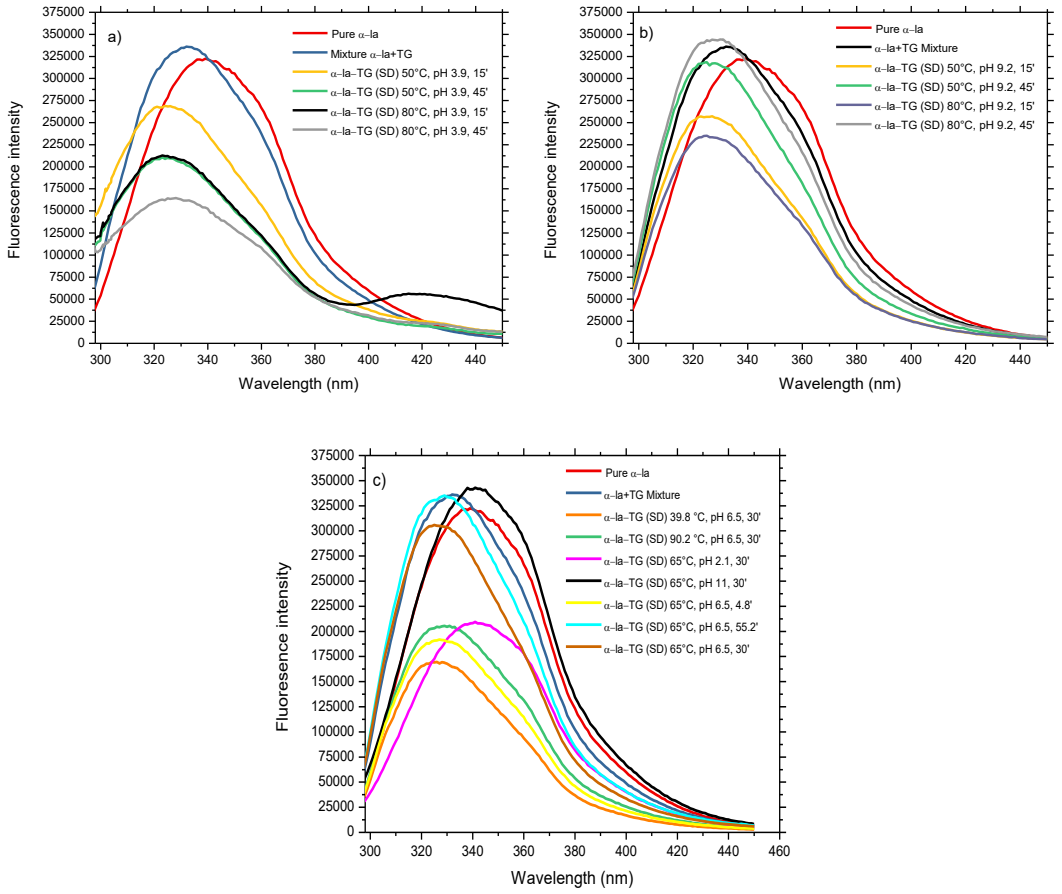

Fig. 5. Emission spectra of chromophores of pure protein (α-la), α-la+TG mixture and the nanostructures in different conditions for α-la-TG (SD) system.

Treatments 8 (80 °C, pH 9.2, 45'), 12 (65 °C, pH 11, 30') and 14 (65°C, pH 6.5, 55.2') for α-la-TG (SD) system showed maximum FI values greater than the controls (Fig. 5b-c). We explain this result as follows. The obtaining of conjugates with spray-dried mixtures occurred at a slower rate, as it was demonstrated in *BI* and *%FAG* analyses

(Fig. 1). Therefore, a smaller number of molecules of TG were bound to the protein, reducing the hydrophobicity of the Trp and Tyr microenvironment. In addition, the effect of the temperature for treatments in these conditions may have caused protein partial denaturation with the corresponding exposure of the chromophores, resulting in greater maximum FI values.

3.3.4. Circular dichroism (CD)

Circular dichroism (CD) is considered as an indicator of conformational changes of proteins at the molecular level. Fig. 6 and 7 show the CD spectra of pure α-la, α-la+TG mixture and the nanostructures from α-la-TG (L) and α-la-TG (SD) systems, respectively. α-la is an α-helical protein evidenced with strong negative peaks at approximately 208 and 222 nm. The results showed that covalent attachment of the polysaccharide to the protein had a big effect on the secondary structure of α-la, and this is represented in the remarkable change of peak height in the CD spectra of the nanostructures compared to the control (pure α-la) (Fig. 6 and 7).

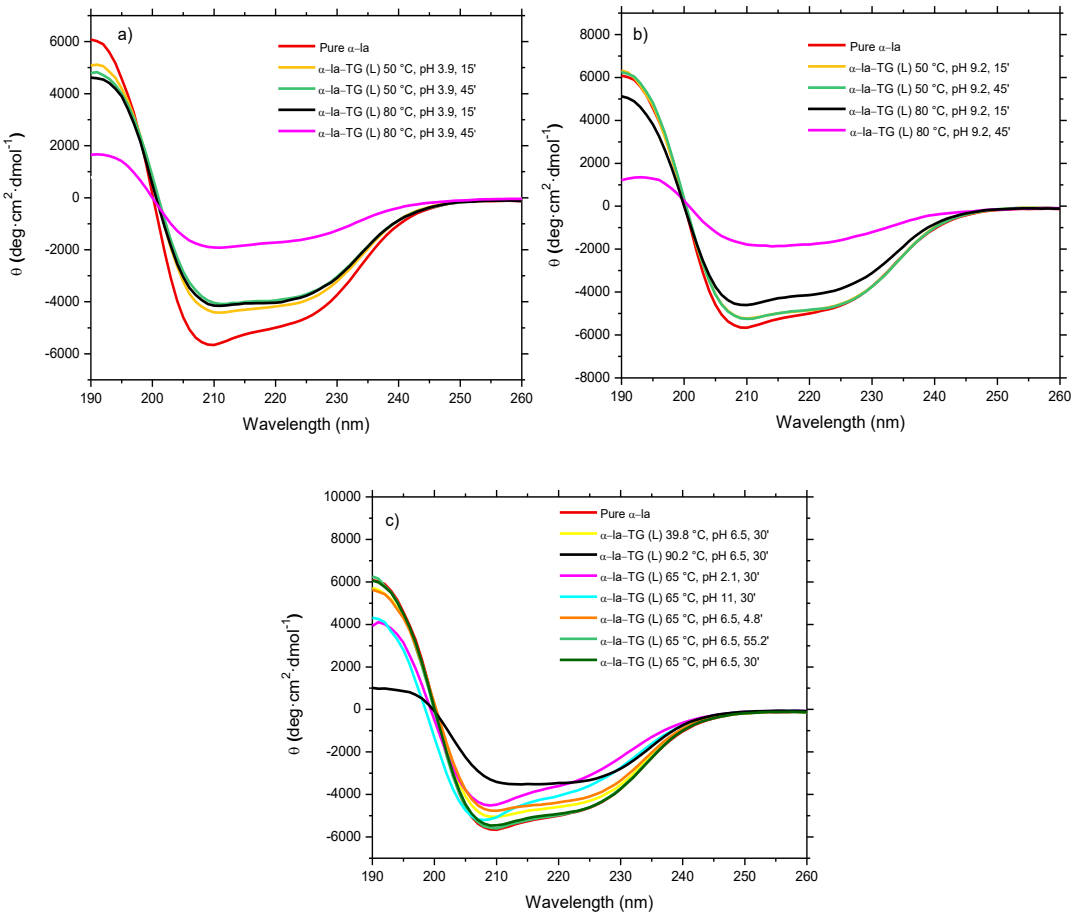

Fig. 6. CD spectra of native protein (α-la), α-la+TG mixture and the nanostructures in different conditions for α-la-TG (L) system.

For α-la-TG (L) system, treatment 6 (80 °C, pH 3.9, 45') showed a remarkable variation of peak height compared to the control (Fig. 6a). This result may have been due to the effect of high temperature and large time of thermal treatment, which caused the possible denaturation of α-la (Day et al., 2014).

According to the results obtained by deconvolution of the CD data of the samples using the CONTIN/LL- Reference 4 analysis method (Sreerama & Woody, 2000), the secondary structure of α-la had changes after glycosylation and the thermal treatments employed. Pure α-la contained 24.3% α-helix, 20.7% β-sheet, 22.0% turns and 30.0% disordered structure. We observed that there was a reduction in the α-helix content and an increase in the percentage of β-sheet and disordered structure in all treatments (Table 5).

Table 5. Mean values of deconvolution of the residual molar ellipticity data for α-la-TG (L) system.

Treatment	System	Alpha-helix (%)	Beta-Sheet (%)	Turns (%)	Disordered structure (%)
	Pure α-la	27.3	20.7	22.0	30.0
1	50 °C, pH 3.9, 15'	15.3	28.3	17.3	39.1
2	50 °C, pH 3.9, 45'	14.3	28.8	17.6	39.2
3	50 °C, pH 9.2, 15'	17.0	26.3	16.7	40.0
4	50 °C, pH 9.2, 45'	17.4	26.1	16.7	39.9
5	80 °C, pH 3.9, 15'	14.5	27.9	17.5	40.2
6	80 °C, pH 3.9, 45'	9.1	32.1	18.3	40.6
7	80 °C, pH 9.2, 15'	8.2	32.7	18.6	40.5
8	80 °C, pH 9.2, 45'	15.4	27.3	17.1	40.2
9	39.8 °C, pH 6.5, 30'	16.5	26.7	16.7	40.1
10	90.2 °C, pH 6.5, 30'	10.2	32.9	16.9	40.1
11	65 °C, pH 2.1, 30'	13.8	28.3	18.3	39.5
12	65 °C, pH 11, 30'	9.0	33.7	18.8	38.6
13	65 °C, pH 6.5, 4.8'	16.0	27.6	16.9	39.6
14	65 °C, pH 6.5, 55.2'	12.4	28.1	17.1	42.4
15	65 °C, pH 6.5, 30'	17.3	26.1	16.6	40.0

*Pure α-la corresponds to the α-la in solution with no heat treatment and no pH adjustment.

Glycosylation of proteins and polysaccharides involves the covalent binding of the carbonyl group of a reducing sugar and the ε-amino group of the protein, which is within the α-helix region or its neighbor of proteins. The decrease in α-helix content is due to the fact that polysaccharide molecules were linked to the ε-amino group in the α-helix regions (Li, Xue, Chen, Ding, & Wang, 2014). Therefore, the attachment of TG molecules to α-la led to changes in spatial structure and protein unfolding. Yi et

al. (2016a) found similar results in α-la-dextran nanocomplexes. In addition, the effect of temperature, pH and heating time could have influenced more acutely the changes in the secondary structure of the protein (Day et al., 2014; Saraiva et al., 2017). This agrees with the larger decrease in the α-helix percentage in treatments 5 (80 °C, pH 3.9, 15'), 6 (80 °C, pH 3.9, 45'), 7 (80 °C, pH 9.2, 15'), 8 (80 °C, pH 9.2, 45'), 10 (90.2 °C, pH 6.5, 30') 12 (65 °C, pH 11, 30'), and 14 (65 °C, pH 6.5, 55.2') according to Table 5.

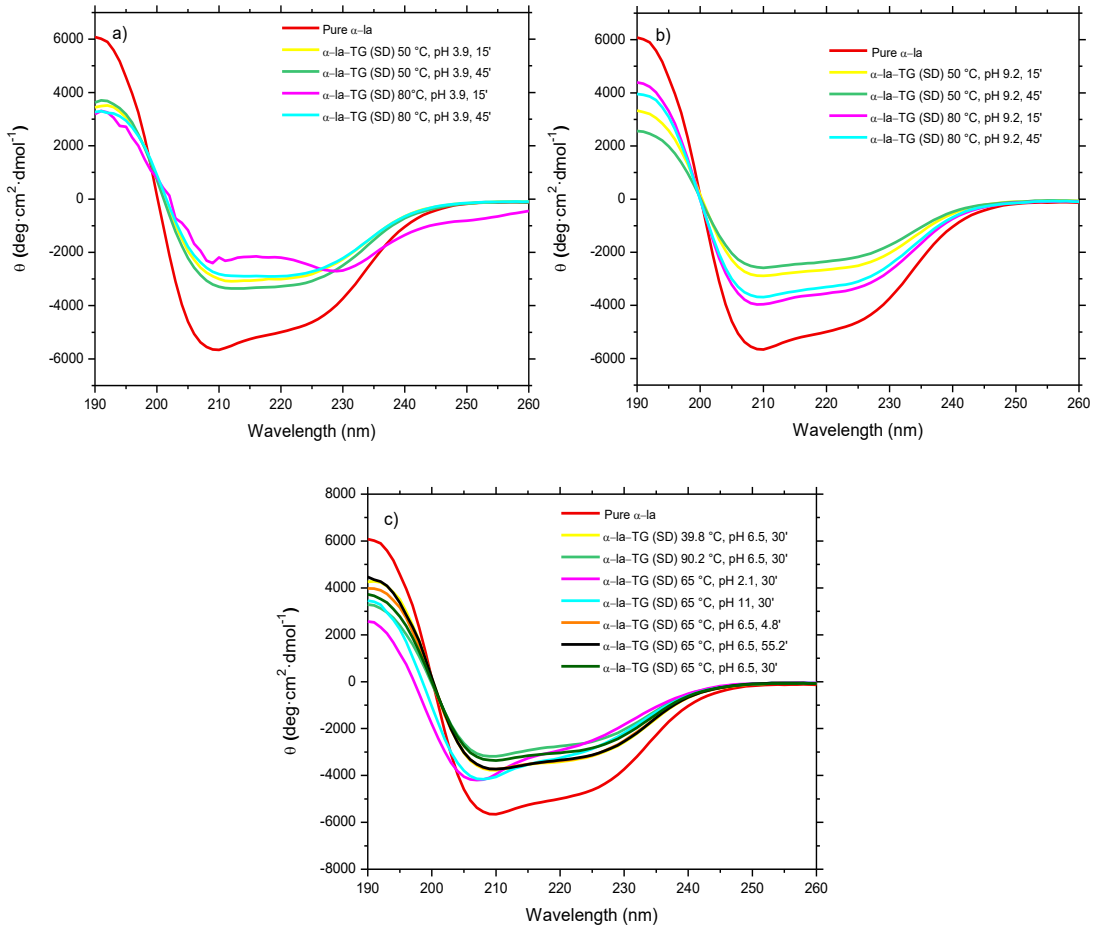

Fig. 7. Spectra of de native protein (α-la), α-la+TG mixture and the nanostructures in different conditions for α-la-TG (SD) system.

On the other hand, for the treatments from α-la-TG (SD) system, the changes in the secondary structure of the protein were more notorious (Fig 7). CD spectra of all treatments showed a large reduction in peak height compared to the control (pure α-la). A possible cause of this result was the effect of the spray dry operation, which uses high temperatures and may cause partial denaturation of the α-la, resulting in changes in the protein conformation (Toro-Sierra et al., 2013). In addition, the effect of the

temperature, pH and the heating time of each treatment contributed to a further change in the secondary structure of proteins. This can be seen in Table 6, which shows that the decrease in the α-helix content was higher than in treatments using conjugates from α-la-TG (L) system.

Table 6. Mean values of deconvolution of the residual molar ellipticity data for α-la-TG (SD) system.

Treatment	System	Alpha-helix (%)	Beta-Sheet (%)	Turns (%)	Disordered structure (%)
	Pure α-la	27.3	20.7	22.0	30.0
1	50 °C, pH 3.9, 15'	17.3	26.1	16.6	40.0
2	50 °C, pH 3.9, 45'	12.7	30.0	17.8	39.5
3	50 °C, pH 9.2, 15'	14.9	28.2	17.1	39.8
4	50 °C, pH 9.2, 45'	16.1	26.7	17.1	40.1
5	80 °C, pH 3.9, 15'	6.6	35.7	18.2	38.5
6	80 °C, pH 3.9, 45'	8.0	38.1	23.5	30.4
7	80 °C, pH 9.2, 15'	18.8	24.8	16.5	40.3
8	80 °C, pH 9.2, 45'	13.4	28.8	17.4	40.5
9	39.8 °C, pH 6.5, 30'	18.1	25.1	16.9	39.9
10	90.2 °C, pH 6.5, 30'	15.5	27.5	17.1	39.9
11	65 °C, pH 2.1, 30'	13.7	26.6	17.4	42.3
12	65 °C, pH 11, 30'	9	38.6	18.8	33.7
13	65 °C, pH 6.5, 4.8'	7.8	35.2	19.1	37.9
14	65 °C, pH 6.5, 55.2'	18.7	25.3	16.8	39.2
15	65 °C, pH 6.5, 30'	16.3	26.6	16.9	40.3

*Pure α-la corresponds to the α-la in solution with no heat treatment and no pH adjustment.

3.3.5. Stability of α-la-TG nanostructures during storage

Table 7 shows the relation of the chosen treatments of each system in which there was formation of nanoparticles. We considered particle sizes between 10 and 300 nm according to Uskoković (2007). In this section, the nanostructures selected were analyzed via DLS for 45 days in order to evaluate their stability during storage at 4 °C.

Table 7. Conditions with formation of nanostructures for α-la-TG (L) and α-la-TG (SD) systems

Treatment	System	Average size (nm)			Zeta potential (mv)	Maximum fluorescence intensity	Circular dichroism			
		Peak 1	Peak 2	Peak 3			Alpha-helix (%)	Beta-sheet (%)	Turns (%)	Disordered structure (%)
8	α-la-TG (L) 80 °C, pH 9.2, 45'	289.5	64.40	4343	-12.765	208978.4	15.4	27.3	17.1	40.2
9	α-la-TG (L) 39.8 °C, pH 6.5, 30'	1028	124.6	4998	-3.333	298300.8	16.5	26.7	16.7	40.1
12	α-la-TG (L) 65 °C, pH 11, 30'	46.26	167.7	-	-13.940	279387.2	9.0	38.6	18.8	33.7
3	α-la-TG (SD) 50 °C, pH 9.2, 15'	44.31	234.34	-	-7.460	257264.8	14.9	28.2	17.1	39.8
4	α-la-TG (SD) 50 °C, pH 9.2, 45'	528,4	290.1	4894	-6.285	318343.2	16.1	26.7	17.1	40.1
9	α-la-TG (SD) 39.8 °C, pH 6.5, 30'	34.29	161.5	210.62	-3.700	169503.2	18.1	25.1	16.9	39.9
14	α-la-TG (SD) 65 °C, pH 6.5, 55.2'	1200	121,4	34,14	-4.065	335060.8	18.7	25.3	16.8	39.2

In general, we observed that the mean diameter of nanostructures was risen with the increasing storage time and was different ($p < 0.05$) when compared to the control (day 1) according to Fig. 8. For the treatments from α-la-TG (L) system with 3 days of storage values of average diameter above 300 nm were observed, indicating that this period was the time necessary for the loss of the colloidal stability of the system, with the consequent aggregation of particles. This phenomenon may have occurred due to the type of polysaccharide used, in this case tara gum, which is characterized by being uncharged (Dea et al., 1977), demonstrating that the hydrophobic interactions and the hydrogen bonds were not sufficient to maintain the systems stable for a longer period.

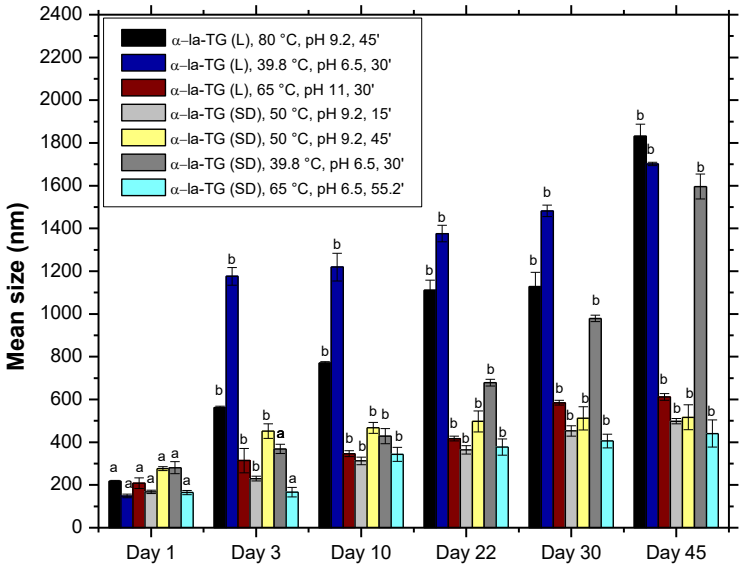

Fig. 8. Effect of time storage at 4°C on the hydrodynamic diameter of nanostructures for α-la-TG (L) and α-la-TG (SD) systems. Values with the same letter were not significantly different when compared to the control (Day 1) by Dunnett test (p>0.05).

For α-la-TG (SD), we observed that the treatments 3 (50 °C, pH 9.2, 15') and 14 (65 °C, pH 6.5, 55.2') showed a maximum stability of 10 days. Fig. 8 shows that the size variation of the α-la-TG (L) system was higher than the α-la-TG (SD) system. This suggests that systems using conjugates with a lower grafting degree present greater stability. One possible explanation for this phenomenon is the conjugate solubility. Several studies report a decrease in protein solubility as result of the Maillard reaction. Al-Hakkak & Al-Hakkak (2010) observed a reduction in the solubility of egg protein-pectin conjugates with increasing grafting degree. Álvarez, García, Rendueles, & Díaz (2012) determined a decrease in the solubility of conjugates from porcine blood protein isolate and dextran. Therefore, lower solubility of the nanostructures from α-la-TG (L)

system resulted in periods of low stability. These results are in agreement with those obtained in the ζ-potential analysis for this system, showing in general that all the treatments did not present electrostatic stability (Table 4).

3.3.6. Foaming properties

Foaming properties include foaming capacity and foaming stability. Foaming capacity indicates the ability of the protein to foam, and the foaming stability refers to the ability of the foam formed to retain the maximum volume of air for a determinate time (Kim, Choi, Shin, & Moon, 2003). Table 8, Fig. 9 and 10 show the values of the foaming capacity (volume increase-*VI*) and foaming stability for the more stable treatments from α-la-TG (L) and α-la-TG (SD) systems.

Table 8. Foaming capacity for systems with α-la.

Foaming capacity	**Pure α-la**	**α-la+TG Mixture**	**α-la-TG (L) 65 °C, pH 11, 30'**	**α-la-TG (SD) 50 °C, pH 9.2, 15'**	**α-la-TG (SD) 65 °C, pH 6.5, 55.2'**
VI	98.31 ± 2.34^{a}	105.00 ± 7.07^{ab}	112.67 ± 2.36^{b}	133.75 ± 5.30^{c}	95.00 ± 7.13^{a}

VI: volume increase. Values with the same letter were not significantly different by Tukey test (p>0.05). The measurements were done in triplicate.

Treatment 12 (65 °C, pH 11, 30') from α-la-TG (L) system showed *VI* values greater than the pure α-la (Table 7). This increase in foaming capacity may be due to the reason that hydrophilic groups of the protein enhanced the solubility when polysaccharides covalently bind to the protein on the dry-heating (Hemar, Tamehana, Munro, & Singh, 2001). In addition, moderate dry-heating in short times is advantageous to increase the foaming capacity due to the partial protein unfolding to the molten globule state, which increases the flexibility of the protein chain as long as there is no formation of aggregates (Hagolle, Launay, & Relkin, 1998; Wooster & Augustin, 2007). This result is in agreement with the deconvolution of the CD data for treatment 12, which indicated an increase in the disordered structure content (Table 5) and fluorescence analysis, which showed a high FI (Fig. 4c). An et al. (2014) found similar values using OVA- CMC conjugates with two days of dry heating time. Similar results were found in WPI-red seaweed conjugates (Chiu et al., 2009). On the other hand, the *VI* value for the treatment from α-la-TG (SD) system was higher than the controls except the treatment 14 (65 °C, pH 6.5, 55.2').

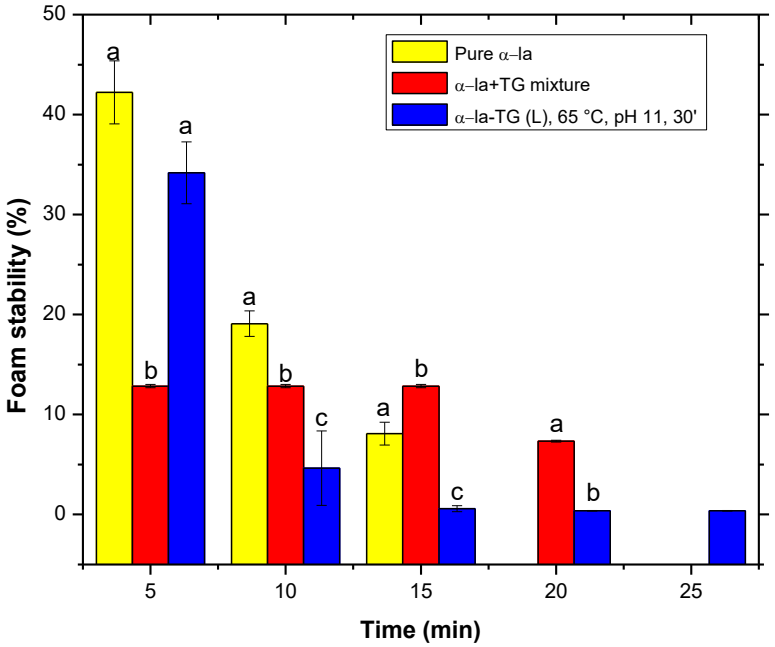

Fig. 9. Foam stability for α-la-TG (L) system. Values with the same letter were not significantly different by Tukey test ($p > 0.05$). The measurements were done in triplicate

The foaming stability of the nanostructures was greater compared to the controls for both systems. For α-la-TG (L) system, we observed at the beginning that the controls showed greater stability compared to the nanostructures from treatment 12 (65 °C, pH 11, 30'). However, for times over 20 minutes, the foaming stability of the controls was reduced, being smaller compared to the treatment 12 (Fig. 9). These results suggest that due to the effect of the grifting between α-la and TG on the dry-heating, the local viscosity in the foam lamellae has been increased and this inhibits film drainage and creates a greater thickness of the mixed biopolymer absorbed layer that tends to increase steric stabilization and inhibit bubble breakage (Dickinson & Izgi, 1996).

On the other hand, the nanostructures from α-la-TG (SD) showed a greater foaming stability compared to the controls. Treatments 3 (50 °C, pH 9.2, 15') and 14 (65 °C, pH 6.5, 55.2') showed stability times above 60 min indicating that the conjugation of α-la with TG improved the foaming stability (Fig. 10).

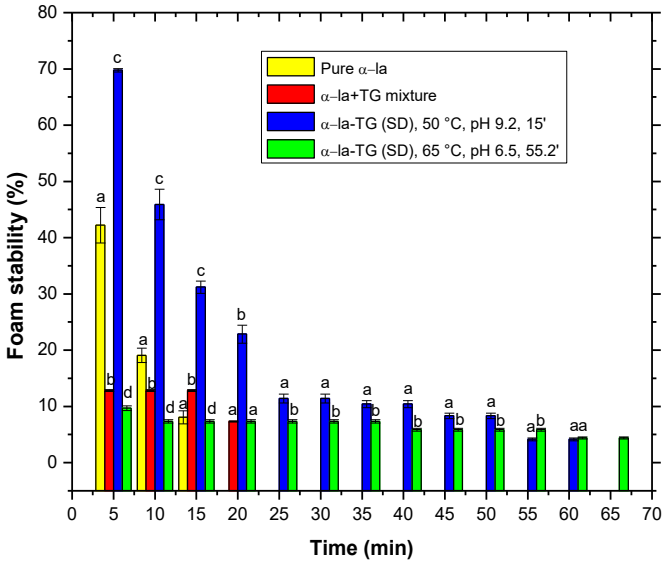

Fig. 10. Foam stability for α-la-TG (SD) system. Values with the same letter were not significantly different by Tukey test ($p > 0.05$). The measurements were done in triplicate.

3.3.7. Emulsion stability index (*ESI*)

In order to investigate the effect of the conjugation of the TG on the stability of emulsions, the *ESI* of the nanostructures from α-la-TG (L) and α-la-TG (SD) systems was determined as shown in Fig. 11. We observed that treatment 3 (50 °C, pH 9.2, 15') from α-la-TG (SD) system showed statistically higher *ESI* values in 30 and 60 min compared to the controls. The great emulsifying stability of this treatment may be attributed to its molecular characteristics, which are able to create a robust macromolecular barrier at the oil-water interfaces to prevent emulsion droplet aggregation (Akhtar & Dickinson, 2003). Guo, Guo, Yu, & Kong (2018) found similar behavior in WPI-sugar beet pectin conjugates.

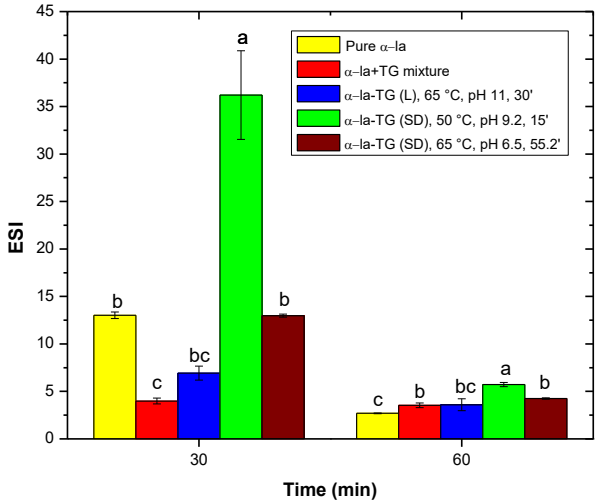

Fig. 11. Emulsion stability index (ESI) for α-la-TG system. Values with the same letter were not significantly different by Tukey test ($p > 0.05$). The measurements were done in triplicate.

On the other hand, treatments 12 (65 °C, pH 11, 30') from α-la-TG (L) system and 14 (65 °C, pH 6.5, 55.2') from α-la-TG (SD) system showed lower *ESI* values in 30 min compared to the control (pure α-la). This suggests that the influence of thermal treatment and pH on the conjugates affected the hydrophilic and hydrophobic properties of the protein causing an imbalance between the hydrophilic and lipophilic phases in the emulsion. Similar results were found by Chiu et al. (2009) in WPI-Green seaweeds conjugates.

3.3.8. Differential scanning calorimetry (DSC)

The nanostructures from α-la-TG (L) system, α-la-TG (SD) system and the pure α-la control were studied in terms of their thermal behavior. DSC measurements revealed the denaturation temperature (T_d) and denaturation enthalpy (ΔH_d) of the treatments 12 (65°C, pH 11, 30') from α-la-TG (L) system and 3 (50 °C, pH 9.2, 15') from α-la-TG (SD) system as well as the pure α-la control (Table 9). The corresponding thermal profile of nanostructures and the pure α-la obtained in the temperature range of 20-98 °C are shown in Fig. 12.

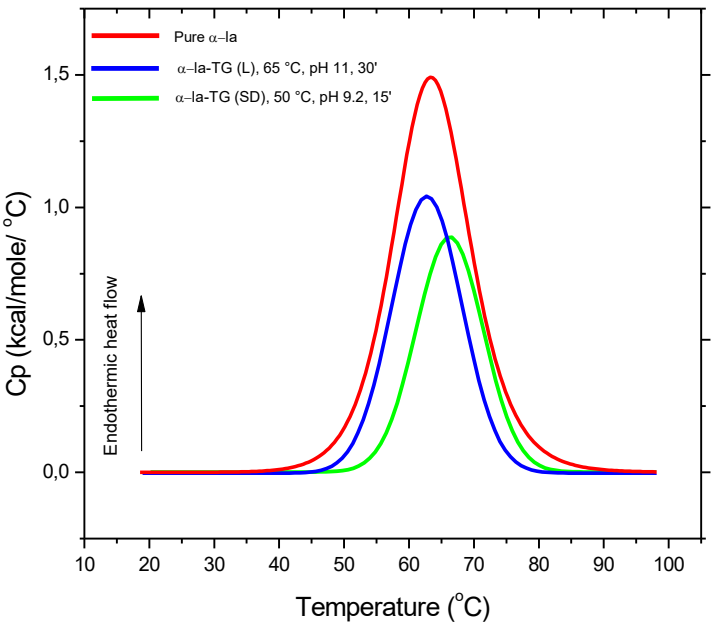

Fig. 12. DSC thermograms of pure α-la, α-la-TG (L) and α-la-TG (SD) systems

The thermograms of each sample exhibited endothermic peaks and the T_d of the α-la control was 63.56 °C. Similar values were found by Diniz et al. (2014) and Monteiro et al. (2016). We observed an increase in T_d (67.5 °C) and a decrease in ΔH_d (1.097×10^4

± 78 kCal·mol^{-1}) of treatment 3 compared to the α-la control (T_d = 63.56 °C; ΔH_d = 2.339×10^4 ± 143 kCal·mol^{-1}). These results indicate that after the glycosylation process of α-la, the protein thermal stability was improved. Wang & Zhong (2014b) found similar behavior in nanostructures from WPI-Maltodextrin conjugates. The reduction of ΔH_d may have occurred due to the processes of aggregation and perturbation of hydrophobic interactions, which are characterized by decreasing the enthalpy (Boye, Alli, & Ismail, 1996). This trend was also observed by Koshani, Aminlari, Niakosari, Farahnaky, & Mesbahi (2015) in lysozyme-tragacanthine conjugates.

Table 9. Thermodynamic parameters obtained from DSC analysis of pure α-la, α-la-TG (L) and α-la-TG (SD) systems.

Treatment	System	T_d (°C)	ΔH_d (kCal·mol^{-1})
12	Pure α-la	63.56 ± 0.04	2.339 × 10^4 ± 143
	α-la-TG (L) 65 °C, pH 11, 30'	63.42 ± 0.06	1.395 × 10^4 ± 141
3	α-la-TG (SD) 50 °C, pH 9.2, 15'	67.5 ± 0.04	1.097 × 10^4 ± 78

T_d: Denaturation temperature; ΔH_d: denaturation enthalpy;

3.3.9. Morphological characterization of nanostructures

AFM and TEM images were captured to determine the nanostructure morphology of the treatment 3 (50 °C, pH 9.2, 15') from α-la-TG (SD) system. Fig. 13a and 13b show the AFM topographical images of individual molecules of TG and α-la. Tara gum is a branched polysaccharide, which has a flexible and extended polymeric structure. In the AFM images, TG presented a broadly flat shape as a random structure on the mica surface (Fig. 13a). Fig. 13b confirmed that α-la had a typical globular structure with a mean diameter of 15 nm, showing greater brightness than the TG, which indicates a greater particle height.

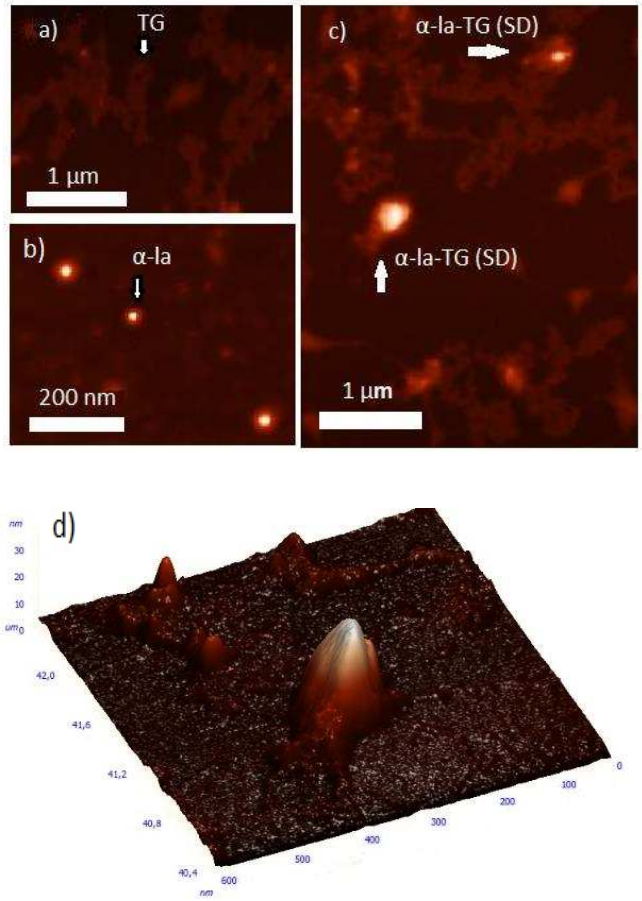

Fig. 13. Atomic force microscopy topographical images of individual molecules of (a) Tara gum (TG), (b) Pure alpha-lactalbumin (α-la), (c) Treatment 3 (50 °C, pH 9.2, 15') from α-la-TG (SD)system and (d) 3D projection of image (c).

Fig. 13c shows images of the nanostructures for treatment 3 from α-la-TG (SD) system. In the image one can observe that the TG molecules appear to be bound to the α-la surface involving totally the molecule. Fig. 13d shows a 3D projection of Fig. 13c, and one can clearly see that the nanostructures exhibited in the center have a conical shape with smooth surfaces that corresponds to the α-la particles. In the surrounding area, there were structures with rougher surfaces and less height corresponding to the TG molecules. The mean diameter of the nanostructures in Fig. 13d was approximately 200 nm with an average height of 30 nm. The mean diameter determined by AFM analysis was smaller than the mean hydrodynamic diameter (234.4 nm) calculated by DLS technique for the same treatment. We expected these results because the DLS technique provides mean particle size data in solution, while AFM analysis present images of spread and dried particle on a mica surface. The value of the nanostructure

height was much larger than the mean diameter, suggesting that the nanostructures are very soft and collapsed on the mica surface. Similar results were found in nanogels from lysozyme-dextran conjugates (Li et al., 2008)

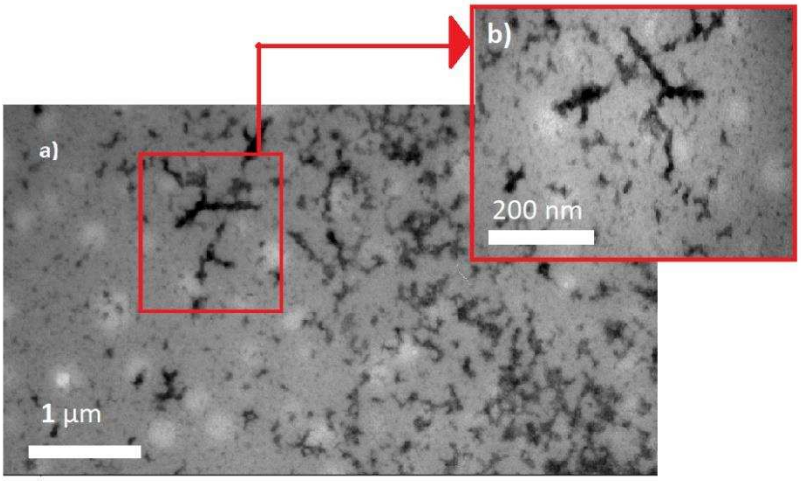

Fig. 14. Transmission electron micrograph of treatment 3 (50 °C, pH 9.2, 15') from α-la-TG (SD) system, (a) α-la-TG (SD) at 2000x, (b) α-la-TG (SD) at 50000x.

In the TEM images (Fig. 14a-b) for treatment 3, nanoparticles with elongated structure were observed, but it is possible to appreciate in the image an association of spherical structures with a diameter of approximately 100 nm.

4. Conclusions

The results of the browning index and percentage of free amino groups confirmed the glycosylation of α-la and tara gum in spray-dried or lyophilized mixtures. The glycosylation rate of the mixtures α-la and tara gum decreased when the spray dry was used instead the lyophilization. The most appropriate time of glycosylation/conjugation reaction was 2 days. Nanostructures from α-la-TG conjugates with a mean diameter among 30 and 300 nm presented changes in the secondary and tertiary structure of α-la. Exposure of the nanostructures from conjugates to thermal treatments at high temperatures (90.2 - 80 °C) was associated with loss of the α-helix content and increased disordered structure for the systems studied. Nanostructured systems composed by protein conjugated with polysaccharide presented an increase in the foaming and emulsifying capacities and thermal stability as compared with systems containing only protein. Overall, this work showed that it is possible to obtain nanostructures from α-la-TG conjugates using the dry-heating and

thermal gelation techniques with pH adjustment. These systems have potential use in the food industry as food additives.

Acknowledgments

The authors thank the Conselho Nacional de Pesquisa e Desenvolvimento Tecnológico (CNPq) for the financial support, the Centro Nacional de Pesquisa em Energia e Materiais-Laboratório Nacional de Biociências (CNPEM-LNBio) for the analyses of circular dichroism, intrinsic fluorescence and differential scanning calorimetry, the Núcleo de Microscopia e Microanálise of Universidade Federal de Viçosa for transmission electron microscopy analysis and the Professor Dr. Sukarno Ferreira from the Departamento de Física for the atomic force microscopy analysis.

References

Adjonu, R., Doran, G., Torley, P., & Agboola, S. (2014). Whey protein peptides as components of nanoemulsions: A review of emulsifying and biological functionalities. *Journal of Food Engineering*, *122*, 15–27. https://doi.org/10.1016/J.JFOODENG.2013.08.034

Akhtar, M., & Dickinson, E. (2003). Emulsifying properties of whey protein–dextran conjugates at low pH and different salt concentrations. *Colloids and Surfaces B: Biointerfaces*, *31*(1–4), 125–132. https://doi.org/10.1016/S0927-7765(03)00049-3

Al-Hakkak, J., & Al-Hakkak, F. (2010). *Journal of food engineering. Journal of Food Engineering* (Vol. 100). Elsevier Science Pub. Co. Retrieved from https://www.cabdirect.org/cabdirect/abstract/20103170180

Álvarez, C., García, V., Rendueles, M., & Díaz, M. (2012). Functional properties of isolated porcine blood proteins modified by Maillard's reaction. *Food Hydrocolloids*, *28*(2), 267–274. https://doi.org/10.1016/J.FOODHYD.2012.01.001

An, Y., Cui, B., Wang, Y., Jin, W., Geng, X., Yan, X., & Li, B. (2014). Functional properties of ovalbumin glycosylated with carboxymethyl cellulose of different substitution degree. *Food Hydrocolloids*, *40*, 1–8. https://doi.org/10.1016/j.foodhyd.2014.01.028

Boye, J. I., Alli, I., & Ismail, A. A. (1996). Interactions Involved in the Gelation of Bovine Serum Albumin. *Journal of Agricultural and Food Chemistry*, *44*(4), 996–1004. https://doi.org/10.1021/jf950529t

Cerqueira, M. A., Pinheiro, A. C., Souza, B. W. S., Lima, A. M. P., Ribeiro, C., Teixeira, J. A., Moreira, R. A., Coimbra, M. A., Gonçalves, M. P., & Vicente, A. A (2009). Extraction, purification and characterization of galactomannans from non-traditional sources. *Carbohydrate Polymers*, *75*(3), 408-414. https://doi.org/10.1016/j.carbpol.2008.07.036

Chen, H., Xu, Z., Mo, J., Lyu, Y., Tang, X., & Shen, X. (2017). Effects of guar gum on adhesion properties of soybean protein isolate onto porcine bones. *International Journal of Adhesion and Adhesives*, *75*(March), 124–131. https://doi.org/10.1016/j.ijadhadh.2017.03.001

Chiu, T. hsin, Chen, M. lun, & Chang, H. chia. (2009). Comparisons of emulsifying properties of Maillard reaction products conjugated by green, red seaweeds and various commercial proteins. *Food Hydrocolloids*, *23*(8), 2270–2277. https://doi.org/10.1016/j.foodhyd.2009.06.003

Corzo-Martínez, M. C., Sánchez, C. C., Moreno, F. J., Patino, J. M. R., and Villamiel, M. (2012). Interfacial and foaming properties of bovine b-lactoglobulin: Galactose Maillard Conjugates. *Food Hydrocolloids*, *27*, 438–447.

Day, L., Zhai, J., Xu, M., Jones, N. C., Hoffmann, S. V., & Wooster, T. J. (2014). Conformational changes of globular proteins adsorbed at oil-in-water emulsion interfaces examined by synchrotron radiation circular dichroism. *Food Hydrocolloids*, *34*, 78–87. https://doi.org/10.1016/j.foodhyd.2012.12.015

de Oliveira, F. C., Coimbra, J. S. dos R., de Oliveira, E. B., Zuñiga, A. D. G., & Rojas, E. E. G. (2014). Food Protein-polysaccharide Conjugates Obtained via the Maillard Reaction: A Review. *Critical Reviews in Food Science and Nutrition*, *56*(7), 1108–1125. https://doi.org/10.1080/10408398.2012.755669

Dea, I. C. M., Morris, E. R., Rees, D. A., Welsh, E. J., Barnes, H. A., & Price, J. (1977). Associations of like and unlike polysaccharides: Mechanism and specificity in galactomannans, interacting bacterial polysaccharides, and related systems. *Carbohydrate Research*, *57*, 249–272. https://doi.org/10.1016/S0008-

6215(00)81935-7

Delavari, B., Saboury, A. A., Atri, M. S., Ghasemi, A., Bigdeli, B., Khammari, A., … Goliaei, B. (2015). Alpha-lactalbumin: A new carrier for vitamin D3 food enrichment. *Food Hydrocolloids*, *45*, 124–131. https://doi.org/10.1016/j.foodhyd.2014.10.017

Dickinson, E., & Izgi, E. (1996). Foam stabilization by protein-polysaccharide complexes. *Colloids and Surfaces A: Physicochemical and Engineering Aspects*, *113*(1–2), 191–201. https://doi.org/10.1016/0927-7757(96)03647-3

Diniz, R. S., Coimbra, J. S. dos R., Teixeira, Á. V. N. de C., da Costa, A. R., Santos, I. J. B., Bressan, G. C., … da Silva, L. H. M. (2014). Production, characterization and foamability of α-lactalbumin/glycomacropeptide supramolecular structures. *Food Research International*, *64*, 157–165. https://doi.org/10.1016/j.foodres.2014.05.079

Donaldson, T. L., Boonstra, E. F., & Hammond, J. M. (1980). Kinetics of protein denaturation at gas—liquid interfaces. *Journal of Colloid and Interface Science*, *74*(2), 441–450. https://doi.org/10.1016/0021-9797(80)90213-1

Fan, Y., Yi, J., Zhang, Y., Wen, Z., & Zhao, L. (2017). Physicochemical stability and in vitro bioaccessibility of β-carotene nanoemulsions stabilized with whey protein-dextran conjugates. *Food Hydrocolloids*, *63*(2017), 256–264. https://doi.org/10.1016/j.foodhyd.2016.09.008

Fink, A. L. (1998). Protein aggregation: folding aggregates, inclusion bodies and amyloid. *Folding and Design*, *3*(1), R9–R23. https://doi.org/10.1016/S1359-0278(98)00002-9

Gu, Y. S., Matsumura, Y., Yamaguchi, S., & Mori, T. (2001). Action of protein-glutaminase on alpha-lactalbumin in the native and molten globule states. *Journal of Agricultural and Food Chemistry*, *49*(12), 5999–6005. Retrieved from http://www.ncbi.nlm.nih.gov/pubmed/11743799

Guo, X., Guo, X., Yu, S., & Kong, F. (2018). Influences of the different chemical components of sugar beet pectin on the emulsifying performance of conjugates formed between sugar beet pectin and whey protein isolate. *Food Hydrocolloids*, *82*, 1–10. https://doi.org/10.1016/j.foodhyd.2018.03.032

Hagolle, N., Launay, B., & Relkin, P. (1998). Impact of structural changes and aggregation on adsorption kinetics of ovalbumin at the water/air interface. *Colloids and Surfaces B: Biointerfaces*, *10*(4), 191–198. https://doi.org/10.1016/S0927-7765(97)00065-9

Hemar, Y., Tamehana, M., Munro, P. A., & Singh, H. (2001). Viscosity, microstructure and phase behavior of aqueous mixtures of commercial milk protein products and xanthan gum. *Food Hydrocolloids*, *15*(4–6), 565–574. https://doi.org/10.1016/S0268-005X(01)00077-7

Jiménez-Castaño, L., Villamiel, M., & López-Fandiño, R. (2007). Glycosylation of individual whey proteins by Maillard reaction using dextran of different molecular mass. *Food Hydrocolloids*, *21*(3), 433–443. https://doi.org/10.1016/j.foodhyd.2006.05.006

Kato, A. (2002). Industrial applications of Millard-type protein– polysaccharide conjugados. *Food Science and Technology Research, 8*, 193–199.

Kim, H. J., Choi, S. J., Shin, W.-S., & Moon, T. W. (2003). Emulsifying properties of bovine serum albumin-galactomannan conjugates. *Journal of Agricultural and Food Chemistry*, *51*, 1049–1056. https://doi.org/10.1021/jf020698v

Koch, L., Emin, M. A., & Schuchmann, H. P. (2017). Influence of processing conditions on the formation of whey protein-citrus pectin conjugates in extrusion. *Journal of Food Engineering*, *193*, 1–9. https://doi.org/10.1016/j.jfoodeng.2016.08.012

Koshani, R., Aminlari, M., Niakosari, M., Farahnaky, A., & Mesbahi, G. (2015). Production and properties of tragacanthin-conjugated lysozyme as a new multifunctional biopolymer. *Food Hydrocolloids*, *47*, 69–78. https://doi.org/10.1016/j.foodhyd.2014.12.023

Le, T. T., Bhandari, B., Holland, J. W., & Deeth, H. C. (2011). Maillard reaction and protein cross-linking in relation to the solubility of milk powders. *Journal of Agricultural and Food Chemistry*, *59*(23), 12473–12479. https://doi.org/10.1021/jf203460z

Lesmes, U., & McClements, D. J. (2012). Controlling lipid digestibility: Response of lipid droplets coated by β-lactoglobulin-dextran Maillard conjugates to simulated

gastrointestinal conditions. *Food Hydrocolloids*, *26*(1), 221–230. https://doi.org/10.1016/j.foodhyd.2011.05.011

Levine, D. ., Berenson, M. ., & Stephan, D. (1998). *Estatística: teoria e aplicações* (Livros Téc). Rio de Janeiro.

Li, C., Xue, H., Chen, Z., Ding, Q., & Wang, X. (2014). Comparative studies on the physicochemical properties of peanut protein isolate-polysaccharide conjugates prepared by ultrasonic treatment or classical heating. *Food Research International*, *57*, 1–7. https://doi.org/10.1016/j.foodres.2013.12.038

Li, J., Shaoyong Yu, Ping Yao, * and, & Jiang, M. (2008). Lysozyme−Dextran Core−Shell Nanogels Prepared via a Green Process. *Langmuir*, *24*, 3486–3492. https://doi.org/10.1021/LA702785B

Liu, F., Ma, C., McClements, D. J., & Gao, Y. (2016). Development of polyphenol-protein-polysaccharide ternary complexes as emulsifiers for nutraceutical emulsions: Impact on formation, stability, and bioaccessibility of β-carotene emulsions. *Food Hydrocolloids*, *61*, 578–588. https://doi.org/10.1016/j.foodhyd.2016.05.031

Liu, J., Ru, Q., & Ding, Y. (2012). Glycation a promising method for food protein modification: Physicochemical properties and structure, a review. *Food Research International*, *49*(1), 170–183. https://doi.org/10.1016/J.FOODRES.2012.07.034

Liu, Y., Zhao, G., Zhao, M., Ren, J., & Yang, B. (2012). Improvement of functional properties of peanut protein isolate by conjugation with dextran through Maillard reaction. *Food Chemistry*, *131*(3), 901–906. https://doi.org/10.1016/J.FOODCHEM.2011.09.074

Livney, Y. D. (2010). Milk proteins as vehicles for bioactives. *Current Opinion in Colloid and Interface Science*, *15*(1–2), 73–83. https://doi.org/10.1016/j.cocis.2009.11.002

Lu, Q., Tang, Q., Xiong, Y., Qing, G., & Sun, T. (2016). Protein/peptide aggregation and amyloidosis on biointerfaces. *Materials*, *9*(9). https://doi.org/10.3390/ma9090740

Markman, G., & Livney, Y. D. (2012). Maillard-conjugate based core-shell co-

assemblies for nanoencapsulation of hydrophobic nutraceuticals in clear beverages. *Food & Function*, *3*(3), 262–70. https://doi.org/10.1039/c1fo10220f

Martinez-Alvarenga, M. S., Martinez-Rodriguez, E. Y., Garcia-Amezquita, L. E., Olivas, G. I., Zamudio-Flores, P. B., Acosta-Muniz, C. H., & Sepulveda, D. R. (2014). Effect of Maillard reaction conditions on the degree of glycation and functional properties of whey protein isolate – Maltodextrin conjugates. *Food Hydrocolloids*, *38*, 110–118. https://doi.org/10.1016/J.FOODHYD.2013.11.006

McClements, D. J. (2004). Protein-stabilized emulsions. *Current Opinion in Colloid & Interface Science*, *9*(5), 305–313. https://doi.org/10.1016/J.COCIS.2004.09.003

McClements, D. J. (2005). *Food Emulsions: principles, practice and techniques* (2nd ed.). Boca Raton: CRC Press.

Monteiro, A. A., Monteiro, M. R., Pereira, R. N., Diniz, R., Costa, A. R., Malcata, F. X., … Ramos, Ó. L. (2016). Design of bio-based supramolecular structures through self-assembly of α-lactalbumin and lysozyme. *Food Hydrocolloids*, *58*, 60–74. https://doi.org/10.1016/j.foodhyd.2016.02.009

Oliver, C. M., Melton, L. D., & Stanley, R. A. (2006). Creating Proteins with Novel Functionality via the Maillard Reaction: A Review. *Critical Reviews in Food Science and Nutrition*, *46*(4), 337–350. https://doi.org/10.1080/10408690590957250

Pirestani, S., Nasirpour, A., Keramat, J., Desobry, S., & Jasniewski, J. (2016). *Effect of glycosylation with gum Arabic by Maillard reaction in a liquid system on the emulsifying properties of canola protein isolate*. *Carbohydrate Polymers*. Elsevier Ltd. https://doi.org/10.1016/j.carbpol.2016.11.044

Qiu, J., Zheng, Q., Fang, L., Wang, Y., Min, M., Shen, C., … Xiong, C. (2018). Preparation and characterization of casein-carrageenan conjugates and self-assembled microcapsules for encapsulation of red pigment from paprika. *Carbohydrate Polymers*. https://doi.org/https://doi.org/10.1016/j.carbpol.2018.05.054

Ramos, O. L., Pereira, R. N., Rodrigues, R., Teixeira, J. A., Vicente, A. A., & Xavier Malcata, F. (2014). Physical effects upon whey protein aggregation for nano-

coating production. *Food Research International*, *66*, 344–355. https://doi.org/10.1016/J.FOODRES.2014.09.036

Randhir, R., Kwon, Y.-I., & Shetty, K. (2008). Effect of thermal processing on phenolics, antioxidant activity and health-relevant functionality of select grain sprouts and seedlings. *Innovative Food Science & Emerging Technologies*, *9*(3), 355–364. https://doi.org/10.1016/J.IFSET.2007.10.004

Riddick, T. (1968). *Zeta-meter manual*. New York: Zeta-meter Inc.

Ryan, K. N., Zhong, Q., & Foegeding, E. A. (2013). Use of Whey Protein Soluble Aggregates for Thermal Stability-A Hypothesis Paper. *Journal of Food Science*, *78*(8), R1105–R1115. https://doi.org/10.1111/1750-3841.12207

Sanmartín, E., Arboleya, J. C., Villamiel, M., & Moreno, F. J. (2009). Recent Advances in the Recovery and Improvement of Functional Proteins from Fish Processing By-Products: Use of Protein Glycation as an Alternative Method. *Comprehensive Reviews in Food Science and Food Safety*, *8*(4), 332–344. https://doi.org/10.1111/j.1541-4337.2009.00083.x

Saraiva, C. S., dos Reis Coimbra, J. S., de Carvalho Teixeira, A. V. N., de Oliveira, E. B., Teófílo, R. F., da Costa, A. R., & de Almeida Alves Barbosa, É. (2017). Formation and characterization of supramolecular structures of β-lactoglobulin and lactoferrin proteins. *Food Research International*, *100*, 674–681. https://doi.org/10.1016/j.foodres.2017.07.065

Sheng, L., Su, P., Han, K., Chen, J., Cao, A., Zhang, Z., … Ma, M. (2017). Synthesis and structural characterization of lysozyme–pullulan conjugates obtained by the Maillard reaction. *Food Hydrocolloids*, *71*, 1–7. https://doi.org/10.1016/j.foodhyd.2017.04.026

Sittikijyothin, W., Torres, D., & Gonçalves, M. P. (2005). Modelling the rheological behaviour of galactomannan aqueous solutions. *Carbohydrate Polymers*, *59*(3), 339–350. https://doi.org/10.1016/J.CARBPOL.2004.10.005

Spotti, M. J., Perduca, M. J., Piagentini, A., Santiago, L. G., Rubiolo, A. C., & Carrara, C. R. (2013). Gel mechanical properties of milk whey protein-dextran conjugates obtained by Maillard reaction. *Food Hydrocolloids*, *31*(1), 26–32. https://doi.org/10.1016/j.foodhyd.2012.08.009

Sreerama, N., & Woody, R. W. (2000). Estimation of Protein Secondary Structure from Circular Dichroism Spectra: Comparison of CONTIN, SELCON, and CDSSTR Methods with an Expanded Reference Set. *Analytical Biochemistry*, *287*(2), 252–260. https://doi.org/10.1006/ABIO.2000.4880

Sun, W.-W., Yu, S.-J., Yang, X.-Q., Wang, J.-M., Zhang, J.-B., Zhang, Y., & Zheng, E.-L. (2011). Study on the rheological properties of heat-induced whey protein isolate–dextran conjugate gel. *Food Research International*, *44*(10), 3259–3263. https://doi.org/10.1016/J.FOODRES.2011.09.019

Taheri-Kafrani, A., Choiset, Y., Faizullin, D. A., Zuev, Y. F., Bezuglov, V. V., Chobert, J.-M., … Haertlé, T. (2011). Interactions of β-lactoglobulin with serotonin and arachidonyl serotonin. *Biopolymers*, *95*(12), 871–880. https://doi.org/10.1002/bip.21690

Teófilo, R. F., & Ferreira, M. M. C. (2006). Quimiometria II: Planilhas eletrônicas para cálculus de planejamentos experimentais, um tutorial. *Quimica Nova*, *29*(2), 338–350. https://doi.org/10.1590/S0100-40422006000200026

Toro-Sierra, J., Schumann, J., & Kulozik, U. (2013). Impact of spray-drying conditions on the particle size of microparticulated whey protein fractions. *Dairy Science and Technology*, *93*(4–5), 487–503. https://doi.org/10.1007/s13594-013-0124-7

Uskoković, V. (2007). Nanotechnologies: What we do not know. *Technology in Society*, *29*(1), 43–61. https://doi.org/10.1016/J.TECHSOC.2006.10.005

Vigo, M. S., Malec, L. S., Gomez, R. G., & Llosa, R. A. (1992). Spectrophotometric assay using o-phthaldialdehyde for determination of reactive lysine in dairy products. *Food Chemistry*, *44*(5), 363–365. https://doi.org/10.1016/0308-8146(92)90269-8

Wang, W., & Zhong, Q. (2014a). Improved thermal stability of whey protein-maltodextrin conjugates at pH 5.0 by d-Glucose, sucrose, d-cellobiose, and lactose. *Food Hydrocolloids*, *41*, 257–264. https://doi.org/10.1016/j.foodhyd.2014.04.025

Wang, W., & Zhong, Q. (2014b). Properties of whey protein-maltodextrin conjugates as impacted by powder acidity during the Maillard reaction. *Food Hydrocolloids*,

38, 85–94. https://doi.org/10.1016/j.foodhyd.2013.11.018

Wong, B. T., Day, L., & Augustin, M. A. (2011). Deamidated wheat protein-dextran Maillard conjugates: Effect of size and location of polysaccharide conjugated on steric stabilization of emulsions at acidic pH. *Food Hydrocolloids*, *25*(6), 1424–1432. https://doi.org/10.1016/j.foodhyd.2011.01.017

Wooster, T. J., & Augustin, M. A. (2007). Rheology of whey protein-dextran conjugate films at the air/water interface. *Food Hydrocolloids*, *21*(7), 1072–1080. https://doi.org/10.1016/j.foodhyd.2006.07.015

Yang, J.-E., Chun, S.-H., Kim, H. H., Choi, H.-D., & Lee, K.-W. (2017). Characterization of Maillard-type lysozyme-galactomannan conjugate having immune-enhancing effects. *Food Chemistry*, *227*, 149–157. https://doi.org/10.1016/J.FOODCHEM.2017.01.076

Yi, J., Fan, Y., Yokoyama, W., Zhang, Y., & Zhao, L. (2016a). Characterization of milk proteins–lutein complexes and the impact on lutein chemical stability. *Food Chemistry*, *200*, 91–97. https://doi.org/10.1016/j.foodchem.2016.01.035

Yi, J., Fan, Y., Zhang, Y., Wen, Z., Zhao, L., & Lu, Y. (2016b). Glycosylated α-lactalbumin-based nanocomplex for curcumin: Physicochemical stability and DPPH-scavenging activity. *Food Hydrocolloids*, *61*, 369–377. https://doi.org/10.1016/j.foodhyd.2016.05.036

Yi, J., Fan, Y., Zhang, Y., Wen, Z., Zhao, L., & Lu, Y. (2016a). Glycosylated α-lactalbumin-based nanocomplex for curcumin: Physicochemical stability and DPPH-scavenging activity. *Food Hydrocolloids*, *61*, 369–377. https://doi.org/10.1016/j.foodhyd.2016.05.036

Yi, J., Lam, T. I., Yokoyama, W., Cheng, L. W., & Zhong, F. (2014). Controlled Release of β-Carotene in β-Lactoglobulin–Dextran-Conjugated Nanoparticles' in Vitro Digestion and Transport with Caco-2 Monolayers. *Journal of Agricultural and Food Chemistry*, *62*(35), 8900–8907. https://doi.org/10.1021/jf502639k

Supplementary material

1. x-ray crystal of α-la in native state with lysine marked in red color

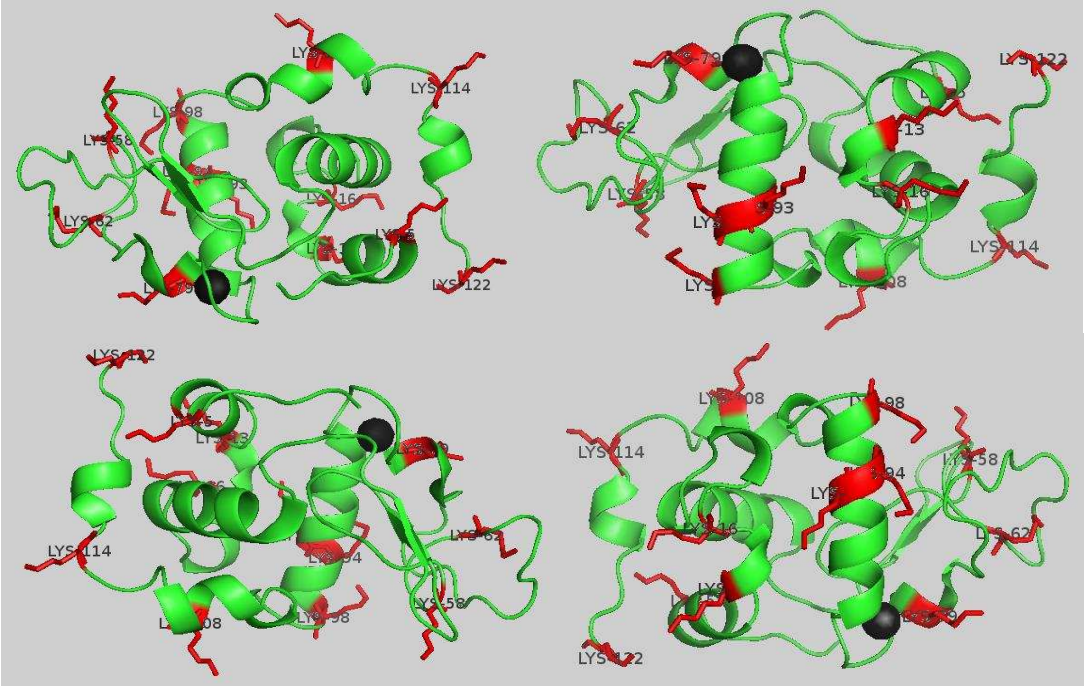

Source: Chrysina, Brew, & Acharya (2000) PDB. PyMOL-Molecular Graphics System 1.7.0.0 was used on the image processing.

2. Regression analysis for α-la-TG (L) and α-la-TG (SD) systems

System	α-la-TG (L)		α-la-TG (SD)	
Term	**Regression coefficient for Size (Y_1)**	***p***	**Regression coefficient for Size (Y_1)**	***p***
Constant	1017,102	0,6299	2365,988	0,1837
Linear				
X_1	-20,516	0,6658	-25,601	0,5019
X_2	174,054	0,4273	-178,550	0,5019
X_3	-26,670	0,4652	-39,811	0,1901
Quadratic				
X_1*X_1	0,245	0,4691	0,075	0,7761
X_2*X_2	6,619	0,5429	4,337	0,6142
X_3*X_3	0,349	0,3112	0,135	0,6124
Interaction				
X_1*X_2	-3,290	0,1697	1,109	0,5366
X_1*X_3	0,239	0,5489	0,430	0,1967
X_2*X_3	-1,954	0,3934	0,449	0,8001
R^2	0,46949		0,53184	

Note: Statistically significant (p-value < 0,05);
X_1:temperature; X_2:pH; X_3: heating time; Y_1: Mean diameter;
R^2:coefficient of determination

ARTICLE 2

Nanostructured systems formed from conjugates of β-lactoglobulin and tara gum

ABSTRACT

Nanostructures from conjugates of β-lactoglobulin (β-lg) and Tara Gum (TG) were obtained via heat-gelation process with pH adjustment. The conjugates were produced by Maillard reaction using the dry-heating method and they were characterized by browning index (*BI*) and percentage of free amino groups (*% FAG*). The nanostructured systems were characterized by (*i*) dynamic light scattering, zeta potential, circular dichroism and intrinsic fluorescence to evaluate the structures, (*ii*) transmission electron microscopy to evaluate the morphology, and (*iii*) foaming ability and emulsifying stability to determinate if the systems exhibit technological functionalities. The most appropriate time of conjugation was 2 days. The spray-dried and lyophilized mixtures presented different values of *BI* and *% FAG* ($p < 0.05$). Nanostructures from conjugates with average sizes lower than 300 nm were formed under different process conditions. Analyses of circular dichroism and intrinsic fluorescence showed conformational changes in the nanostructures, mainly a decrease in the α-helix content. The use of process conditions at 50 °C, pH 9.2, 45' showed lower foaming capacity and greater emulsifying stability compared to the control (pure β-lg). Nanostructures have potential use in the food industry.

Keywords: Maillard reaction, glycosylation, conjugates, emulsifying stability, foaming ability.

1. Introduction

Several proteins are natural, nontoxic, easily available, and cost-effective emulsifiers with high nutritional values and superior bioavailability. These biomolecules provide techno-functional properties to the systems in which are added such as solubility, foaming ability, emulsification, film formation and gelification (Adjonu, Doran, Torley, & Agboola, 2014; Yi, Fan, Yokoyama, Zhang, & Zhao, 2016).

Whey proteins are being highly used in the nanotechnology and food industries due to their techno-functional properties and their safe nutritional ingredient (GRAS) classification. These proteins can act as gelling agent and can form aggregate whose particle sizes are easily monitored. Moreover, they have the ability to combine polysaccharides and bioactive compounds among other materials (Ramos et al., 2014).

However, the net surface electrical charge of whey proteins is reduced when the pH is close to their isoelectric point (pI), which leads to their aggregation and instability and, consequently, restricts the application in food matrices (Yi, Lam, Yokoyama, Cheng, & Zhong, 2014; Yi, Fan, Zhang, et al., 2016b; Saraiva et al., 2017). The protein stability is affected by the use of high temperatures, prolonged heating times, salt concentration (ionic strength), organic solvents and proteolytic agents (McClements, 2004; Oliver, Melton, & Stanley, 2006; Liu, Zhao, Zhao, Ren, & Yang, 2012). The use of these type of agents results in flocculation and aggregation process. Conjugation of whey proteins with polysaccharides through the Maillard reaction can enhance the protein stability at certain environmental conditions and intensify techno-functional properties (Sanmartín, Arboleya, Villamiel & Moreno, 2009; Álvarez, García, Rendueles, & Díaz, 2012; Corzo-Martínez, Sánchez, Moreno, Patino, & Villamiel, 2012; Spotti et al., 2013). In the Maillard reaction, the protein and the polysaccharide are linked by a covalent bond between the ε-amino group of the lysine residues, and the carbonyl group of the polysaccharides (Kato, 2002; J. Liu, Ru, & Ding, 2012; Markman & Livney, 2012). This process occurs under controlled conditions of time, temperature, and relative humidity. Whey proteins are resistant to aggregation after grafting with maltodextrins (Wang & Zhong, 2014a). WPI-red seaweed conjugates revealed better foaming stability (Chiu, Chen, & Chang, 2009). Lesmes & McClements (2012) recently reported that the stability of nanoemulsions was significantly improved in gastrointestinal digestion conditions when the lipolysis were controlled by β-lactoglobulin-dextran conjugates. Glycosylated β-lactoglobulin can be

used as food ingredient and it reduces oxidative reactions (Morgan, Léonil, Mollé, & Bouhallab, 1997).

β-lactoglobulin (β-lg), the first most abundant whey protein in cow's milk, is characterized by having a globular three-dimensional structure, presenting in its primary structure 162 amino acid residues, molecular weight of approximately 18.3 kDa, isoelectric point equal to 5.4 (Bromley, Krebs, & Donald, 2005; Alves, Brenneisen, Ninni, Meirelles, & Maurer, 2008; Wijaya, Van der Meeren, & Patel, 2017). This protein presents high solubility (~ 97%) over a wide pH range, but mainly at low pH values (3 pH), being stable under these conditions (Chatterton, Smithers, Roupas, & Brodkorb, 2006).

Among the diverse polysaccharides present on the market, one can find the tara gum (TG), which is recognized as food additive in several countries and it is mainly used as a thickener and stabilizer whose rheological properties are crucial for the consistency and viscosity of food products (Sittikijyothin, Torres, & Gonçalves, 2005). In addition, some studies described the possibility of using this biomolecule in the formation of gels, films and coatings with other polysaccharides and/or proteins (Cerqueira et al., 2009). There are many studies that report the behavior of the tara gum, however, research involving conjugation of whey proteins with tara gum are scarce (Jiménez-Castaño et al., 2007). Thus, we assume that β-lactoglobulin conjugated with tara gum through the Maillard reaction will improve the stability under severe environmental condition of protein.

In this research, the production of nanostructures from conjugates of β-lg-tara gum was investigated. The characterization of conjugates was performed using dynamic light scattering, zeta potential, circular dichroism and intrinsic fluorescence. Techno-functional properties were also determined. The morphological characteristics were assessed through transmission electronic microscopy.

2. Material and methods

Powder of β-lactoglobulin (β-lg; 95% protein, 90% of which is β-lg) was kindly donated by Davisco Food International, Inc. (Eden Prairie, MN, USA). Tara gum (TG) was purchased from GastronomyLab (Brasilia, Brazil). Both chemicals were used as furnished without further purification. All other chemicals were of analytical grade

and also used without further purification. Deionized water (Millipore Co., MA, USA) was used in all the experiments

2.1. Preparation of β-lg-TG conjugates

Individually dispersions of β-lg and TG were prepared at 2 $mg \cdot mL^{-1}$ concentration. Mixtures of β-lg+TG were formed by adding dispersions of α-la and TG (1:1, w/w) and stirring the mixtures at 25 $\pm$ 0.1 °C for 12 h (Kato, 2002). Two drying methods for mixture dehydration were tested, the lyophilization (L) and the spray dry (SD) methods. In the first one, the mixtures were frozen at -55 ºC for 5 h (Ultra freezer, Terroni, Brazil) and lyophilized (Lyophilizer LS 3000, Terroni, SP, Brazil) by a first drying step at -45 °C and pressure of 400 mTorr during 40 h, followed by a secondary drying step at 20 °C and pressure of 200 mTorr during 8 h. In the second method, the mixtures were spray-dried (Mini-Spray Dryer model B-290, Büchi Laboratoriums-Technik, Flawil, Switzerland) by using inlet temperature (T_{inlet}) of 160 °C, outlet temperature (T_{outlet}) of 90 °C, air flowrate (F_{air}) of 40 $m^3 \cdot h^{-1}$, and feeding rate (F_r) of 250 $mL \cdot h^{-1}$ (Wang & Zhong, 2014b). Mass of 0.250 g of lyophilized, and/or spray-dried, mixture powder was incubated at 60 °C and 79 % of relative humidity in a desiccator (approx. 0.8 L volume). Relative humidity was maintained constant by using saturated KBr (Vetec, RJ, Brazil) solution. Each system required 3 h to reach the equilibrium condition (60 °C and 79 % RH). After this interval, the heating time was immediately recorded, then samples were collected during 9 days (at the days 1, 2, 3, 5, 7, and 9) and they were kept refrigerated (4 ºC) until analysis.

2.2. Conjugate characterization

The browning index (*BI*) and the percentage the free primary amino groups (*% FAG*) of systems were evaluated in order to determine the most appropriate incubation time to obtain the conjugates.

2.2.1. Browning index determination

The extent of the Maillard reaction of the β-lg -TG conjugate powders (L or SD) was monitored by means of the brown color appearance using a colorimeter (Chroma Meter CR-300 series, Konica Minolta Sensing, Inc., USA). The CIE Lab system defined in rectangular coordinates (*L**, *a**, *b**), with diffuse illumination/0° was applied and then the browning index (*BI*) was calculated according to Equations (1) and (2) (Martinez-Alvarenga et al., 2014)

$$BI = \frac{100(x - 0.31)}{0.172} \quad (1)$$

$$x = \frac{a + 1.75\,(L)}{5.645(L) + a - 3.012(b)} \quad (2)$$

Where *L*, *a*, and *b* are, respectively, the values of lightness, of green–red and of blue–yellow color components obtained in the colorimeter, *BI* is the browning index, and *x* is the value obtained in Equation (2). Mixture (L or SD) of β-lg+TG without heat treatment was used as control.

2.2.2. Free amino groups detection

The degree of modification of the primary amino groups was measured indirectly using a colorimetric assay based on the reaction between o-phthalaldehyde (OPA, Sigma-Aldrich, Austria) and the primary amine group (-NH_2) in proteins (OPA technique) (Vigo, Malec, Gomez, & Llosa, 1992; Sun et al., 2011). A volume of 200 μL of β-lg-TG conjugate dispersion (2 mg·mL^{-1}) prepared with L or SD powder was mixed with 800 μL of 0.1 mol·L^{-1} sodium tetraborate buffer solution (Fmaia, São Paulo, Brazil), 100 μL of 20 % (w/v) sodium dodecyl sulfate (SDS) (USB, Cleveland, USA), and 100 μL 2-mercaptoethanol (Vetec, RJ, Brazil). Then, the systems were subjected to heating in a thermostatic bath (Tecnal, Sao Paulo, Brazil) at 90 °C for 5 min. OPA reagent was prepared immediately before using: 80 mg of OPA was dissolved in 2 mL of pure ethanol (Sigma-Aldrich, St. Louis, USA) and added of 50 mL of 0.1 mol·L^{-1} sodium tetraborate buffer solution (pH 9.85), 0.2 mL of 2-mercaptoethanol (Vetec, RJ , Brazil), and 5 mL of 20 % (w/v) SDS. The reagent was made up to 100 mL with deionized water. Conjugate dispersion (100 μL) was mixed with 2 mL of OPA reagent and the resulted mixture was stirred in vortex (Phoenix, São Paulo, Brazil). Absorbance of systems was measured at 340 nm (Spectrophotometer Care 50 Probe, Varian, Japan). The decrease in free amino groups (*FAG*) of conjugates was calculated using pure β-lg dispersion, without incubation stage, as control and reference (100 %), by means of Equation (3):

$$FAG\ (\%) = \frac{A_C}{A_{\beta-\mathrm{lg}}} * 100 \quad (3)$$

Where A_C is the absorbance of the conjugates and $A_{\beta-\mathrm{lg}}$ the of β-lg control absorbance.

2.3. Production of nanostructures from β-lg-TG conjugates

The heat-gelation process with pH adjustment was used to produce nanostructures from β-lg-TG conjugates (Li, Yu, Yao, & Jiang, 2008). Dispersions of 2 mg·mL^{-1} from β-lg-TG conjugates (L or SD) were prepared, pH value was adjusted using HCl (Vetec, RJ, Brazil) (0.1 mol·L^{-1}) or NaOH (Vetec, St. Louis, USA) (0.1 mol·L^{-1}). The systems were subjected to heating in a thermostatic bath (TE-184, Tecnal, Brazil). The dispersions containing the formed nanostructures were immediately cooled in an ice bath and kept at 4 °C until their characterization. Different values of pH, temperatures and heating times (Table 1) were evaluated following a central composite design (CCD) in order to evaluate the combined effect of these variables on the particle size of α-la-TG nanostructures, with 2^3 factorial and star design with three central points as shown in Table 2. The values of pH and temperature were defined according to the isoelectric point (5.4) and the denaturation temperature (85 °C) of pure β-lg in aqueous solution, respectively as suggested by Teófilo & Ferreira (2006).

Table 1. Uncoded and coded levels of independent variables used in the CCD

Independent variable	Coded and uncoded levels				
	-α	-1	0	1	+α
Temperature (°C)	39.8	50	65	80	90.2
pH	2.1	3.9	6.5	9.2	11
Time (min)	4.8	15	30	45	55.2

2.4. Characterization of the nanostructures

2.4.1. Dynamic light scattering analysis (DLS)

DLS measurements of 2 mg·mL^{-1} β-lg-TG (L or SD) nanostructured dispersions were used in order to determine the mean hydrodynamic diameter of their particles (Z-average). Experimental runs in triplicate were conducted at (25.0 ± 0.1) °C in polystyrene cuvettes by using a particle size instrument (Zetasizer Nano ZS, Malvern Instruments Ldt, United Kingdom) equipped with an avalanche photodiode detector, a digital correlator (TurboCor), and a helium–neon (HeNe) laser (4 mW and 632.8 nm) as source of linearly polarized light. The scattered intensity was measured under a 173° detection angle with respect to the source. The autocorrelation function was analyzed by the CONTIN algorithm to determine the size distribution (in nanometers). Dispersions of pure β-lg and of β-lg+TG mixture (without heat treatment) were used as control.

2.4.2. ζ-potential analysis

ζ-potential measurements of 2 mg·mL^{-1} β-lg-TG nanostructured dispersions were performed in triplicate using the technique of laser doppler micro electrophoresis to determinate the net surface electrical charge of the nanostructures. The experimental runs were conducted at (25.0 ± 0.1) °C in disposable folded capillary cuvettes by using an apparatus (Zetasizer Nano ZS, Malvern Instruments Ldt, United Kingdom) equipped with a HeNe laser (4 mW). Dispersions of pure β-lg and of β-lg+TG mixture (without heat treatment) were used as control.

Table 2. Central composite design with decoded values of three variables (temperature, pH, time) with three central points (assays 15, 16, 17).

Assay	Temperature (°C)	pH	Time (min)
1	50.0	3.9	15.0
2	50.0	3.9	45.0
3	50.0	9.2	15.0
4	50.0	9.2	45.0
5	80.0	3.9	15.0
6	80.0	3.9	45.0
7	80.0	9.2	15.0
8	80.0	9.2	45.0
9	39.8	6.5	30.0
10	90.2	6.5	30.0
11	65.0	2.1	30.0
12	65.0	11.0	30.0
13	65.0	6.5	4.8
14	65.0	6.5	55.2
15	65.0	6.5	30.0
16	65.0	6.5	30.0
17	65.0	6.5	30.0

2.4.3. Molecular fluorescence spectroscopy analysis (FI)

Fluorimetry measurements of 2 mg·mL^{-1} β-lg-TG nanostructured suspensions were obtaining in order to determinate conformational changes in the structures. The experimental runs were conducted at (25.0 ± 0.1) °C by using a spectrofluorometer (ISS, K2, USA), at wavelength ranging from 290 to 450 nm, quartz cuvettes of 10 mm path length (Hellma Analytics, Germany), and with tryptophan (Trp) and tyrosine (Tyr) excitation source of 285 nm (Taheri-Kafrani et al., 2011). Spectra were baseline-

corrected by subtracting blank spectra (Milli-q water). Dispersions of pure β-lg and β-lg+TG mixture (without heat treatment) were used as control.

2.4.4. Circular dichroism (CD) spectroscopy

CD measurements of 2 mg·mL^{-1} β-lg-TG nanostructured dispersions were determined in order to assess modifications in the secondary structure of the particles. The experimental runs were conducted at (25.0 $\pm$ 0.1) °C by using a spectropolarimeter (Jasco Corporation, J-810, Japan), equipped with a temperature controller (Jasco Corporation, Peltier PFD 425S, Japan) coupled to a thermostatic bath (Julabo, AWC 100, Germany), in quartz cuvettes of 10 mm path length (Hellma Analytics, Germany), at wavelength ranging from 190 to 260 nm, under constant nitrogen rate. Each spectrum was obtained by averaging ten consecutive measurements and was baseline-corrected by subtracting blank spectra (Milli-q water). Dispersions of pure β-lg (without heat treatment) were used as control. CD data were normalized to mean residual molar ellipticity, applying Equation (4):

$$[\theta] = \frac{\theta \cdot 100 \cdot MM}{aa \cdot c \cdot l} \quad (4)$$

Where θ is the CD signal (degrees), *MM* is the protein molar mass (kDa), *aa* is the number of amino acid residues, *c* is the protein concentration (mg·mL^{-1}) and *l* is the optical path of the cuvette (cm). Deconvolution of the residual molar ellipticity data of the systems was performed by means the CONTIN/LL - Reference 4 analysis method, according to Sreerama & Woody (2000).

2.4.5. Stability of β-lg-TG nanostructures during storage

Nanostructured systems presenting mean hydrodynamic diameters varying between 10 and 300 nm (Uskoković, 2007) were selected to carry out stability analysis of particle size over 45 days, at 4 °C. Nanostructure sizes were measured at 1, 3, 10, 22, 30 and 45 days of storage.

2.5. Techno-functional properties of β-lg-TG nanostructures

Foaming ability and emulsifying stability were evaluated for systems, which present the most stable distribution of particle size during storage. Foaming ability

2.5.1. Foaming ability

In order to evaluate the foaming ability of the systems, aliquots (15 mL) of nanostructured dispersions (2 mg·mL^{-1}) were added in a beaker (50 mL) and then

homogenized (Ultra turrax, IKA, DI 25 Basic, Germany) during 72 s, at 13,500 rpm. Dispersions of pure β-lg and β-lg+TG mixture (without heat treatment) were used as control. The increase of the volume was determined by measuring the total volume and the foam volume, immediately after homogenization, according to Equation (5):

$$VI\ (\%) = \frac{B - A}{A} * 100 \quad (5)$$

Where *VI* is the volume increase (%), *A* is the initial volume of samples before agitation (mL), and *B* is the final volume of samples after agitation (mL).

Foam stability (*FS*) was measured immediately after stirring. The change in foam volume was calculated after agitation and at 5 min intervals up to 120 min. Equation (6) was used to determinate the foam stability (%):

$$FS\ (\%) = \frac{V_{ft}}{V_{f0}} * 100 \quad (6)$$

Where V_{f0} is the foam volume (mL) of samples at time 0 and V_{ft} is the foam volume of samples after time *t*. Experiments were done in triplicate.

2.5.2. Emulsifying stability

To evaluate the emulsifying stability of β-lg-TG nanostructures, the emulsion stability index (*ESI*) was calculated according to McClements (2005). Oil-in-water emulsion (15 % w/w) was prepared with 0.91 g of soy oil and 5.17 g of β-lg-TG nanostructure dispersions (2 mg·mL^{-1}). The mixture was kept in agitation (Ultra Turrax, IKA, DI 25 Basic, Germany) at 13,500 rpm for 1 min, at 25 °C; after that, it was immediately homogenized (Ultrason Unique homogenizer, DES500, Brazil) at amplitude of 40 % and power of 300 W for 1 min in ice-water bath. The oil droplet size (Z-average) of the emulsions was measured on the Zetasizer Nano ZS (Malvern Instruments Inc., UK) at 0, 30 and 60 min after the formation of emulsions. Equation (7) was used to calculate *ESI*:

$$ESI = \frac{d(0)}{d(t) - d(0)} \quad (7)$$

Where $d(0)$ is the initial mean droplet diameter (nm) of the emulsion and $d(t)$ is the mean droplet diameter (nm) measured at time *t* (30 and 60 min). Pure β-lg and β-lg+TG

mixture without heat treatment were used as control. Experiments were done in triplicate.

2.6. Morphological characterization

2.6.1. Transmission electronic microscopy (TEM)

Systems used in the TEM analysis were prepared by drying β-lg-TG nanostructure dispersions at room temperature for 24 h. A drop of the dispersion was deposited onto 200 mesh copper grids coated with thin films of Formvare carbon (Koch Electron Microscopy, Brazil). The samples were then negatively stained with uranyl acetate (2 % w/w) (Merck, Germany) for 15 s. Images of β-lg-TG nanostructures was obtaining on the equipment (transmission electron microscopy Zeiss, 43 model 109, Oberkochen, Germany) with accelerating voltage of 80 kV.

2.7. Data analysis

In aiming to select the most appropriate incubation time to form nanostructured β-lg-TG conjugates, significant differences among means of both variables the browning index and the percentage of free amino groups were evaluated by means of the Tukey HSD test with $p < 0.05$ using the *Statistica* 10® software. Data were expressed as mean ± standard deviation. Normal probability plots were constructed by using *Statistica* 10® software. Through of the DLS analysis, the most appropriate conditions for obtaining the nanostructures were determined. Data of techno-functional properties and stability during storage were evaluated using the analysis of variance (ANOVA) and the Tuckey and Dunnett tests ($p < 0.05$) with the *Statistica* 10® software, respectively.

3. Results and discussion

3.1. Characterization of β-lg-TG (L) and β-lg-TG (SD) conjugates

3.1.1. Browning index and percentage of free amine groups

The brown color occurrence and reduction on the percentage of free amine groups of proteins are clear indicators of the progression of the Maillard reaction (de Oliveira, Coimbra, de Oliveira, Zuñiga, & Rojas, 2014; Wooster & Augustin, 2007). In the present research, the color development and the percentage of free amino groups were measured by *BI* and OPA method, respectively.

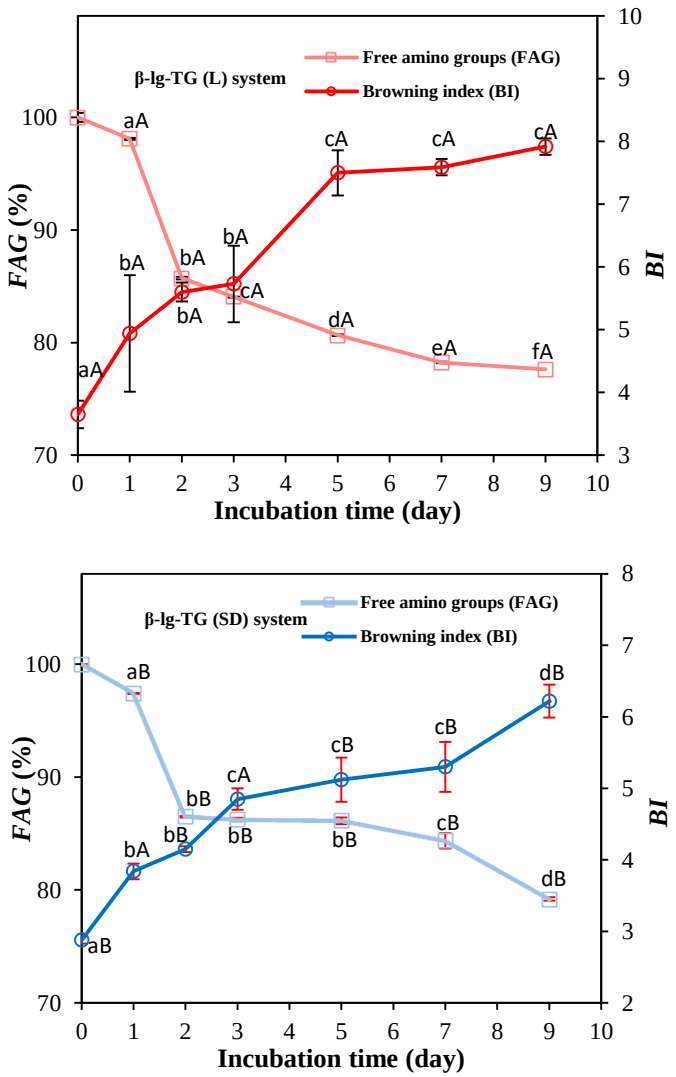

Fig. 1. Browning Index (*BI*) and percentage of free amine groups (% *FAG*) for (a) β-lg-TG (L) and (b) β-lg -TG (SD) systems. Values with the same lower-case letter in each line are not different by Tukey test ($p > 0.05$). Values with the same upper-case letter for each day and the same response are not different by Tukey test ($p > 0.05$). The measurements were done in triplicate.

The results are shown in Fig. 1 for β-lg-TG (L) and β-lg-TG (SD) conjugates obtained by the dry-heating method. Both systems showed a significant increase in *BI* values with increasing heating time ($p < 0.05$). Spotti et al. (2013) and Martinez-Alvarenga et al. (2014) found an increase in *BI* with increasing heating time in WPI-dextran and WPI-maltodextrins conjugates, respectively. The major color difference was noted after 5 days of dry-heating. In smaller periods, the changes occurred more slowly (Fig. 2). These color differences from day 5 may give some indication of stage transitions from the Maillard reaction (intermediate or advanced stage) in which the production of colored compounds known as melanoidins occurs.

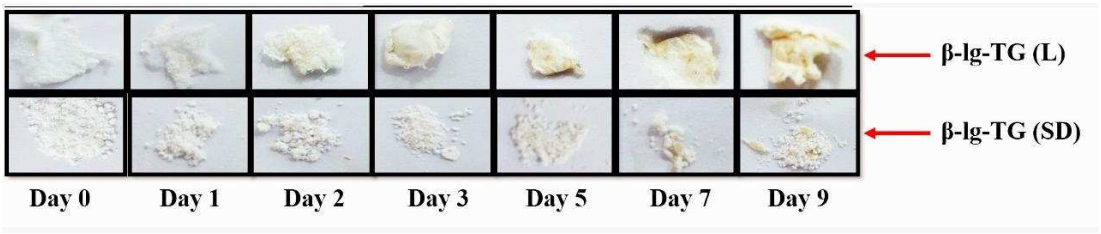

Fig. 2. Images of β-lg-TG (L) and β-lg-TG (SD) systems with different heating times.

On the other hand, the progress of the Maillard reaction was studied by the determination of free amino groups (% *FAG*), because changes in coloration may be related to caramelization reactions (Randhir, Kwon, & Shetty, 2008). The results observed in Fig. 1 showed that *% FAG* decreases with increasing heating time for both systems. These results were expected since the progression of Maillard reaction increases over longer times. One may notice that glycosylation is more pronounced in the first days of heating (1 and 2 days), indicating a reduction of *% FAG* at higher intensity. This suggests that the covalent attachment to the polysaccharides occurs on the first days of heating. Similar results were found by Aoki et al. (1999), Morris, Sims, Robertson, & Furneaux (2004) and Y. Sun, Hayakawa, & Izumori (2004) in lysozyme, ovalbumin, and soy protein fraction.

The decrease in the *% FAG* coincided with the increase in *BI*. This suggests that the β-lg glycosylation with TG occurred satisfactorily. Based on the results obtained, we considered that the appropriate time of glycosylation for the β-lg-TG (L) and β-lg-TG (SD) systems for was 2 days. In larger reaction times with higher *BI* values and lower *% FAG* values (Fig. 1), the glycosylation reaction may occur simultaneously with the formation of final products of the Maillard reaction, which may cause damages to human health.

On the other hand, the effect of the lyophilization and spray dry operations on the glycosylation reaction was evaluated. *BI* values and *% FAG* for β-lg-TG (SD) systems (Fig. 1b) were statistically different ($p < 0.05$) compared to the β-lg-TG (L) system values (Fig. 1a), suggesting that the Maillard reaction rate was lower in spray-dried mixtures. The spray dry operation employs high temperatures (160-210 °C), which may promote the partial unfolding of β-lg, resulting in an irreversible aggregation of this protein (Toro-Sierra, Schumann, & Kulozik, 2013). This process occurs at an air-water interface and the partially unfolding proteins expose the hydrophobic groups to

the air, promoting self-association with the protein aggregates formation (Donaldson, Boonstra, & Hammond, 1980; Fink, 1998; Lu, Tang, Xiong, Qing, & Sun, 2016). These agglomerates are in a dry environment in which hydrophilic residues such as lysine are inside the interior of the molecule. Therefore, the number of amino groups available from lysine is reduced. This fact and a reduction in the interfacial area of the system decrease the probability of the occurrence of β-lg glycosylation with TG, resulting in a decrease in the reaction progress. In contrast, in the lyophilization operation, β-lg maintains a higher proportion of the native state, which is characterized by having the largest lysine number on the protein surface (see supplementary material, item 1), increasing the probability of occurrence of covalent bonds between β-lg and TG.

3.2. Production of nanostructures from α-la-TG conjugates

β-lg-TG conjugates obtained under controlled conditions (60 ° C, 79 % RH and heating time of 2 days) showed an appropriate relationship between *BI* and *% FAG*. Nanostructures from this conjugates were produced by heat-gelation process, evaluating the effect of temperature, pH and heating time (Table 2).

3.3. Characterization of nanostructures from β-lg-TG conjugates

3.3.1. Dynamic light scattering analysis (DLS)

Data of size of β-lg-TG nanostructured systems and controls (pure β-lg and β-lg+TG mixture without heat treatment and pH adjustment) are shown in Table 3. The main populations defined here refer to those as the highest percentage in size distribution by volume.

In general, the size distribution of both systems showed mean diameter values greater than the mean diameter of the pure β-lg. This protein exhibits 15 amino acid residues of lysine (Sgarbieri, 2005) with potential amino groups that could bind covalently to the carbonyl groups of TG, resulting in an increase in particle size (Sheng et al., 2017). A similar trend was found in lysozyme-galactomannan nanostructures (Yang, Chun, Kim, Choi, & Lee, 2017).

Table 3. Dynamic light scattering of (L) and (SD) β-lg-TG nanostructures, β-lg+TG mixture and native β-lg protein at different process conditions.

Treatment	System		β-lg-TG (L)			β-lg-TG (SD)		
			D_h	% VD	PDI	D_h	% VD	PDI
1	50 °C, pH 3.9, 15'	Peak 1	2171	96.8		1577	100	
		Peak 2	351.1	3.2	0.731	-	-	0.773
		Peak 3	-	-		-	-	
2	50 °C, pH 3.9, 45'	Peak 1	1590	84.7		692.4	85.2	
		Peak 2	4935	5.1	1.000	71.7	14.8	0.872
		Peak 3	56.4	10.2		-	-	
3	50 °C, pH 9.2, 15'	Peak 1	837.4	29.8		1047	2.1	
		Peak 2	110.2	6.4	0.652	143.3	97.2	0.659
		Peak 3	27.4	62.6		5438	0.7	
4	50 °C, pH 9.2, 45'	Peak 1	1015	64.2		1132	17.5	
		Peak 2	4521	24.3	0.891	96.9	74.6	0.437
		Peak 3	81.88	11.14		4858	7.9	
5	80 °C, pH 3.9, 15'	Peak 1	2047	98.8		1298	93.1	
		Peak 2	154.5	1.2	0.660	96.9	3.4	0.830
		Peak 3	-	-		5176	3.6	
6	80 °C, pH 3.9, 45'	Peak 1	1106	93.2		2107	100	
		Peak 2	92.7	4.2	0.814	-	-	0.577
		Peak 3	5551	2.5		-	-	
7	80 °C, pH 9.2, 15'	Peak 1	30.5	60.2		73.9	23.9	
		Peak 2	2107	1.8	0.530	204.1	76.1	0.467
		Peak 3	267.3	38.0		-	-	
8	80 °C, pH 9.2, 45'	Peak 1	278.9	98.7		1271	77.4	
		Peak 2	26.1	0.7	0.430	78.4	11.9	1.000
		Peak 3	113.1	0.1		4356	10.7	
9	39.8 °C, pH 6.5, 30'	Peak 1	648.4	14.0		70.41	25.1	
		Peak 2	3536	78.3	1.000	278.4	66.4	0.376
		Peak 3	61.65	7.7		4404	8.5	
10	90.2 °C, pH 6.5, 30'	Peak 1	746.6	69.8		53.46	22.6	
		Peak 2	80.4	27.3	0.804	288	67.1	0.528
		Peak 3	5590	2.9		2269	10.2	
11	65 °C, pH 2.1, 30'	Peak 1	41.7	36.2		34.7	41	
		Peak 2	1467	57.3	1.000	187.6	55.7	0.515
		Peak 3	4979	6.4		1692	3.3	
12	65 °C, pH 11, 30'	Peak 1	978.2	43.9		779.2	53.8	
		Peak 2	2891	51.6	1.000	4370	30.9	0.890
		Peak 3	122.9	4.5		86.16	15.3	
13	65 °C, pH 6.5, 4.8'	Peak 1	3026	62.6		873.3	46.1	
		Peak 2	817.7	28.7	1.000	4333	39.2	1.000
		Peak 3	99.46	8.8		91.2	14.7	
14	65 °C, pH 6.5, 55.2'	Peak 1	56.1	16.4		76.6	10.7	
		Peak 2	358.2	6.7	1.000	2344	89.3	1.000
		Peak 3	2172	76.9		-	-	
15	65 °C, pH 6.5, 30' (CP)	Peak 1	1378	52.0		2336	43.9	
		Peak 2	195.1	4.2	1.000	386.2	6.4	1.000
		Peak 3	4940	43.8		31.9	49.7	
16	Pure β-lg	Peak 1	2.577	99.8		2.5	99.8	
		Peak 2	102.7	0.1	0.478			
		Peak 3	781.0	0.1				
17	β-lg+TG mixture	Peak 1	1348	47.7				
		Peak 2	221.5	40.6	0.602			
		Peak 3	5107	11.7				

D_h: hydrodynamic diameter; VD: volume distribution; PDI: polydispersity index; CP: central point

For β-lg-TG (L) system, heat treatments at 80 °C, pH 9.2 with 15 and 45 minutes of heating time showed a main population in the particle size of 30.49 and 278.9 nm, respectively. This suggests that under the mentioned conditions there was nanoparticle formation (Uskoković, 2007). The more basic the pH, the more negative charges the β-lg acquires, thus increasing electrostatic repulsion between particles. Saraiva et al (2017) found similar results in β-lg and lactoferrin nanostructures. At pH 3.9 and 6.5, most treatments showed values of the main population above 700 nanometers (Table 3). These values suggest that at pH close to the Isoelectric point of β-lg (pI = 5.4) the protein surface charge is close to zero, leading to the formation of agglomerates with the consequent increase in the mean particle diameter (Phan-Xuan et al., 2011; Wong, Day, & Augustin, 2011).

For β-lg-TG (SD) system, treatments with acid (2.1) and basic (9.2) pH showed a main population with mean diameter lower than 300 nm. On the other hand, treatments using high and low temperatures (90.2-39.8 °C) at pH 6.5 with 30 minutes of heating indicated the formation of nanoparticles. These results are similar to those found by Jiang & Brodkorb (2012) who obtained β-lg-Ribose nanostructures using a heat treatment of 95 °C and pH 8.5. In other conditions, mean particle diameter values were greater than 1000 nm.

On the other hand, the influence of different values of pH, temperature and heating time on the average size of the nanostructures was evaluated following the central rotational composite design. The regression analysis revealed that linear and quadratic coefficients and interaction effects of the three factors evaluated were not significant ($p > 0.05$) and there was no model adjustment according to the coefficient of determination (see supplementary material, item 2). However, an alternative way for determining the influence of the factors evaluated on the mean diameter of the nanostructures are the normal probability plots. The utilization of this type of graphs is based on the fact that the main effects (linear and quadratic) or interaction effects are distributed according to a normal distribution centered at zero with σ^2 variance, in other words, these effects have to be concentrated over a straight line in the graph. However, if the points marked on the graph seem to deviate somewhat from this line, there is reason to believe that this data is not distributed in a normal way, therefore, are significant effects, which should be analyzed in detail (Levine, Berenson, & Stephan, 1998).

Figure 3 shows the normal probability plots of the β-lg-TG (L) and β-lg-TG (SD) systems. The linear effect of the pH, the quadratic effect of temperature and the interaction between the linear effects of the temperature and pH for β-lg-TG (L) system were shown to be distant from the line (Fig. 3a). This suggests that these effects are significantly different from zero and therefore they have influence on the average diameter of the nanoparticles. For the β-lg-TG (SD) system, the linear effect of pH and the heating time showed influence (Fig. 3b).

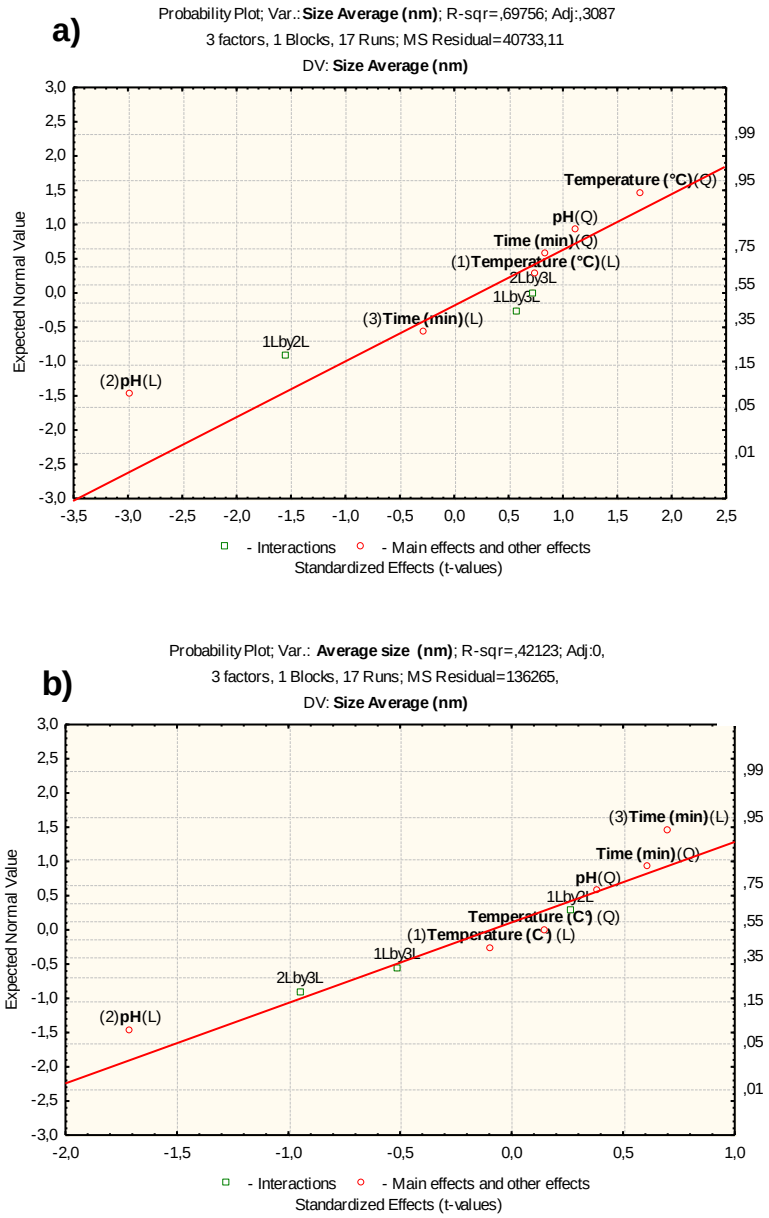

Fig. 3. Normal probability plots for β-lg-TG (L) (a) and β-lg-TG (SD) (b) systems.

3.3.2. ζ-potential analysis

The ζ-potential analysis allow to determine the net surface charge of the system. Values of zeta potential of nanostructures and controls (pure β-lg and β-lg+TG mixture without heat treatment and pH adjustment) are shown in Table 4. In general, treatments with pH values below the isoelectric point of β-lg (pI = 5.4) showed positive ζ-potential values for both systems studied. In contrast, in pH 6.5, 9.2 and 11, the surface net charge of the protein became negative because these values are above the IP of β-lg. In treatments at pH 3.9 and 6.5, close to the isoelectric point of β-lg, ζ-potential potential values were close to zero. Therefore, the net surface charge of β-lg was partially neutralized with the consequent aggregation of particles. These results are in agreement with the DLS analysis for these treatments, which indicated values of average diameter above 1000 nanometers.

Table 4. Variation of zeta potential (mV) of native protein (β-lg), β-lg+TG mixture and the nanostructures in different conditions for the β-lg-TG (L) and β-lg-TG (SD) systems.

		Zeta potential (mV)	
Treatment	**System**	**β-lg-TG (L)**	**β-lg-TG (SD)**
1	50 °C, pH 3.9, 15'	0.261	-0.086
2	50 °C, pH 3.9, 45'	1.058	0.080
3	50 °C, pH 9.2, 15'	-3.193	-3.200
4	50 °C, pH 9.2, 45'	-5.133	-4.780
5	80 °C, pH 3.9, 15'	0.611	0.037
6	80 °C, pH 3.9, 45'	0.327	0.161
7	80 °C, pH 9.2, 15'	-2.310	-7.235
8	80 °C, pH 9.2, 45'	-9.480	-2.920
9	39.8 °C, pH 6.5, 30'	-3.597	-14.150
10	90.2 °C, pH 6.5, 30'	-4.135	-2.825
11	65 °C, pH 2.1, 30'	1.523	2.305
12	65 °C, pH 11, 30'	-6.575	-8.350
13	65 °C, pH 6.5, 4.8'	-2.875	-2.680
14	65 °C, pH 6.5, 55.2'	-1.920	-3.120
15	65 °C, pH 6.5, 30'	-1.580	-2.165
16	Pure β-lg	-22.700	
17	β-lg+TG mixture	-7.740	

On the other hand, ζ-potential values for treatments at pH 6.5 were higher than the pure control β-lg (-22.70 mV). This can be attributed to the shielding effect of the TG layer outside the nanostructures, which was bound through the glycosylation reaction leading to the remarkable decrease in the ζ-potential. Similar results were found in

β-lg-dextran and α-la-dextran conjugates (Fan, Yi, Zhang, Wen, & Zhao, 2017; Lesmes & McClements, 2012). According to Riddick (1968), ζ-potential values between -30 and 30 mV indicate instability in the system. Values above 30 mV or below -30 mV indicate a high stability. In this study, all treatments showed values in the range of -30 to 30 mV for both systems studied. This result indicates that the stability of the system is not determined by electrostatic interactions but defined by hydrogen bonds and/or hydrophobic interactions (Chen et al., 2017). The decrease of the amino groups due to the glycosylation reaction and the steric hindrance of the uncharged polysaccharide may have contributed to the reduction of the ζ-potential. Similar results were found in soy protein isolate-Guar gum conjugates (Chen et al., 2017).

3.3.3. Fluorescence spectroscopy

The intrinsic fluorescence spectra of pure β-lg, β-lg+TG mixture and nanostructures for β-lg-TG (L) and β-lg-TG (SD) systems are shown in Fig. 4 and 5, respectively.

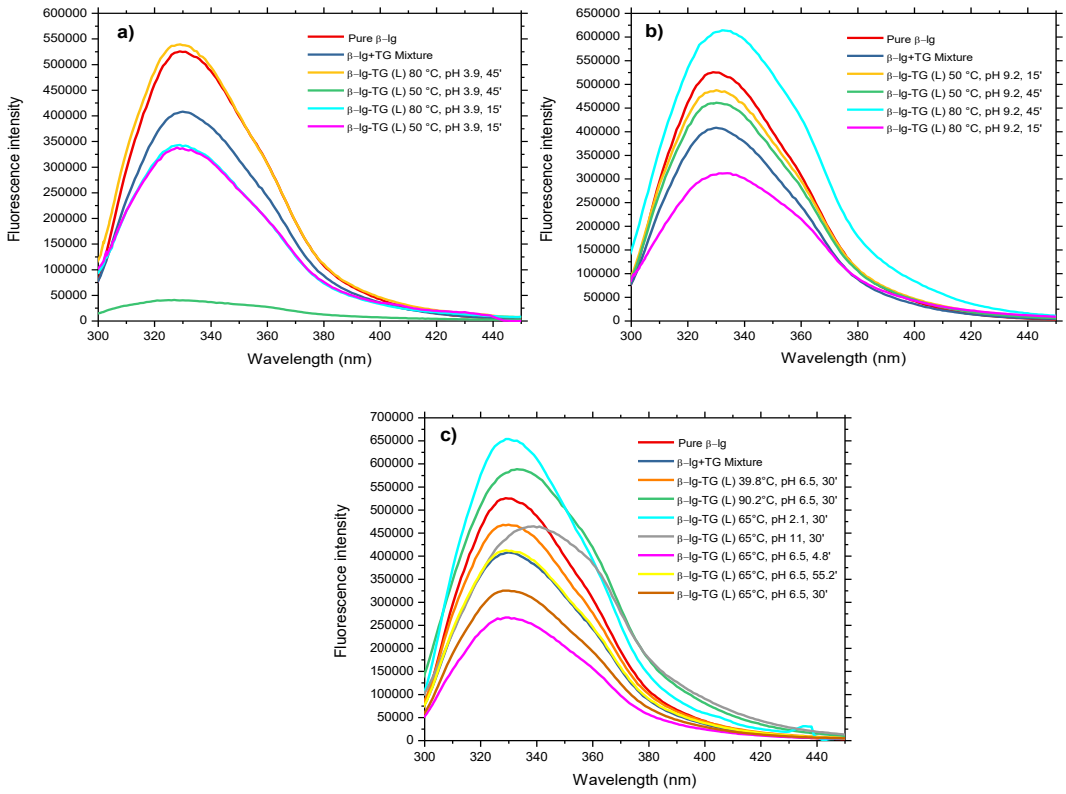

Fig. 4. Emission spectra of chromophores of pure protein (β-lg), β-lg+TG mixture and nanostructures in different conditions for β-lg-TG (L) system.

For treatments from β-lg-TG (L) system, the maximum fluorescence intensity (FI) had a decrease in value compared to the emission spectrum of the control (pure β-lg),

except for treatments 6 (80 °C, pH 3.9, 45'), 8 (80 °C, pH 9.2, 45'), 10 (90.2 °C, pH 6.5, 30') and 11 (65 °C, pH 2.1, 30') according to Fig 4. It is probable that the binding site between β-lg and TG were in the microenvironment of tryptophan and tyrosine residues (Lys 60-Trp 61; Try 99-Lys 100; Lys 101-Tyr 102), which contributed to changes in fluorescence spectra. Similar results were found in nanostructures from β-lg-PEG conjugates (Zhong et al., 2016). We noticed that samples that did not have this behavior underwent thermal treatments with high temperature and heating time, suggesting that the molecules of the chromophores were exposed to the solvent, and this could have caused the possible protein unfolding. Koch, Emin, & Schuchmann (2017) observed a similar behavior in WPI-pectin conjugates.

On the other hand, the fluorescence spectra for treatments 8 (80 °C, pH 9.2, 45') and 12 (65 °C, pH 11, 30') exhibited a marked red shift at the maximum IF compared to the emission spectrum of pure β-lg. This indicates that the surrounding microenvironment of tryptophan and tyrosine became more hydrophilic. Corzo-Martínez, Moreno, Olano, & Villamiel (2008) and Hattori, Numamoto, Kobayashi, & Takahashi (2000) found similar results in conjugates of β-lg with galactose and anionic saccharides, respectively. A possible cause of this phenomenon is the effect of the pH and temperature used in the thermal treatments. For treatment 8, the possible unfolding of β-lg due to the effect of temperature may have caused exposure of the chromophores to the solvent, which is characterized by having a higher polarity (Fig. 4b). For treatment 12, the pH highly alkaline (pH 11) may have caused an unbalance of charges resulting in a pH-induced protein unfolding, which led to the chromophores to be exposed to a more hydrophilic environment (Hidaka et al., 2015).

For the β-lg-TG (SD) system, treatments 7 (80 °C, pH 9.2, 15'), 8 (80 °C, pH 9.2, 45') and 14 (65 °C, pH 6.5, 55.2') showed higher FI values than the controls with red shift (Fig. 5b-c). The effect of higher temperatures of thermal treatments (90.2-80 °C), spray dry (160-210 °C) and high pH values may have caused conformational changes in the protein with the corresponding exposure of the chromophores in more hydrophilic environments. In addition, the β-lg glycosylation in spray-dried mixtures occurred at slower rate. This was demonstrated in the *BI* and % *FAG* analyses (Fig. 1). Therefore, a lower number of TG molecules was attached to the protein, reducing the hydrophobicity of the tryptophan surrounding microenvironment compared to other treatments.

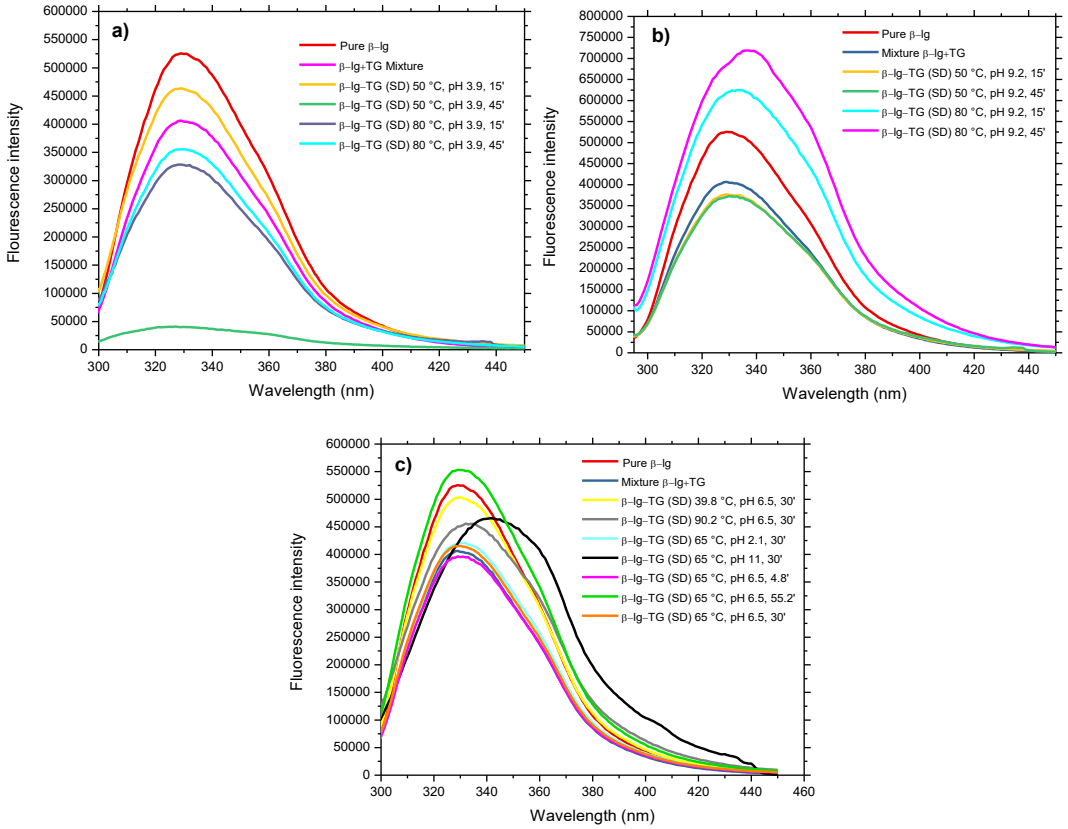

Fig. 5. Emission spectra of chromophores of pure protein (β-lg), β-lg+TG mixture and nanostructures in different conditions for β-lg-TG (SD) system.

3.3.4. Circular dichroism (CD)

Fig. 6 and 7 show the CD spectra of pure β-lg, β-lg+TG mixture and the nanostructures from β-lg-TG (L) and β-lg-TG (SD) systems, respectively. β-lg had a maximum peak negative at 216 nm since this protein is rich in β-sheet. The results showed that the covalent bond between the polysaccharide and the protein had an effect on the secondary structure of β-lg, and this is represented by changes in the height of the negative peaks in the CD spectra of the nanostructures compared to the control (Fig. 6 and 7).

For β-lg-TG (L) system, treatments 7 (80 °C, pH 9.2, 15'), 8 (80 °C, pH 9.2, 45'), 10 (90.2 °C, pH 6.5, 30') and 12 (65, pH 11, 30') showed a polysaccharide-dependence decrease of the negative absorption peak at 216 to and positive absorption peak at 195 nm (Fig. 6b-c) compared to the β-lg control. A slight shift of peak at 216 nm toward lower wavelength (blue shift) can be observed for these treatments. This suggests that the effect of high temperature values (80-90.2 °C) led to the β-lg partial unfolding (Day et al., 2014).

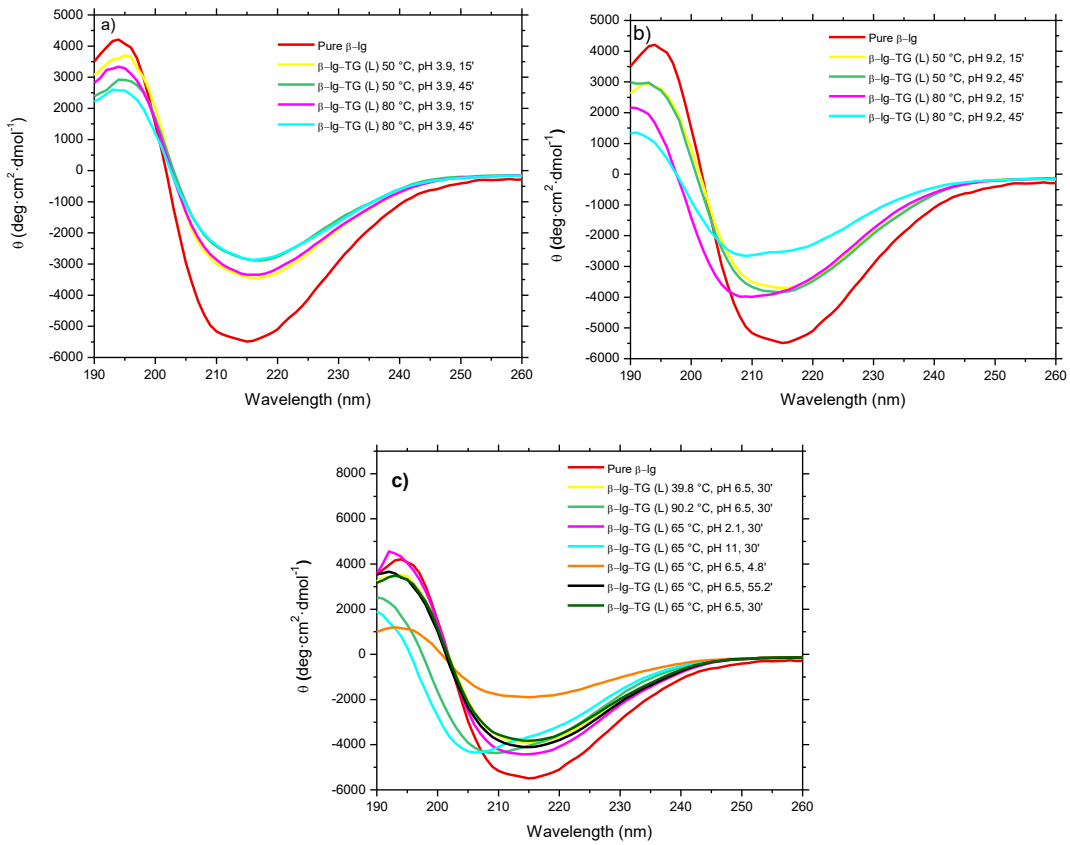

Fig. 6. CD spectra of native protein (β-lg), β-lg+TG mixture and nanostructures in different conditions for β-lg-TG (L) system.

In addition, high pH values in these treatments could have caused the increase of the polarity of the solvent resulting in blue-shifted negative peaks (Cascio & Wallace, 1999). These results are in agreement with those obtained in the fluorescence analysis for these treatments (Fig. 4b-c), which showed a red shift due to increased polarity in the Trp surrounding environment. Stanic-Vucinic, Prodic, Apostolovic, Nikolic, & Cirkovic Velickovic (2013) and Chamani, Moosavi-Movahedi, & Hakimelahi (2005) found a similar trend in conjugates of β-lg-fructose/ribose/lactose and β-lg-Cyclodextrins, respectively.

According to the results obtained by deconvolution of the CD data of the samples using the CONTIN/LL- Reference 4 analysis method (Sreerama & Woody, 2000), the secondary structure of β-lg had changes after glycosylation and the thermal treatments employed. Pure β-lg contained 14.2 % α-helix, 30.1 % β-sheet, 19.8 % turns, and 36.6 % disordered structure. We observed that there was a slight reduction in α-helix content and a small increase in β-sheet and disordered structure percentage in most treatments for β-lg-TG (L) system (Table 5). We assumed that the polysaccharide

binding sites on the β-lg were located in the α-helix regions (see supplementary material, item 1), which led to changes in spatial structure and protein unfolding(Li, Xue, Chen, Ding, & Wang, 2014). The effect of temperature, pH and heating time may have reduced more sharply the α-helix content (Day et al., 2014). This agrees with the larger decrease of α-helix in treatments 5 (80 °C, pH 3.9, 15 °C), 6 (80 °C, pH 3.9, 45'), 7 (80 °C, pH 9.2, 15'), 8 (80 °C, pH 9.2, 45'), 10 (90.2 °C, pH 6.5, 30') and 12 (65 °C, pH 11, 30') (Table 5).

Table 5. Mean values of deconvolution of the residual molar ellipticity data for β-lg-TG (L) system.

Treatment	System	Alpha-helix (%)	Beta-Sheet (%)	Turns (%)	Disordered structure (%)
	Pure β-lg	14.2	30.1	19.8	36.6
1	50 °C, pH 3.9, 15'	10.2	33.5	19.5	36.7
2	50 °C, pH 3.9, 45'	8.8	34.3	19.4	37.5
3	50 °C, pH 9.2, 15'	10.5	32.3	20.0	37.8
4	50 °C, pH 9.2, 45'	10.3	32.1	19.3	38.3
5	80 °C, pH 3.9, 15'	9.7	34.0	19.7	36.6
6	80 °C, pH 3.9, 45'	8.9	33.6	19.4	38.1
7	80 °C, pH 9.2, 15'	10.0	30.3	19.0	40.6
8	80 °C, pH 9.2, 45'	8.5	33.0	18.9	40.6
9	39.8 °C, pH 6.5, 30'	10.7	33.3	19.6	37.4
10	90.2 °C, pH 6.5, 30'	10.4	29.8	19.1	40.7
11	65 °C, pH 2.1, 30'	12.3	31.4	20.0	36.2
12	65 °C, pH 11, 30'	9.5	29.0	18.6	42.9
13	65 °C, pH 6.5, 4.8'	11.0	33.5	20.0	37.5
14	65 °C, pH 6.5, 55.2'	9.0	34.0	22.0	33.0
15	65 °C, pH 6.5, 30'	10.6	33.0	19.5	36.9

*Pure β-lg corresponds to the β-lg in solution with no heat treatment and no pH adjustment.

In addition, the antiparallel β-sheets present in β-lg could be more stable to structural changes resulting in poor variation in β-sheet content after glycosylation and thermal treatments used. A study employing β-lactamase demonstrated that β-sheet structure is more heat-stable than α-helix (Vijayakumar, Vishveshwara, Ravishanker, & Beveridge, 1993). Similar results were obtained in this study.

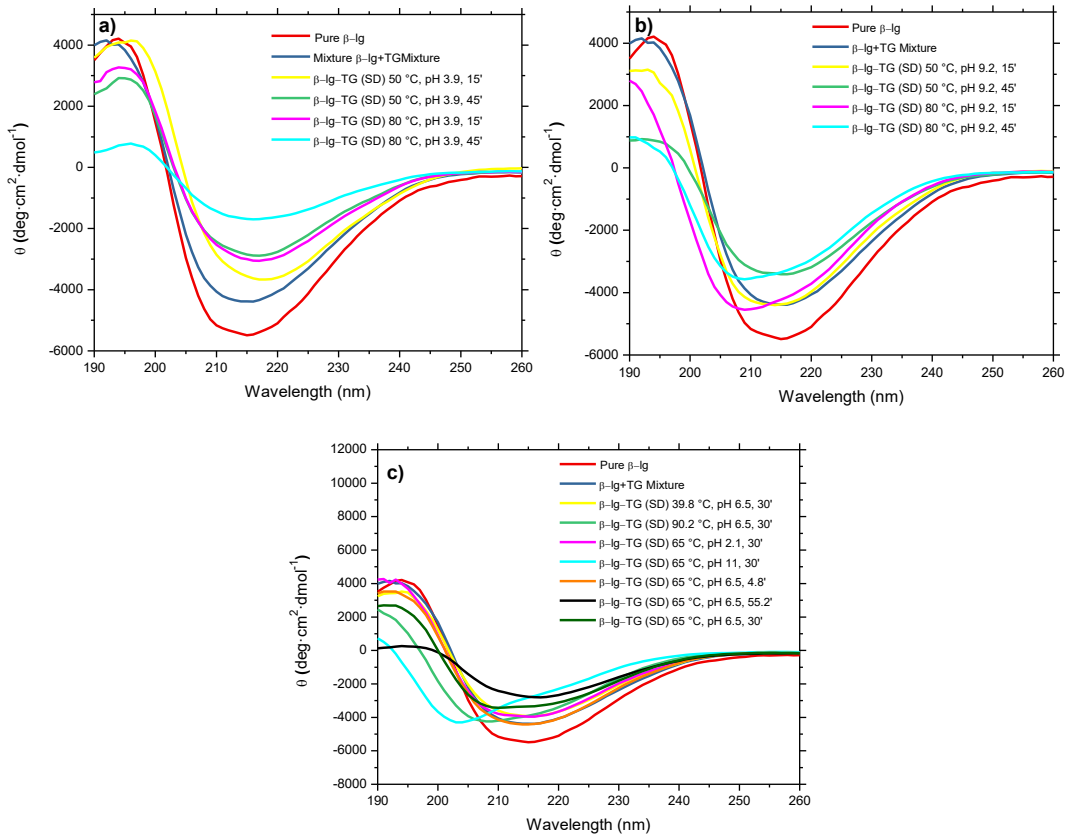

Fig. 7. CD spectra of native protein (β-lg), β-lg+TG mixture and nanostructures in different conditions for β-lg-TG (SD) system.

Table 6. Mean values of deconvolution of the residual molar ellipticity data for β-lg-TG (SD) system.

Treatment	System	Alpha-helix (%)	Beta-Sheet (%)	Turns (%)	Disordered structure (%)
	Pure β-lg	14.2	30.1	19.8	36.6
1	50 °C, pH 3.9, 15'	10.6	41.3	19.8	35.4
2	50 °C, pH 3.9, 45'	8.8	34.3	019.4	37.5
3	50 °C, pH 9.2, 15'	11.3	31.5	19.7	37.6
4	50 °C, pH 9.2, 45'	12.2	31.7	19.2	36.9
5	80 °C, pH 3.9, 15'	9.3	33.8	19.7	37.3
6	80 °C, pH 3.9, 45'	7.0	33.7	18.9	40.3
7	80 °C, pH 9.2, 15'	10.4	30.1	19.0	40.5
8	80 °C, pH 9.2, 45'	9.2	31	18.8	41.0
9	39.8 °C, pH 6.5, 30'	10.7	33.5	19.6	37.4
10	90.2 °C, pH 6.5, 30'	9.8	30.4	18.9	40.8
11	65 °C, pH 2.1, 30'	10.9	32.3	19.7	37.2
12	65 °C, pH 11, 30'	8.2	29.6	18.3	43.9
13	65 °C, pH 6.5, 4.8'	11.1	31.1	19.5	37.3
14	65 °C, pH 6.5, 55.2'	7.9	32.6	19.0	40.4
15	65 °C, pH 6.5, 30'	10.6	31.2	18.8	39.3

*Pure β-lg corresponds to the β-lg in solution with no heat treatment and no pH adjustment.

On the other hand, the treatments of the β-lg-TG (SD) system showed a similar behavior to the β-lg-TG (L) system, indicating that the effect of spray dry unit operation was insignificant (Fig. 7 and Table 6). These results were expected since β-lg is characterized by having two internal disulfide bonds, which confer a better stability (Creamer, Loveday, & Sawyer, 2011).

3.3.5. Stability of α-la-TG nanostructures during storage

Table 7 shows the relation of the chosen treatments of each system in which there was formation of nanoparticles. We considered particle sizes between 10 and 300 nm according to Uskoković (2007). In this section, the nanostructures selected were analyzed via DLS for 45 days in order to evaluate their stability during storage at 4 °C. For treatments from β-lg-TG (L) system from day 3 of storage, the particle average diameter values were higher than 300 nm (Fig 8). This indicates that the loss of colloidal stability occurs from this period, resulting in the consequent aggregation of particles.

A possible explanation for this phenomenon may be due to the type of polysaccharide used, in this case tara gum, which is characterized by being uncharged (Dea et al., 1977). This suggests that hydrophobic interactions and hydrogen bonds were not sufficient to maintain system stability for longer periods. Based on these results, we considered that there were no stable treatments for β-lg-TG (L) system. For β-lg-TG (SD) system, Treatment 4 (50 °C, pH 9.2, 45') showed a maximum stability of 10 days (Fig 8).

Table 7. Conditions with formation of nanostructures for β-lg-TG (L) and β-lg-TG (SD) systems.

Treatment	System	Average size (nm)			Zeta potential (mv)	Maximum fluorescence intensity	Circular dichroism			
		Peak 1	Peak 2	Peak 3			Alpha-helix (%)	Beta-Sheet (%)	Turns (%)	Disordered structure (%)
7	β-lg-TG (L) 80 °C, pH 9.2, 15'	30.49	2107	267.3	-2.310	614346,4	10.0	30.3	19.0	40.6
8	β-lg-TG (L) 80 °C, pH 9.2, 45'	278.9	26.09	113.1	-9.480	426664,2	8.5	33.0	18.9	40.6
3	β-lg-TG (SD) 50 °C, pH 9.2, 15'	1047	143.3	5438	-3.200	376892,8	11.3	31.5	19.7	37.6
4	β-lg-TG (SD) 50 °C, pH 9.2, 45'	1132	96,86	4858	-4.780	372419,2	9.1	31.7	19.2	39.9
7	β-lg-TG (SD) 80 °C, pH 9.2, 15'	73.89	23.9	-	-7.235	624619,2	10.4	30.1	19.0	40.5
9	β-lg-TG (SD) 39.8 °C, pH 6.5, 30'	70.41	278.4	4404	-14,50	503784,8	10.7	33.5	19.6	37.4
10	β-lg-TG (SD) 90.2 °C, pH 6.5, 30'	53.46	288	2269	-2.825	458175,2	9.8	30.4	18.9	40.8
11	β-lg-TG (SD) 65 °C, pH 2.1, 30'	34.69	187.69	1692	2.305	455976	10.9	32.3	19.7	37.2

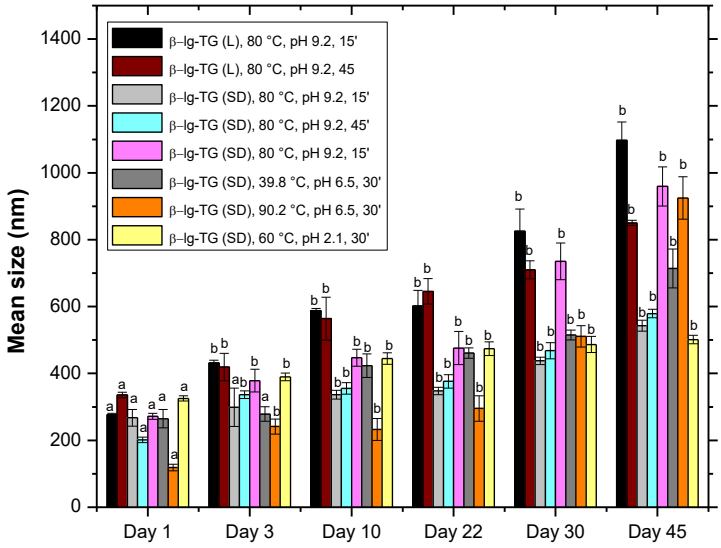

Fig. 8. Effect of time storage at 4°C on the hydrodynamic diameter of nanostructures for β-lg-TG (L) and β-lg-TG (SD) systems. Values with the same letter were not significantly different when compared to the control (Day 1) by Dunnett test ($p > 0.05$).

On the other hand, in Fig. 8 one can observe that the variation of the average size for the treatments from β-lg-TG (L) system was higher than the β-lg-TG (SD) system. This result suggests that systems using β-lg with a lower grafting degree present greater stability. A possible explanation for this phenomenon could be the solubility of these conjugates. Studies report a decrease in the protein solubility with the increase of the progression of the Maillard reaction. Al-Hakkak & Al-Hakkak (2010) observed the reduction of solubility of egg protein-pectin conjugates using proteins with a higher glycosylation degree. Therefore, the treatments that were obtained from β-lg-TG (L) (with a higher glycosylation degree) presented lower solubility, leading to the aggregation of the particles with the consequent decrease in the stability during storage

3.3.6. Foaming properties

Foaming properties include foaming capacity and foaming stability. Foaming capacity indicates the ability of the protein to foam, and the foaming stability refers to the ability of the foam formed to retain the maximum volume of air for a determinate time (Kim, Choi, Shin, & Moon, 2003). Table 8 and Fig. 9 show the values of the foaming capacity (volume increase-*VI*) and foaming stability for the more stable treatment from β-lg-TG (SD) system.

Table 8. Foam capacity for systems with β-lg.

Foaming capacity	Pure β-lg	β-lg+TG Mixture	β-lg-TG (SD) 50 °C, pH 9.2, 45'
VI	181.00 ± 1.41^{a*}	100.75 ± 1.06^{b}	102.50 ± 3.54^{b}

VI: volume increase. *Values with the same letter were not significantly different by Tukey test (p > 0.05). The measurements were done in triplicate.

Treatment 4 (50 °C, pH 9.2, 45') from β-lg-TG (SD) system showed *VI* values lower and significant (p < 0.05) than the control (pure β-lg). This decrease in the foaming capacity is probably due to the diffusion rate of this treatment at the interface and the dilatational characteristics of adsorbed film are not good enough to stabilize the bubbles during their formation. Corzo-Martínez, M. C., Sánchez, C. C., Moreno, F. J., Patino, J. M. R., and Villamiel (2012) found a similar result in β-lg-galactose nanostructured conjugates at pH 7.

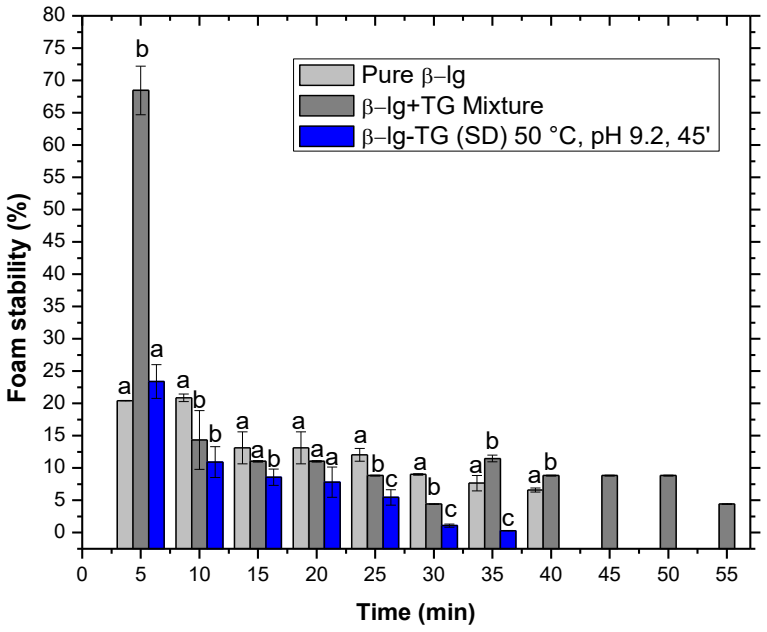

Fig. 9. Foam stability for β-lg-TG (SD) system. Values with the same letter were not significantly different by Tukey test (p > 0.05).

Foaming stability of treatment 4 (50 °C, pH 9.2, 45') was lower when compared to the control (p < 0.05) according to Fig. 9. We had expected that the decrease in foaming stability in treatment 4 would occur primarily due to the decrease in surface hydrophobicity after glycosylation, but the result of the intrinsic fluorescence analysis for this treatment clearly indicated the opposite, showing the lower maximum *FI*

compared to the pure β-lg. This indicates that the surface hydrophobicity was increased. A possible explanation for this phenomenon could be that other factors such as solubility and interfacial properties of the protein could affect foam stability. Considering that the solubility of the protein may have been reduced after glycosylation (Al-Hakkak & Al-Hakkak, 2010), we may conclude that the greater foaming stability of pure β-lg might be due to a higher solubility of this protein. Of course, the detailed mechanism should be further studied using other methods.

3.3.7. Emulsion stability index (*ESI*)

In order to investigate the effect of the conjugation of the TG on the stability of emulsions, the *ESI* of the nanostructures from β-lg -TG (SD) system was determined as shown in Fig. 10. We observed that treatment 4 (50 °C, pH 9.2, 45') from β-lg-TG (SD) system showed statistically higher *ESI* values in 30 and 60 min compared to the controls. The great emulsifying stability of this treatment may be attributed to its molecular characteristics, which are able to create a robust macromolecular barrier at the oil-water interfaces to prevent emulsion droplet aggregation (Akhtar & Dickinson, 2003). Guo, Guo, Yu, & Kong (2018) found similar behavior in WPI-sugar beet pectin conjugates.

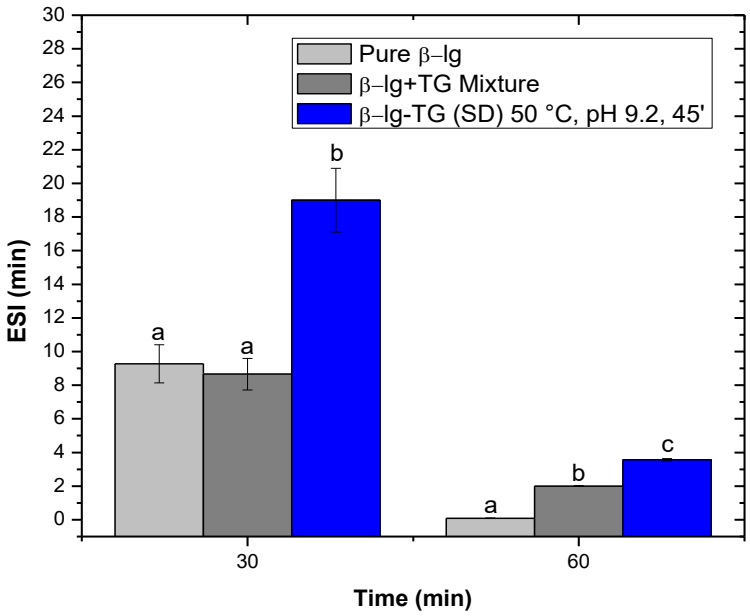

Fig. 10. Emulsion stability index (ESI) for β-lg-TG system. Values with the same letter were not significantly different by Tukey test ($p > 0.05$). The measurements were done in triplicate.

3.3.8. Morphological characterization of nanostructures

TEM images were captured to determine the nanostructure morphology of the treatment 4 (50 °C, pH 9.2, 45') from β-lg-TG (SD) system.

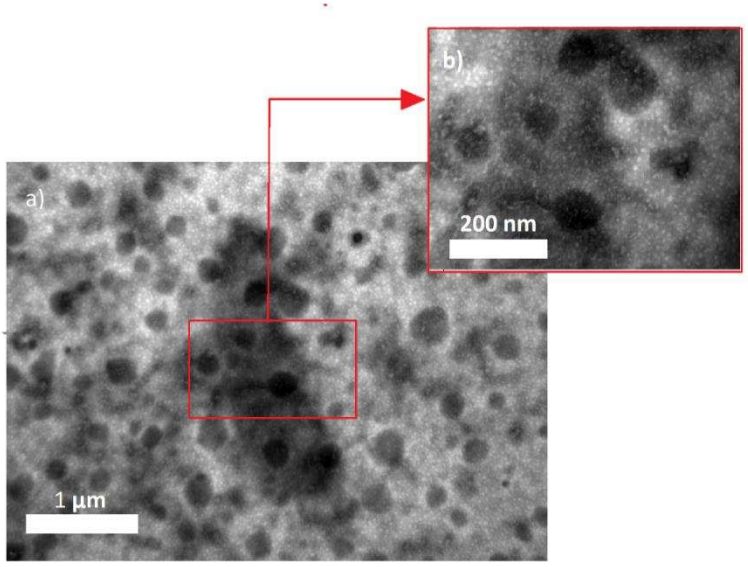

Fig. 11. Transmission electron micrograph of treatment 4 (50 °C, pH 9.2, 45') from β-lg-TG (SD) system, (a) β-lg-TG (SD) at 2000x, (b) β-lg-TG (SD) at 50000x.

In TEM images (Fig. 11a-b) for treatment 4, one can observe the presence of nanostructures with spherical shape with a diameter of approximately 60 nm. This size is much smaller than the mean hydrodynamic diameter obtained in the DLS technique for the same treatment (96.86 nm). We expected these results because the DLS technique provides mean particle size data in solution, while TEM analysis present images of spread and dried particle.

4. Conclusions

The browning index and percentage of free amino groups confirmed the glycosylation of β-lg with tara gum in spray-dried or lyophilized mixtures. The unitary operation of spray dry decreased markedly the glycosylation rate of the mixtures (β-lg and tara gum) when they were submitted to dry-heating. For conjugates obtained from spray-dried or lyophilized mixtures, the most appropriate reaction time was 2 days according to the results of browning index and percentage of free amino groups. Nanostructures from β-lg-TG conjugates were obtained under different temperature, pH and heating time conditions. Nanostructures with a mean diameter in the range of 30 and 300 nm presented changes in the secondary and tertiary structure of β-lg. Exposure of the

conjugates to thermal treatments at high temperatures (80-90.2 °C) was associated with loss of the α-helix content and increased disordered structure for the systems studied. The presence of nanostructures promoted a decrease in the foaming properties of β-lg but an increase in the emulsifying stability. Overall, this work showed that it is possible to obtain nanostructures from β-lg-TG conjugates using the dry-heating and thermal gelation techniques with pH adjustment and that they have potential use in the food industry as food additives.

Acknowledgments

The authors thank the Conselho Nacional de Pesquisa e Desenvolvimento Tecnológico (CNPq) for the financial support, the Centro Nacional de Pesquisa em Energia e Materiais-Laboratório Nacional de Biociências (CNPEM-LNBio) for the analyses of circular dichroism, intrinsic fluorescence and differential scanning calorimetry, the Núcleo de Microscopia e Microanálise of Universidade Federal de Viçosa for transmission electron microscopy analysis.

References

Adjonu, R., Doran, G., Torley, P., & Agboola, S. (2014). Whey protein peptides as components of nanoemulsions: A review of emulsifying and biological functionalities. *Journal of Food Engineering*, *122*, 15–27. https://doi.org/10.1016/J.JFOODENG.2013.08.034

Akhtar, M., & Dickinson, E. (2003). Emulsifying properties of whey protein–dextran conjugates at low pH and different salt concentrations. *Colloids and Surfaces B: Biointerfaces*, *31*(1–4), 125–132. https://doi.org/10.1016/S0927-7765(03)00049-3

Al-Hakkak, J., & Al-Hakkak, F. (2010). Functional egg white–pectin conjugates prepared by controlled Maillard reaction. *Journal of Food Engineering*, *100*(1), 152–159. https://doi.org/10.1016/J.JFOODENG.2010.03.040

Álvarez, C., García, V., Rendueles, M., & Díaz, M. (2012). Functional properties of isolated porcine blood proteins modified by Maillard's reaction. *Food Hydrocolloids*, *28*(2), 267–274. https://doi.org/10.1016/J.FOODHYD.2012.01.001

Alves, J. G. L. F., Brenneisen, J., Ninni, L., Meirelles, A. J. A., & Maurer, G. (2008).

Aqueous Two-Phase Systems of Poly(ethylene glycol) and Sodium Citrate: Experimental Results and Modeling. *Journal of Chemical & Engineering Data*, *53*(7), 1587–1594. https://doi.org/10.1021/je800137f

Aoki, T., Hiidome, Y., Kitahata, K., Sugimoto, Y., Ibrahim, H. R., & Kato, Y. (1999). Improvement of heat stability and emulsifying activity of ovalbumin by conjugation with glucuronic acid through the Maillard reaction. *Food Research International*, *32*(2), 129–133. https://doi.org/10.1016/S0963-9969(99)00039-3

Bromley, E. H., Krebs, M. R. H., & Donald, A. M. (2005). Aggregation across the length-scales in beta-lactoglobulin. *Faraday Discussions*, *128*, 13–27. Retrieved from http://www.ncbi.nlm.nih.gov/pubmed/15658764

Cascio, M., & Wallace, B. . (1999). Red- and Blue-Shifting in the Cicular Dichroism spectra of polypeptides due to dipole effect. *Protein and Peptide Letters*, *1*(2), 136–140.

Chamani, J., Moosavi-Movahedi, A. A., & Hakimelahi, G. H. (2005). Structural changes in ??-lactoglobulin by conjugation with three different kinds of carboxymethyl cyclodextrins. *Thermochimica Acta*, *432*(1), 106–111. https://doi.org/10.1016/j.tca.2005.04.014

Chatterton, D. E. W., Smithers, G., Roupas, P., & Brodkorb, A. (2006). Bioactivity of β-lactoglobulin and α-lactalbumin—Technological implications for processing. *International Dairy Journal*, *16*(11), 1229–1240. https://doi.org/10.1016/J.IDAIRYJ.2006.06.001

Chen, H., Xu, Z., Mo, J., Lyu, Y., Tang, X., & Shen, X. (2017). Effects of guar gum on adhesion properties of soybean protein isolate onto porcine bones. *International Journal of Adhesion and Adhesives*, *75*(March), 124–131. https://doi.org/10.1016/j.ijadhadh.2017.03.001

Chiu, T. hsin, Chen, M. lun, & Chang, H. chia. (2009). Comparisons of emulsifying properties of Maillard reaction products conjugated by green, red seaweeds and various commercial proteins. *Food Hydrocolloids*, *23*(8), 2270–2277. https://doi.org/10.1016/j.foodhyd.2009.06.003

Corzo-Martínez, M. C., Sánchez, C. C., Moreno, F. J., Patino, J. M. R., and Villamiel, M. (2012). Interfacial and foaming properties of bovine b-lactoglobulin:

Galactose Maillard Conjugates. *Food Hydrocolloids*, *27*, 438–447.

Corzo-Martínez, M., Moreno, F. J., Olano, A., & Villamiel, M. (2008). Structural characterization of bovine β-lactoglobulin-galactose/ tagatose maillard complexes by electrophoretic, chromatographic, and spectroscopic methods. *Journal of Agricultural and Food Chemistry*, *56*(11), 4244–4252. https://doi.org/10.1021/jf7036714

Creamer, L. ., Loveday, S. ., & Sawyer, L. (2011). β-Lactoglobulin. In *Encycclopedia of Dairy Sciences* (2nd ed., pp. 787–794). Oxford: Academic Press.

Day, L., Zhai, J., Xu, M., Jones, N. C., Hoffmann, S. V., & Wooster, T. J. (2014). Conformational changes of globular proteins adsorbed at oil-in-water emulsion interfaces examined by synchrotron radiation circular dichroism. *Food Hydrocolloids*, *34*, 78–87. https://doi.org/10.1016/j.foodhyd.2012.12.015

de Oliveira, F. C., Coimbra, J. S. dos R., de Oliveira, E. B., Zuñiga, A. D. G., & Rojas, E. E. G. (2014). Food Protein-polysaccharide Conjugates Obtained via the Maillard Reaction: A Review. *Critical Reviews in Food Science and Nutrition*, *56*(7), 1108–1125. https://doi.org/10.1080/10408398.2012.755669

Dea, I. C. M., Morris, E. R., Rees, D. A., Welsh, E. J., Barnes, H. A., & Price, J. (1977). Associations of like and unlike polysaccharides: Mechanism and specificity in galactomannans, interacting bacterial polysaccharides, and related systems. *Carbohydrate Research*, *57*, 249–272. https://doi.org/10.1016/S0008-6215(00)81935-7

Donaldson, T. L., Boonstra, E. F., & Hammond, J. M. (1980). Kinetics of protein denaturation at gas—liquid interfaces. *Journal of Colloid and Interface Science*, *74*(2), 441–450. https://doi.org/10.1016/0021-9797(80)90213-1

Fan, Y., Yi, J., Zhang, Y., Wen, Z., & Zhao, L. (2017). Physicochemical stability and in vitro bioaccessibility of β-carotene nanoemulsions stabilized with whey protein-dextran conjugates. *Food Hydrocolloids*, *63*(2017), 256–264. https://doi.org/10.1016/j.foodhyd.2016.09.008

Fink, A. L. (1998). Protein aggregation: folding aggregates, inclusion bodies and amyloid. *Folding and Design*, *3*(1), R9–R23. https://doi.org/10.1016/S1359-0278(98)00002-9

Guo, X., Guo, X., Yu, S., & Kong, F. (2018). Influences of the different chemical components of sugar beet pectin on the emulsifying performance of conjugates formed between sugar beet pectin and whey protein isolate. *Food Hydrocolloids*, *82*, 1–10. https://doi.org/10.1016/j.foodhyd.2018.03.032

Hattori, M., Numamoto, K., Kobayashi, K., & Takahashi, K. (2000). Functional changes in beta-lactoglobulin by conjugation with cationic saccharides. *J Agric Food Chem*, *48*(6), 2050–2056. https://doi.org/10.1021/jf991105s

Hidaka, T., Shimada, A., Nakata, Y., Kodama, H., Kurihara, H., Tokihiro, T., & Ihara, S. (2015). Simple model of pH -induced protein denaturation. *Physical Review E - Statistical, Nonlinear, and Soft Matter Physics*, *92*(1), 1–7. https://doi.org/10.1103/PhysRevE.92.012709

Jiang, Z., & Brodkorb, A. (2012). Structure and antioxidant activity of Maillard reaction products from α-lactalbumin and β-lactoglobulin with ribose in an aqueous model system. *Food Chemistry*, *133*(3), 960–968. https://doi.org/10.1016/j.foodchem.2012.02.016

Kato, A. (2002). Industrial applications of Millard-type protein– polysaccharide conjugados. *Food Science and Technology Research, 8*, 193–199.

Kim, H. J., Choi, S. J., Shin, W.-S., & Moon, T. W. (2003). Emulsifying properties of bovine serum albumin-galactomannan conjugates. *Journal of Agricultural and Food Chemistry*, *51*, 1049–1056. https://doi.org/10.1021/jf020698v

Koch, L., Emin, M. A., & Schuchmann, H. P. (2017). Influence of processing conditions on the formation of whey protein-citrus pectin conjugates in extrusion. *Journal of Food Engineering*, *193*, 1–9. https://doi.org/10.1016/j.jfoodeng.2016.08.012

Le, T. T., Bhandari, B., Holland, J. W., & Deeth, H. C. (2011). Maillard reaction and protein cross-linking in relation to the solubility of milk powders. *Journal of Agricultural and Food Chemistry*, *59*(23), 12473–12479. https://doi.org/10.1021/jf203460z

Lesmes, U., & McClements, D. J. (2012). Controlling lipid digestibility: Response of lipid droplets coated by β-lactoglobulin-dextran Maillard conjugates to simulated gastrointestinal conditions. *Food Hydrocolloids*, *26*(1), 221–230.

https://doi.org/10.1016/j.foodhyd.2011.05.011

Levine, D. ., Berenson, M. ., & Stephan, D. (1998). *Estatística: teoria e aplicações* (Livros Téc). Rio de Janeiro.

Li, C., Xue, H., Chen, Z., Ding, Q., & Wang, X. (2014). Comparative studies on the physicochemical properties of peanut protein isolate-polysaccharide conjugates prepared by ultrasonic treatment or classical heating. *Food Research International*, *57*, 1–7. https://doi.org/10.1016/j.foodres.2013.12.038

Li, J., Shaoyong Yu, Ping Yao, * and, & Jiang, M. (2008). Lysozyme−Dextran Core−Shell Nanogels Prepared via a Green Process. *Langmuir*, *24*, 3486–3492. https://doi.org/10.1021/LA702785B

Liu, J., Ru, Q., & Ding, Y. (2012). Glycation a promising method for food protein modification: Physicochemical properties and structure, a review. *Food Research International*, *49*(1), 170–183. https://doi.org/10.1016/J.FOODRES.2012.07.034

Liu, Y., Zhao, G., Zhao, M., Ren, J., & Yang, B. (2012). Improvement of functional properties of peanut protein isolate by conjugation with dextran through Maillard reaction. *Food Chemistry*, *131*(3), 901–906. https://doi.org/10.1016/J.FOODCHEM.2011.09.074

Lu, Q., Tang, Q., Xiong, Y., Qing, G., & Sun, T. (2016). Protein/peptide aggregation and amyloidosis on biointerfaces. *Materials*, *9*(9). https://doi.org/10.3390/ma9090740

Loch, J., Polit, A., Gorecki, A., Bonarek, P., & Kurpieswska, K. (2011). Two modes of fatty acid binding to bovine beta-lactoglobulin-crystallographic and spectroscopic studies. *J. Mol. Recongnit*, *24*, 341-349. https://doi.org/ 10.2210/PDB3NPO/PDB

Markman, G., & Livney, Y. D. (2012). Maillard-conjugate based core-shell co-assemblies for nanoencapsulation of hydrophobic nutraceuticals in clear beverages. *Food & Function*, *3*(3), 262–70. https://doi.org/10.1039/c1fo10220f

Martinez-Alvarenga, M. S., Martinez-Rodriguez, E. Y., Garcia-Amezquita, L. E., Olivas, G. I., Zamudio-Flores, P. B., Acosta-Muniz, C. H., & Sepulveda, D. R. (2014). Effect of Maillard reaction conditions on the degree of glycation and

functional properties of whey protein isolate – Maltodextrin conjugates. *Food Hydrocolloids*, *38*, 110–118. https://doi.org/10.1016/J.FOODHYD.2013.11.006

McClements, D. J. (2004). Protein-stabilized emulsions. *Current Opinion in Colloid & Interface Science*, *9*(5), 305–313. https://doi.org/10.1016/J.COCIS.2004.09.003

McClements, D. J. (2005). *Food Emulsions: principles, practice and techniques* (2nd ed.). Boca Raton: CRC Press.

Morgan, F., Léonil, J., Mollé, D., & Bouhallab, S. (1997). Nonenzymatic lactosylation of bovine beta-lactoglobulin under mild heat treatment leads to structural heterogeneity of the glycoforms. *Biochemical and Biophysical Research Communications*, *236*(2), 413–7. Retrieved from http://www.ncbi.nlm.nih.gov/pubmed/9240451

Morris, G. A., Sims, I. M., Robertson, A. J., & Furneaux, R. H. (2004). Investigation into the physical and chemical properties of sodium caseinate-maltodextrin glyco-conjugates. *Food Hydrocolloids*, *18*(6), 1007–1014. https://doi.org/10.1016/j.foodhyd.2004.04.013

Oliver, C. M., Melton, L. D., & Stanley, R. A. (2006). Creating Proteins with Novel Functionality via the Maillard Reaction: A Review. *Critical Reviews in Food Science and Nutrition*, *46*(4), 337–350. https://doi.org/10.1080/10408690590957250

Phan-Xuan, T., Durand, D., Nicolai, T., Donato, L., Schmitt, C., & Bovetto, L. (2011). On the Crucial Importance of the pH for the Formation and Self-Stabilization of Protein Microgels and Strands. *Langmuir*, *27*(24), 15092–15101. https://doi.org/10.1021/la203357p

Ramos, O. L., Pereira, R. N., Rodrigues, R., Teixeira, J. A., Vicente, A. A., & Xavier Malcata, F. (2014). Physical effects upon whey protein aggregation for nano-coating production. *Food Research International*, *66*, 344–355. https://doi.org/10.1016/J.FOODRES.2014.09.036

Randhir, R., Kwon, Y.-I., & Shetty, K. (2008). Effect of thermal processing on phenolics, antioxidant activity and health-relevant functionality of select grain sprouts and seedlings. *Innovative Food Science & Emerging Technologies*, *9*(3),

355–364. https://doi.org/10.1016/J.IFSET.2007.10.004

Riddick, T. (1968). *Zeta-meter manual*. New York: Zeta-meter Inc.

Sanmartín, E., Arboleya, J. C., Villamiel, M., & Moreno, F. J. (2009). Recent Advances in the Recovery and Improvement of Functional Proteins from Fish Processing By-Products: Use of Protein Glycation as an Alternative Method. *Comprehensive Reviews in Food Science and Food Safety*, *8*(4), 332–344. https://doi.org/10.1111/j.1541-4337.2009.00083.x

Saraiva, C. S., dos Reis Coimbra, J. S., de Carvalho Teixeira, A. V. N., de Oliveira, E. B., Teófílo, R. F., da Costa, A. R., & de Almeida Alves Barbosa, É. (2017). Formation and characterization of supramolecular structures of β-lactoglobulin and lactoferrin proteins. *Food Research International*, *100*, 674–681. https://doi.org/10.1016/j.foodres.2017.07.065

Sgarbieri, V. C. (2005). Structural and Physicochemical Properties of Milk Proteins. *Brazilian Journal of Food Technologies*, *8*, 43–56.

Sheng, L., Su, P., Han, K., Chen, J., Cao, A., Zhang, Z., … Ma, M. (2017). Synthesis and structural characterization of lysozyme–pullulan conjugates obtained by the Maillard reaction. *Food Hydrocolloids*, *71*, 1–7. https://doi.org/10.1016/j.foodhyd.2017.04.026

Spotti, M. J., Perduca, M. J., Piagentini, A., Santiago, L. G., Rubiolo, A. C., & Carrara, C. R. (2013). Gel mechanical properties of milk whey protein–dextran conjugates obtained by Maillard reaction. *Food Hydrocolloids*, *31*(1), 26–32. https://doi.org/10.1016/J.FOODHYD.2012.08.009

Sreerama, N., & Woody, R. W. (2000). Estimation of Protein Secondary Structure from Circular Dichroism Spectra: Comparison of CONTIN, SELCON, and CDSSTR Methods with an Expanded Reference Set. *Analytical Biochemistry*, *287*(2), 252–260. https://doi.org/10.1006/ABIO.2000.4880

Stanic-Vucinic, D., Prodic, I., Apostolovic, D., Nikolic, M., & Cirkovic Velickovic, T. (2013). Structure and antioxidant activity of β-lactoglobulin-glycoconjugates obtained by high-intensity-ultrasound-induced Maillard reaction in aqueous model systems under neutral conditions. *Food Chemistry*, *138*(1), 590–599. https://doi.org/10.1016/j.foodchem.2012.10.087

Sun, W.-W., Yu, S.-J., Yang, X.-Q., Wang, J.-M., Zhang, J.-B., Zhang, Y., & Zheng, E.-L. (2011). Study on the rheological properties of heat-induced whey protein isolate–dextran conjugate gel. *Food Research International*, *44*(10), 3259–3263. https://doi.org/10.1016/J.FOODRES.2011.09.019

Sun, Y., Hayakawa, S., & Izumori, K. (2004). Modification of Ovalbumin with a Rare Ketohexose through the Maillard Reaction: Effect on Protein Structure and Gel Properties. *Journal of Agricultural and Food Chemistry*, *52*(5), 1293–1299. https://doi.org/10.1021/jf030428s

Taheri-Kafrani, A., Choiset, Y., Faizullin, D. A., Zuev, Y. F., Bezuglov, V. V., Chobert, J.-M., … Haertlé, T. (2011). Interactions of β-lactoglobulin with serotonin and arachidonyl serotonin. *Biopolymers*, *95*(12), 871–880. https://doi.org/10.1002/bip.21690

Teófilo, R. F., & Ferreira, M. M. C. (2006). Quimiometria II: Planilhas eletrônicas para cálculus de planejamentos experimentais, um tutorial. *Quimica Nova*, *29*(2), 338–350. https://doi.org/10.1590/S0100-40422006000200026

Toro-Sierra, J., Schumann, J., & Kulozik, U. (2013). Impact of spray-drying conditions on the particle size of microparticulated whey protein fractions. *Dairy Science and Technology*, *93*(4–5), 487–503. https://doi.org/10.1007/s13594-013-0124-7

Uskoković, V. (2007). Nanotechnologies: What we do not know. *Technology in Society*, *29*(1), 43–61. https://doi.org/10.1016/J.TECHSOC.2006.10.005

Vigo, M. S., Malec, L. S., Gomez, R. G., & Llosa, R. A. (1992). Spectrophotometric assay using o-phthaldialdehyde for determination of reactive lysine in dairy products. *Food Chemistry*, *44*(5), 363–365. https://doi.org/10.1016/0308-8146(92)90269-8

Vijayakumar, S., Vishveshwara, S., Ravishanker, G., & Beveridge, D. L. (1993). Differential stability of beta-sheets and alpha-helices in beta-lactamase: a high temperature molecular dynamics study of unfolding intermediates. *Biophysical Journal*, *65*(6), 2304–2312. https://doi.org/10.1016/S0006-3495(93)81288-8

Wang, W., & Zhong, Q. (2014). Properties of whey protein-maltodextrin conjugates as impacted by powder acidity during the Maillard reaction. *Food Hydrocolloids*,

38, 85–94. https://doi.org/10.1016/j.foodhyd.2013.11.018

Wijaya, W., Van der Meeren, P., & Patel, A. R. (2017). Cold-set gelation of whey protein isolate and low-methoxyl pectin at low pH. *Food Hydrocolloids*, *65*, 35–45. https://doi.org/10.1016/J.FOODHYD.2016.10.037

Wong, B. T., Day, L., & Augustin, M. A. (2011). Deamidated wheat protein-dextran Maillard conjugates: Effect of size and location of polysaccharide conjugated on steric stabilization of emulsions at acidic pH. *Food Hydrocolloids*, *25*(6), 1424–1432. https://doi.org/10.1016/j.foodhyd.2011.01.017

Wooster, T. J., & Augustin, M. A. (2007). Rheology of whey protein-dextran conjugate films at the air/water interface. *Food Hydrocolloids*, *21*(7), 1072–1080. https://doi.org/10.1016/j.foodhyd.2006.07.015

Yang, J.-E., Chun, S.-H., Kim, H. H., Choi, H.-D., & Lee, K.-W. (2017). Characterization of Maillard-type lysozyme-galactomannan conjugate having immune-enhancing effects. *Food Chemistry*, *227*, 149–157. https://doi.org/10.1016/J.FOODCHEM.2017.01.076

Yi, J., Fan, Y., Yokoyama, W., Zhang, Y., & Zhao, L. (2016). Characterization of milk proteins–lutein complexes and the impact on lutein chemical stability. *Food Chemistry*, *200*, 91–97. https://doi.org/10.1016/j.foodchem.2016.01.035

Yi, J., Fan, Y., Zhang, Y., Wen, Z., Zhao, L., & Lu, Y. (2016). Glycosylated α-lactalbumin-based nanocomplex for curcumin: Physicochemical stability and DPPH-scavenging activity. *Food Hydrocolloids*, *61*, 369–377. https://doi.org/10.1016/j.foodhyd.2016.05.036

Yi, J., Lam, T. I., Yokoyama, W., Cheng, L. W., & Zhong, F. (2014). Controlled Release of β-Carotene in β-Lactoglobulin–Dextran-Conjugated Nanoparticles' in Vitro Digestion and Transport with Caco-2 Monolayers. *Journal of Agricultural and Food Chemistry*, *62*(35), 8900–8907. https://doi.org/10.1021/jf502639k

Zhong, J., Cai, X., Liu, C., Liu, W., Xu, Y., & Luo, S. (2016). Purification and conformational changes of bovine PEGylated β-lactoglobulin related to antigenicity. *Food Chemistry*, *199*, 387–392. https://doi.org/10.1016/J.FOODCHEM.2015.12.047

Supplementary material

1. β-lg crystal in native state with lysine marked in red color

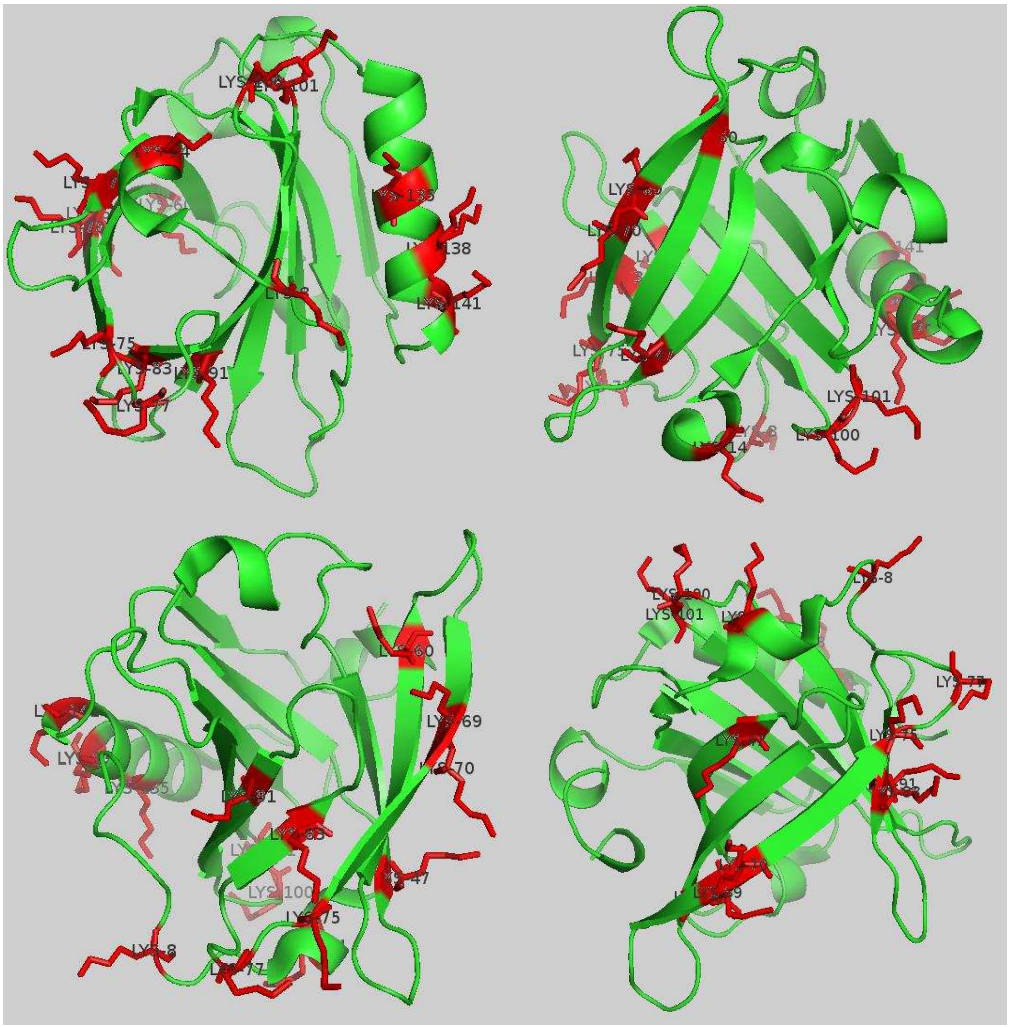

Source: Loch, Polit, Gorecki, Bonarek, & Kurpieswska (2011) PDB. PyMOL-Molecular Graphics System 1.7.0.0 was used on the image processing.

2. **Regression analysis for β-lg-TG (L) and β-lg-TG (SD) systems**

System	**β-lg-TG L**		**β-lg-TG SD**	
Term	**Regression coefficient for Size (Y_1)**	***p***	**Regression coefficient for Size (Y_1)**	***p***
Constant	2558,531	0,1730	701,467	0,8266
Linear				
X_1	-44,269	0,2824	-6,775	0,9251
X_2	-47,222	0,7922	-108,945	0,7400
X_3	-35,169	0,2622	26,308	0,6333
Quadratic				
X_1*X_1	0,459	0,1295	0,072	0,8871
X_2*X_2	9,648	0,3013	6,163	0,7083
X_3*X_3	0,226	0,4250	0,300	0,5586
Interaction				
X_1*X_2	-2,768	0,1670	0,874	0,7978
X_1*X_3	0,184	0,5796	-0,296	0,6252
X_2*X_3	1,313	0,4882	-3,104	0,3759
R^2	0,69756		0,42123	

Note: Statistically significant (p-value < 0,05); X_1:temperature of heating; X_2:pH; X_3: time of heating; Y_1: Mean diameter; R^2:coefficient of determination.

GENERAL CONCLUSIONS

In this study, the Maillard reaction was used to obtain nanostructured conjugates formed by whey proteins (α-1a, β-1g) and Tara gum. The results of the conjugate characterization showed that the increase in the browning index and the reduction of the free amino groups are directly proportional to the increase in the heating time. The unit operations of spray dry and lyophilization affected the progress of the Maillard reaction. The most appropriate time of glycosylation was of 2 days for both systems studied.

Regarding to the formation of nanostructures from α-1a-TG system, nanoparticles with a hydrodynamic diameter varying from 34.3 to 290.1 nm were obtained at different conditions of temperature (39.8, 50, 65, and 80 °C), pH (6.5, 9.2, and11) and heating time (15, 30, 45, and 55.2 min). Process conditions of 50 °C, pH 9.2, 15' for α-1a-TG (SD) system presented a conic shape with foaming and emulsifying capacities and thermal stability greater than the control (pure α-1a). Analyses of circular dichroism and fluorimetry showed protein conformational changes after the glycosylation and the application of thermal treatments in the nanostructures, mainly in treatments for α-1a-TG (SD) system.

Nanostructures from β-1g-TG system presented mean diameter varying from 30.5 to 278.9 nm at different conditions of temperature (39.8, 50, 65, 80, and 90.2 °C), pH (2.1 6.5, and 9.2) and heating time (15, 30, and 45 min) with a major influence of pH in the formation of the nanoparticles. Lyophilized and spray-dried systems showed electrostatic instability with ζ-potential values varying from -30 to 30 mV. There was conformational changes in the nanostructures for β-1g-TG (L) system, mainly at process conditions of (90.2 °C, pH 6.5, 30') and of (65 °C, pH 2.1, 30') due to the effect of temperature and pH. Process conditions of (50 °C, pH 9.2, 45') for β-1g-TG (SD) system presented spherical shape and emulsifying stability greater than the control (pure β-1g).

More studies are necessary on the characterization of these nanostructures using, for example, stability measures to denaturants, toxicological studies to determine the effect of these nanoparticles on the human organism and tests to determine the viability for being used as carrier matrices of active compounds.